SCI INSTITUTE
TECHNICAL REPORT

Uintah User Guide

Jim Guilkey, Todd Harman, Justin Luitjens, John Schmidt, Jeremy Thornock, J. Davison de St. Germain, Siddharth Shankar, Joseph Peterson, Carson Brownlee

UUSCI-2009-007

Scientific Computing and Imaging Institute
University of Utah
Salt Lake City, UT 84112 USA

September 15, 2009

THE UNIVERSITY OF UTAH

Uintah User Guide

Jim Guilkey, Todd Harman, Justin Luitjens,
John Schmidt, Jeremy Thornock, J. Davison de St. Germain,
Siddharth Shankar, Joseph Peterson, Carson Brownlee

Version 1.1

Contents

Chapter 1

Overview of Uintah

1.1 The Center for the Simulation of Accidental Fires and Explosions (C-SAFE)

1.1.1 Center History

The Uintah software suite was created by the Center for the Simulation of Accidental Fires and Explosions (C-SAFE). C-SAFE was originally created at the University of Utah in 1997 by the Department of Energy's Accelerated Strategic Computing Initiative's (ASCI) Academic Strategic Alliance Program (ASAP). (ASCI has since been renamed to the Advanced Simulation and Computing (ASC) program.)

Center Objective

C-SAFE's primary objective has been to provide a software system in which fundamental chemistry and engineering physics are fully coupled with nonlinear solvers, visualization, and experimental data verification, thereby integrating expertise from a wide variety of disciplines. Simulations using the Uintah software can help to better evaluate the risks and safety issues associated with fires and explosions in accidents involving both hydrocarbon and energetic materials.

Target Simulation

The Uintah software system was designed to support the solution of a wide range of highly dynamic physical processes using a large number of processors. However, our specific target simulation has been the heating of an explosive device placed in a large hydrocarbon pool fire and the subsequent deflagration explosion and blast wave (Figure 1.1). The explosive device is a small cylindrical steel container (4" outside diameter) filled with plastic bonded explosive (PBX-9501). Convective and radiative heat fluxes from the fire heat the outside of the container and subsequently the PBX.

After some amount of time the critical temperature in the PBX is reached and the explosive begins to rapidly decompose into a gas. The solid-¿gas reaction pressurizes the interior of the steel container causing the shell to rapidly expand and eventually rupture. The gaseous products of reaction form a blast wave that expands outward along with pieces of the container and any unreacted PBX. The physical processes in this simulation have a wide range in time and length scales from microseconds and microns to minutes and meters. Uintah was designed as a general-purpose fluid-structure interaction code that can simulate not only this scenario but a wide range of related problems.

Complex simulations such as this require both immense computational power and complex software. Typical simulations include solvers for structural mechanics, fluids, chemical reactions, and material models. All of these aspects must be integrated in an efficient manner to achieve the scalability required to perform these simulations. The heart of Uintah is a sophisticated computational framework that can integrate multiple simulation components, analyze the dependencies and communication patterns between them, and efficiently execute the resulting multi-physics simulation. Uintah also provides mechanisms for automating load-balancing, checkpoint/restart, and parallel I/O. The Uintah core was designed to be general, and is appropriate for use in a wide range of PDE algorithms based on structured (adaptive) grids and particle-in-cell algorithms.

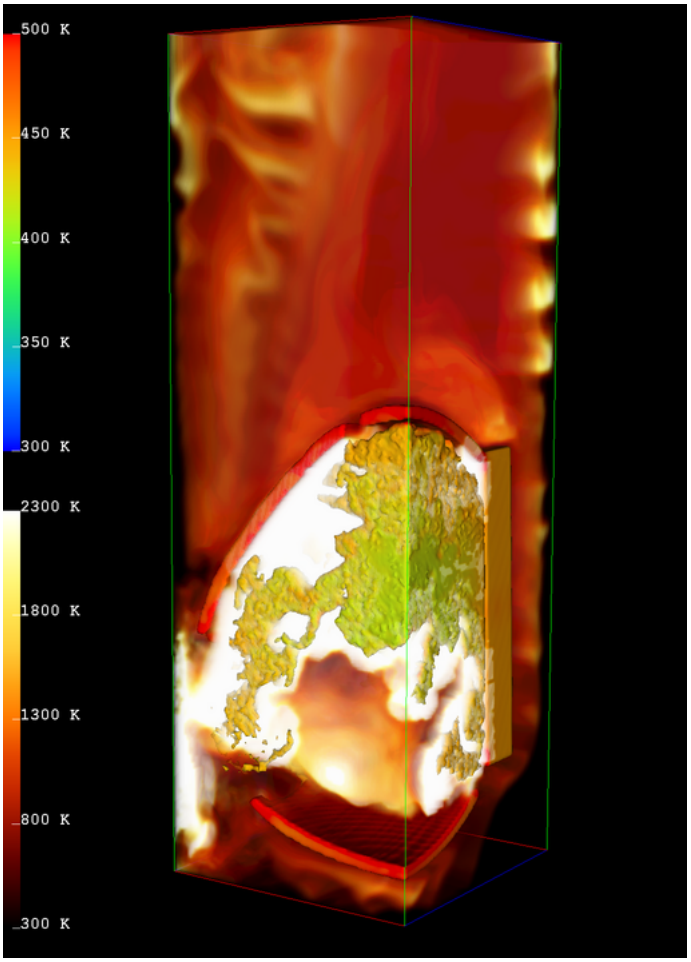

Figure 1.1: Target Simulation - Fire-Container-Explosion.

1.2 Uintah Software

The Uintah Computational Framework (also referred to as Uintah or the UCF) consists of a set of software components and libraries that facilitate the solution of Partial Differential Equations (PDEs) on Structured AMR (SAMR) grids using up to hundreds to thousands of processors.

One of the challenges in designing a parallel, component-based and multi-physics application is determining how to efficiently decompose the problem domain. Components, by definition, make local decisions. Yet parallel efficiency is only obtained through a globally optimal domain decomposition and scheduling of computational tasks. Typical techniques include allocating disjoint sets of processing resources to each component, or defining a single domain decomposition that is a compromise between the ideal load balance of multiple components. However, neither of these techniques will achieve maximum efficiency for complex multi-physics problems.

Uintah uses a non-traditional approach to achieving parallelism by employing an abstract task graph representation to describe computation and communication. The task graph is an explicit representation of the computation and communication that occur in the coarse of a single iteration of the simulation (typically a timestep or nonlinear solver iteration). Uintah components delegate decisions about parallelism to a scheduler component by using variable dependencies to describe communication patterns and characterizing computational workloads to facilitate a global resource optimization. The task graph representation has a number of advantages, including efficient fine-grained coupling of multi-physics components, flexible load balancing mechanisms and a separation of application concerns from parallelism concerns. However, it creates a challenge for scalability which we overcome by creating an implicit definition of this graph and representing it in a distributed fashion.

The primary advantage of a component-based approach is that it facilitates the separate development of simulation algorithms, models, and infrastructure. Components of the simulation can evolve independently. The component-based architecture allows pieces of the system to be implemented in a rudimentary form at first and then evolve as the technologies mature. Most importantly, Uintah allows the aspects of parallelism (schedulers, load-balancers, parallel input/output, and so forth) to evolve independently of the simulation components. Furthermore, components enable replacement of computation pieces without complex decision logic in the code itself.

Please see the Developers Guide (`http://www.uintah.utah.edu/trac/chrome/site/UintahAPI.pdf`) for more information about the internal architecture of Uintah.

1.2.1 Software Ports

Uintah has been ported and runs well on a number of operating systems. These include Linux, Mac OSX, Windows, AIX, and HPuX. Simulating small problems is perfectly feasible on 2-4 processor desktops, while larger problems will need 100s to 1000s of

processors on large computer clusters.

1.2.2 Uintah Software History

The UCF was orginally build upon the SCIRun Problem Solving Environment. SCIRun provided a core set of software building blocks, as well as a powerful visualization package. While Uintah continues to use the SCIRun core libraries, Uintah's use of the SCIRun PSE has been retired in favor of using the VisIt visualization package from LLNL.

Chapter 2

Using Uintah

Several executable programs have been developed using the Uintah Computational Framework (UCF). The primary code that drives the components implemented in Uintah is called `sus`, which stands for Standalone Uintah Simulation. The existing components were originally developed to solve a complex fluid structure problem involving a container filled with an explosive enveloped in a fire.

The code models the fire and the subsequent heat transfer to the container followed by the resultant container deformation and ultimate rupture due to the ignition and burning of the explosive material all running on thousands of processors requiring thousands of hours of computer time and hundreds of gigabytes of data storage. Although Uintah was developed originally to solve this complicated multi-physics problem, the general nature of the algorithms and the framework have allowed researchers to use the code to investigate a wide range of problems. The framework is general purpose enough to allow for the implementation of a variety of implicit and explicit algorithms on structured grids. In addition, particle based algorithms can be implemented using the native particle support found in the framework.

This code leverages the task based parallelism inherent in the UCF to implement several time stepping algorithms for structural mechanics, fluid dynamics, and fluid structure interactions. What follows is a description of using `sus` within the realm of structural mechanics, fluid mechanics, and structure-fluid interactions.

2.1 Installing the Uintah Software

For information on downloading the Uintah software package (via tarball or SVN), and how to setup (configure) and build (make) the system, please refer to the Uintah Installation Guide.

2.2 Mechanics of Running sus

For single processor simulations, the `sus` executable (Standalone Uintah Simulation) is run from the command line prompt like this:

```
sus input.ups
```

where `input.ups` is an XML formatted input file. The Uintah software release contains numerous example input files located in the `src/StandAlone/inputs/UintahRelease` directory.

For multiprocessor runs, the user generally uses `mpirun` to launch the code. Depending on the environment, batch scheduler, launch scripts, etc, `mpirun` may or may not be used. However, in general, something like the following is used:

```
mpirun -np num_processors sus -mpi input.ups
```

`num_processors` is the number of processors that will be used. The input file must contain a patch layout that has at least the same number (or greater) of patches as processors specified by a number following the -np option shown above.

In addition, the `-mpi` is optional but often times necessary if the mpi environment is not automatically detected from within the sus executable.

Uintah provides for restarting from checkpoint as well. For information on this, see Section 2.6, which describes how to create checkpoint data, and how to restart from it.

2.3 Uintah Problem Specification (UPS)

The Uintah framework uses XML like input files to specify the various parameters required by simulation components. These Uintah Problem Specification (.ups) files are validated based on the specification found in `src/StandAlone/inputs/UPS_SPEC/ups_spec.xml` (and its sibling files).

The application developer is free to use any of the specified tags to specify the data needed by the simulation. The essential tags that are required by Uintah include the following:

```
<Uintah_specification>

<SimulationComponent>

<Time>

<DataArchiver>

<Grid>
```

Individual components have additional tags that specify properties, algorithms, materials, etc. that are unique to that individual components. Within the individual

sections on MPM, ICE, MPMICE, Arches, and MPMArches, the individual tags will be explained more fully.

The sus executable verifies that the input file adheres to a consistent specification and that all necessary tags are specified. However, it is up to the individual creating or modifying the input file to put in physically reasonable set of consistent parameters.

2.4 Simulation Components

The input file tag for SimulationComponent has the `type` attribute that must be specified with either `mpm, mpmice, ice, arches,` or `mpmarches,` as in:

```
<SimulationComponent type = "mpm" />
```

2.5 Time Related Variables

Uintah components are time dependent codes. As such, one of the first entries in each input file describes the time-stepping parameters. An input file segment is given below that encompasses all of the possible parameters. Most are self-explanatory, and not all are required, (e.g `<max_Timestep>, <max_delt_increase>, <end_on_max_time_exactly>` and `<delt_init>` are all optional). `<timestep_multiplier>` serves as a CFL number, that is, a number, usually less than 1.0, that is used to moderate the timestep automatically calculated by the individual components.

```
<Time>
    <maxTime>            1.0         </maxTime>
    <initTime>           0.0         </initTime>
    <delt_min>           0.0         </delt_min>
    <delt_max>           1.0         </delt_max>
    <delt_init>          1.0e-9      </delt_init>
    <max_delt_increase>  2.0         </max_delt_increase>
    <timestep_multiplier>1.0         </timestep_multiplier>
    <max_Timestep>       100         </max_Timestep>
    <end_on_max_time_exactly>true    </end_on_max_time_exactly>
</Time>
```

2.6 Data Archiver

The Data Archiver section specifies the directory name where data will be stored and what variables will be saved and how often data is saved and how frequently the simulation is checkpointed.

The `<filebase>` tag is used to specify the directory name and by convention, the `.uda` suffix is attached denoting the "Uintah Data Archive".

Data can be saved based on a frequency setting that is either based on time intervals;
`<outputTimestepInterval> floating_point_time_increment </outputTimestepInterval>`
or timestep intervals;
`<outputInterval> integer_number_of_steps </outputInterval>`

Each simulation component specifies variables with label names that can be specified for data output. By convention, particle data are denoted by `p.` followed by a particular variable name such as mass, velocity, stress, etc. Whereas for node based data, the convention is to use the `g.` followed by the variable name, such as mass, stress, velocity, etc. Similarly, cell-centered and face-centered data typically end with the a trailing `CC` or `FC,` respectively. Within the DataArchiver section, variables are specified with the following format:

```
<save label = "p.mass" />
<save label = "g.mass" />
```

To see a list of variables available for saving for a given component, execute the following command from the `StandAlone` directory:

```
inputs/labelNames component
```

where `component` is, e.g., `mpm, ice,` etc.

Check-pointing information can be created that provides a mechanism for restarting a simulation at a later point in time. The `<checkpoint>` tag with the `cycle` and `interval` attributes describe how many copies of checkpoint data is stored (cycle) and how often it is generated (interval).

As an example of checkpoint data that has two timesteps worth of checkpoint data that is created every .01 seconds of simulation time are shown below:

```
<checkpoint cycle = "2" interval = "0.01"/>
```

To restart from a checkpointed archive, simply put "`-restart`" in the sus command-line arguments and specify the .uda directory instead of a ups file (sus reads the copied `input.xml` from the archive). One can optionally specify a certain timestep to restart from with `-t timestep` with multiple checkpoints, but the last checkpointed timestep is the default. When restarting, sus copies all of the appropriate information from the old uda directory to its new uda directory.

Here are some examples:

```
./sus -mpm -restart disks.uda.000 -nocopy
./sus -mpm -restart disks.uda.000 -t 29
```

2.7 Simulation Options

There are many options available when running MPM simulations. These are generally specified in the `<MPM>` section of the input file. A list of these options taken from `inputs/UPS_SPEC/mpm_spec.xml` is given in section 7.4.

2.8 Geometry objects

Within several of the components, the material is described by a combination of physical parameters and the geometry. Geometry objects use the notion of constructive solid geometry operations to compose the layout of the material from simple shapes such as boxes, spheres, cylinders and cones, as well as operators which include the union, intersections, differences of the simple shapes. In addition to the simple shapes, triangulated surfaces can be used in conjunction with the simple shapes and the operations on these shapes.

Each geometry object has the following properties, label (string name), type (box, cylinder, sphere, etc), resolution (vector quantity), and any unique geometry parameters such as origin, corners, triangulated data file, etc. The operators which include, the union, the difference, and intersection tags contain either lists of additional operators or the primitives pieces.

As an example of a non-trivial geometry object is shown below:

```
<geom_object>
     <intersection>
       <box label = "Domain">
          <min>[0.0,0.0,0.0]</min>
          <max>[0.1,0.1,0.1]</max>
       </box>
       <union>
         <sphere label = "First node">
            <origin>[0.022,0.028,0.1  ]</origin>
            <radius>0.01</radius>
         </sphere>
         <sphere label = "2nd node">
            <origin>[0.030,0.075,0.1  ]</origin>
            <radius>0.01</radius>
         </sphere>
       </union>
     </intersection>
     <res>[2,2,2]</res>
     <velocity>[0.,0.,0.]</velocity>
     <temperature>0 </temperature>
</geom_object>
```

The following geometry objects are given with their required tags:

`box` has the following tags: min and max which are vector quantities specified in the `[a, b, c]` format.

`sphere` has an origin tag specified as a vector and the radius tag specified as a float.

`cone` has a tag for the top and bottom origins (vector) as well as tags for the top and bottom radius (float) to create a right circular cone/frustum.

`cylinder` has a tag for the top and bottom origins (vector) plus a tag for the radius (float).

`parallelepiped` requires that four points be specified as illustrated by the ASCII art snippet taken from the source code:

```
//*****************************************
//                                        //
//             *-------------*            //
//            / .           / \           //
//           /   .         /   \          //
//          P4-------------*    \         //
//           \    .         \    \        //
//            \   P2.........\....*        //
//             \ .            \  /         //
//             P1--------------P3          //
//
//  Returns true if the point is inside (or on) the parallelepiped.
//  (The order of p2, p3, and p4 doesn't really matter.)
```

`tri` is a tag for describing a triangulated surface. The name tag specifies the file name to use for reading in the triangulated surface description and the points file. The triangulated surface (file_name.tri) contains a list of integers describing the connectivity of points specified in file_name.pts. Here is an excerpt from a tri file and a points file:

```
Triangulated file

1 39 41
1 41 38
38 41 42
. . .

Points file

0 0.03863 -0.005
0.35227 0.13023 -0.005
0.00403479 0.0296797 -0.005
. . .
```

The Mach 2 Wedge example in Section 8.4 depicts usage of this option.

The boolean operators on the geometry pieces include `difference, intersection,` and `union.`

The `difference` takes two geometry pieces and subtracts the second geometry piece from the first geometry piece. The `intersection` operator requires at least two geometry pieces in forming an intersection geometry piece. Whereas the `union` operator aggregates a collection of geometry pieces. Multiple operators can be used to form very complex geometry pieces.

An additional input in the `<geom_object>` field is the `<res>` tag. In MPM, this simply refers to how many particles are placed in each cell in each coordinate direction. For multi-material ICE simulations, the `<res>` serves a similar purpose in that one can

specify the subgrid resolution of the initial material distribution of mixed cells at the interface of geometry objects.

In addition to the above, it is also possible in MPM simulations to describe geometry by providing a file containing a series of particle locations. These can be in either ASCII or binary format. In addition, it is also possible to provide initial data for certain variables on the particles, including volume, temperature, external force, fiber direction (used in material models with transverse isotropy) and velocity. The following is an example in which external force and fiber direction are specified:

```
<file>
    <name>LVcoarse.pts</name>
    <var>p.externalforce</var>
    <var>p.fiberdir</var>
</file>
```

where the text file LVcoarse.pts looks like:

```
0.0385 0.0335 0.0015 0 0 0 0.248865 -0.0593421 -0.966718
0.0395 0.0335 0.0015 0 0 0 0.254892 -0.0220365 -0.966718
0.0405 0.0335 0.0015 0 0 0 0.267002 0.0197728 -0.963493
0.0415 0.0335 0.0015 0 0 0 0.261177 0.0588869 -0.963493
       .
       .
       .
```

Because these files can be arbitrarily large, an additional preprocessing step must be taken before issuing the `sus` command. `pfs` for "Particle File Splitter" is a utility that splits the data in the `.pts` file into a series of files (`file.pts.0, file.pts.1,` , etc), one for each patch. By doing this, each processor needs only read in the data for the patches that it contains, rather than each processor reading in the entire file, which can be hard on the file system. Note, that this step is required, even if only using a single patch, and must be reissued any time the patch configuration is changed. Usage of this utility, which is compiled into the `StandAlone/tools/pfs` directory, is:

```
pfs input.ups
```

One final option is available for initializing particle positions in MPM simulations, and that is through the use of three dimensional image data, such as might be collected via CT scans or confocal microscopy. The image data are provided as 8-bit raw files, and usage in the input file is given as:

```
<image>
  <name>spheres.raw</name>
  <res>[1600, 1600, 1600]</res>
  <threshold>[1, 25]</threshold>
</image>
<file>
```

```
        <name>spheres.pts</name>
        <format>bin</format>
      </file>
```

The <image> section gives the name of the file, the resolution, in pixels, in the various coordinate directions, and threshold range. Particles will be generated at voxels within the specified range. The <file> section is the same as that described above. A different preprocessing utility is provided when using image data (for the same reasons described previously). Usage is as follows:

```
pfs2 -b input.ups
```

The -b indicates that binary spheres.pts.# files will be created, which saves considerable disk space when performing large simulations.

2.9 Boundary conditions

Boundary conditions are specified within the <Grid> but are described separately for clarity. The essential idea is that boundary conditions are specified on the domain of the grid. Values can be assigned either on the entire face, or parts of the face. Combinations of various geometric descriptions are used to aid in the assignment of values over specific regions of the grid. Each of the six faces of the grid is denoted by either the minus or plus side of the domain.

The XML description of a particular boundary condition includes which side of the domain, the material id, what type of boundary condition (Dirichlet or Neumann) and which variable and the value assigned. The following is a an MPM specification of a Dirichlet boundary condition assigned to the velocity component on the x minus face (the entire side) with a vector value of [0.0,0.0,0.0] applied to all of the materials.

```
<Grid>
      <BoundaryConditions>
        <Face side = "x-">
            <BCType id = "all" var = "Dirichlet" label = "Velocity">
                  <value> [0.0,0.0,0.0] </value>
            </BCType>
        </Face>
        <Face side = "x+">
           <BCType id = "all" var = "Dirichlet" label = "Velocity">
                <value> [0.0,0.0,0.0] </value>
           </BCType>
        </Face>
       . . . .
       <BoundaryCondition>
  . . . .
 <Grid>
```

The notation `<Face side = "x-">` indicates that the entire x minus face of the boundary will have the boundary condition applied. The `id = "all"` means that all the materials will have this value. To specify the boundary condition for a particular material, specify an integer number instead of the "all". The `var = "Dirichlet"` is used to specify whether it is a Dirichlet or Neumann or symmetry boundary conditions. Different components may use the `var` to include a variety of different boundary conditions and are explained more fully in the following component sections. The `label = "Velocity"` specifies which variable is being assigned and again is component dependent. The `<value> [0.0,0.0,0.0] </value>` specifies the value.

An example of a more complicated boundary condition demonstrating a hot jet of fluid issued into the domain is described. The jet is described by a circle on one side of the domain with boundary conditions that are different in the circular jet compared to the rest of the side.

```
<Face circle = "y-" origin = "0.0 0.0 0.0" radius = ".5">
       <BCType id = "0"   label = "Pressure" var = "Neumann">
                             <value> 0.0   </value>
       </BCType>
       <BCType id = "0" label = "Velocity" var = "Dirichlet">
                             <value> [0.,1.,0.] </value>
       </BCType>
       <BCType id = "0" label = "Temperature" var = "Dirichlet">
                             <value> 1000.0  </value>
       </BCType>
       <BCType id = "0" label = "Density" var = "Dirichlet">
                             <value> .35379  </value>
       </BCType>
       <BCType id = "0" label = "SpecificVol"  var = "computeFromDensity">
                             <value> 0.0  </value>
       </BCType>
     </Face>
     <Face side = "y-">
       <BCType id = "0"   label = "Pressure"     var = "Neumann">
                             <value> 0.0   </value>
       </BCType>
       <BCType id = "0" label = "Velocity"     var = "Dirichlet">
                             <value> [0.,0.,0.] </value>
       </BCType>
       <BCType id = "0" label = "Temperature"  var = "Neumann">
                             <value> 0.0  </value>
       </BCType>
       <BCType id = "0" label = "Density"      var = "Neumann">
                             <value> 0.0  </value>
       </BCType>
       <BCType id = "0" label = "SpecificVol"  var = "computeFromDensity">
                             <value> 0.0  </value>
       </BCType>
```

```
    </Face>
```

The jet is described by the circle on the y minus face with the origin at 0,0,0 and a radius of .5. For the region outside of the circle, the boundary conditions are different. Each side must have at least the `"side"` specified, but additional circles and rectangles can be specified on a given face.

An example of the `rectangle` is specified as with the lower corner at 0,0.181,0 and upper corner at 0,0.5,0.

```
<Face rectangle = "x-" lower = "0.0 0.181 0.0" upper = "0.0 0.5 0.0">
```

2.10 Grid specification

The `<Grid>` section specifies the domain of the structured grid and includes tags which indicate the lower and upper corners, the number of extra cells which can be used by various components for the application of boundary conditions or interpolation schemes.

The grid is decomposed into a number of patches. For single processor problems, usually one patch is used for the entire domain. For multiple processor simulations, there must be at least one patch per processor. Patches are specified along the x,y,z directions of the grid using the `<patches> [2,5,3] </patches>` which specifies two patches along the x direction, five patches along the y direction and 3 patches along the z direction. The maximum number of processors that `sus` could use is $2 * 5 * 3 = 30$. Attempting to use more processors than patches will cause a run time error during initialization.

Finally, the grid spacing can specified using either a fixed number of cells along each x,y,z direction or by the size of the grid cell in each direction. To specify a fixed number of grid cells, use the `<resolution> [20,20,3] </resolution>` . This specifies 20 grid cells in the x direction, 20 in the y direction and 3 in the z direction. To specify the grid cell size use the `<spacing> [0.5,0.5,0.3] </spacing>` . This specifies the a grid cell size of .5 in the x and y directions and .3 in the z direction. The `<resolution>` and `<spacing>` cannot be specified together. The following two examples would generate identical grids:

```
<Level>
    <Box label="1">
       <lower>        [0,0,0]          </lower>
       <upper>        [5,5,5]          </upper>
       <extraCells>   [1,1,1]          </extraCells>
       <patches>      [1,1,1]          </patches>
    </Box>
    <spacing>         [0.5,0.5,0.5]    </spacing>
</Level>
```

```
<Level>
    <Box label="1">
       <lower>        [0,0,0]          </lower>
       <upper>        [5,5,5]          </upper>
       <resolution>   [10,10,10]       </resolution>
       <extraCells>   [1,1,1]          </extraCells>
       <patches>      [1,1,1]          </patches>
    </Box>
</Level>
```

The above examples indicate that the grid domain has a lower corner at 0,0,0 and an upper corner at 5,5,5 with one extra cell in each direction. The domain is broken down into one patch covering the entire domain with a grid spacing of .5,.5,.5. Along each dimension there are ten cells in the interior of the grid and one layer of "extraCells" outside of the domain. extraCells are the Uintah nomenclature for what are frequently referred to as "ghost-cells".

2.11 Regridder

The regridder creates a multilevel grid from the refinement flags. Each level will completely cover the refinement flags from the coarser level. The primary regridder used in Uintah is the `Tiled` regridder. The tiled regridder creates a set of evenly sized tiles across the domain that will become patches if refinement is required in the tiles region.

The following is an example of this regridder.

```
<Regridder type="Tiled">
    <max_levels>2</max_levels>
    <cell_refinement_ratio> [[2,2,1]] </cell_refinement_ratio>
    <cell_stability_dilation> [2,2,0] </cell_stability_dilation>
    <min_boundary_cells> [1,1,0] </min_boundary_cells>
    <min_patch_size>  [[8,8,1]] </min_patch_size>
    <dynamic_size> true </dynamic_size>
    <patches_per_level_per_proc>8</patches_per_level_per_proc>
</Regridder>
```

The `max_levels` tag specifies the maximum number of levels to be created. The `cell_refinement_ratio` tag specifies the refinement ratio between the levels. This can be specified on a per level basis as follows:

```
    <cell_refinement_ratio> [[2,2,1],[4,4,1]] </cell_refinement_ratio>
```

The `cell_stability_dilation` tag specifies how many cells around the refinement flags are also guaranteed to be refined. The `min_boundary_cells` tag specifies the size of the boundary layers. The size of the tiles is specified using the `min_patch_size` tag and can also be specified on a per level basis.

Finally the size of the tiles can change at run time. If the number of patches is higher than what is needed then the tile size will double in the smallest dimension. Conversely if the target number of patches is low then the tile size will halve in the longest dimension but will never go below the `min_patch_size` . The target number of patches per processor is specified using the `patches_per_level_per_proc` tag. To prevent the resizing of tiles set the tag `dynamic_size` to false.

2.12 Load Balancer

The load balancer assigns patches to processors such that work is evenly distributed. Uintah currently supports a wide array of load balancing algorithms. To specify a load balancing algorithm add a block similar to the following:

```
<LoadBalancer type="DLB">
     <dynamicAlgorithm>patchFactor</dynamicAlgorithm>
     <timestepInterval>50</timestepInterval>
     <gainThreshold>0.05</gainThreshold>
</LoadBalancer>
```

The type specifies which load balancer is used. The type can be `DLB, RoundRobin, SimpleLoadBalancer,` or `SingleProcessorLoadBalancer.` If no load balancer is specified than either the SimpleLoadBalancer or the SingleProcessorLoadBalancer will be used. For complex problems including AMR the DLB load balancer should be used. This load balancer uses advanced algorithms to achieve more efficient patch assignments. To use the DLB load balancer you must include the `dynamicAlgorithm` tag. This tag can be `PatchFactor` or `Zoltan.`

```
<dynamicAlgorithm>patchFactor</dynamicAlgorithm>
```

Both of these algorithms compute the weight of a patch using either a profiling model or an algorithm cost model. By default the profiling model is used as it provides highly accurate estimates and does not require the specification of model parameters. To disable profiling add the tag

```
<doCostProfiling>false</doCostProfiling>
```

This will cause the load balancer to use the cost model $W_p = N_p c_1 + N_c c_2 + c_3$ to determine the weight of a patch, where N_p is the number of particles in the patch, N_c is the number of cells on the patch, c_1 is the weight per particle, c_2 is the weight per cell, and c_3 is a constant cost on the patch. These constants can be specified with the following tags:

```
<cellCost>1</cellCost>
<particleCost>1.25</particleCost>
<patchCost>4</patchCost>
```

The number of particles will always be zero unless the algorithm is instructed to collect particles with the collectParticles tag.

```
<collectParticles>true</collectParticles>
```

The following are a couple of extra load balancer parameters that may be useful.

```
<timestepInterval>50</timestepInterval>
<gainThreshold>0.05</gainThreshold>
<outputNthProc>8</outputNthProc>
```

The `timestepInterval` tag specifies the maximum number of timesteps the simulation can run without attempting to load balance. The `gainThreshold` tag specifies the percent improvement that a load balance must provide over the old load balance in order for the new load balance to be used. Finally the `outputNthProc` tag causes the data archive to be written to by every Nth processor instead of every processor. This can alleviate problems caused by having to many processors attempting to write to the same file system at the same time.

If the dynamic algorithm is set to `Zoltan` then the user must also specify which Zoltan algorithm to use with the `zoltanAlgorithm` tag.

```
<zoltanAlgorithm>HSFC</zoltanAlgorithm>
```

The Zoltan algorithm can be set to `HSFC, RIB, RCB.`

2.13 UDA

The UDA is a file/directory structure used to save Uintah simulation data. For the most part, the user need not concern himself with the UDA layout, but it is a good idea to have a general feeling for how the data is stored on disk.

Every time a simulation (sus) is run, a new UDA is created. Sus uses the <filebase> tag in the simulation input file to name the UDA directory (appending a version number). If an UDA of that name already exists, the next version number is used. Additionally, a symbolic link named "disks.uda" (is updated to and) will point to the newest version of this simulations UDA. Eg:

```
disks.uda.000
disks.uda.001
disks.uda.001 <- disks.uda
```

Each UDA consists of a number of top level files, a checkpoints subdirectory, and subdirectories for each saved timestep. These files include:

- `.dat` files contain global information about the simulation (each line in the .dat files contains: simulation_time value).

- `checkpoints` directory contains a limited number of time step data subdirectories that contain a complete snapshot of the simulation (allowing for the simulation to be restarted from that time).
- `input.xml` contains the original problem specification (the .ups file).
- `index.xml` contains information on the actual simulation run.
- `t0000#` contains data saved for that specific time step. The data saved is specified in .ups file and may be a very limited subset of the full simulation data.

See Section 2.6 for a description of how to specify what data are saved and how frequently.

Chapter 3

Visualization tools – VisIt

Visualization of Uintah data is currently possible using any of two software packages. These are SCIRun and VisIt. Of these, SCIRun is no longer supported, although legacy versions will continue to work. The VisIt package from LLNL is general purpose visualization software that offers all of the usual capabilities for rendering scientific data. It is still developed and maintained by LLNL staff, and its interface to Uintah data is supported by the Uintah team.

3.1 Reading Uintah Data Archives

Once you have installed VisIt and the UDA reader plugin, you can launch VisIt and start visualizing UDA's. To open a UDA, select `Open File` from the `File` menu. Browse into the UDA you want to load and select the `index.xml` file. Then hit on `OK` and a list of timesteps should now appear on the gui. Figure 3.1 illustrates this process.

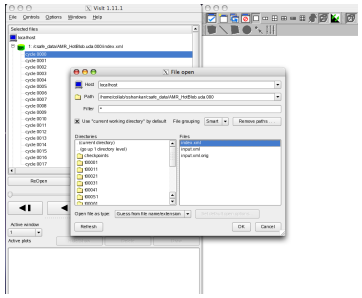

Figure 3.1: Opening an UDA with VisIt

3.2 Plots

VisIt displays data as plots. A plot might render a specific variable or it might render the structure of the mesh. Figure 3.2 illustrates this.

Note that VisIt attempts to analyze the variables and associate them with the appropriate plots. As shown in Fig-

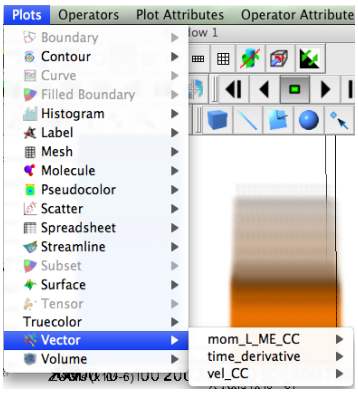

Figure 3.2: Various plots in VisIt

ure 3.2, only vector variables are available for the vector plot. The most commonly used plots for visualizing UDA's are Pseudocolor, Volume and the Vector plot. The Subset plot can be used to visualize the structure of patches in an AMR dataset.

Once you have a plot, you change plot attributes by clicking on the PlotAtts menu and selecting the plot of you choice. Alternatively, you may double click on the plot itself in Active plots window. For example, if you have a Volume plot and you want to change its attributes, the window shown in Figure 3.3 pops up.

As seen in Figure 3.3, you can change the color map, opacity curve, rendering method, no. of samples, lighting options, etc. in this window.

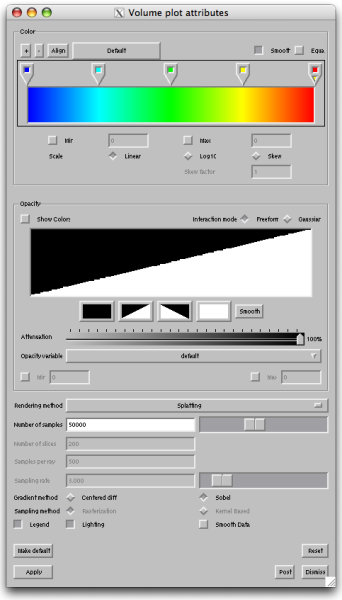

Figure 3.3: Volume plot attributes in VisIt

3.3 Operators

A wide variety of operators can be applied to the plots, as mentioned earlier. These modify the incoming datasets in some way (eg., a slice formats a 3D dataset into a 2D slice), which can then be plotted. However, you will first need to select a plot and then only you can apply an operator to it (though the order of operation is opposite). An important thing to keep in mind is that when you select an operator, by default it gets applied to all the plots in the Active plots window. You will need to uncheck the Apply operators checkbox, in case you just want to apply the operator to a single plot as shown in Figure 3.4.

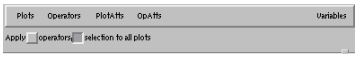

Figure 3.4: Unchecking "selection to all plots"

The entire list of operators that VisIt supports can be seen by clicking on the Operators menu. Also, once you have applied an operator, you can change its attributes by clicking on the OpAtts menu and then clicking on the desired operator. Figures 3.5a and 3.5b illustrate how you can apply a Slice operator to a Pseudocolor plot and then change the operator attributes. First, apply the Pseudocolor plot to a desired variable, and then select the Slice operator from the Operators menu.

At this point in time, you should have an ordering similar to that in Figure 3.6a. Once you have this order, select Slice from the OpAtts menu. This will pop up the Slice operator attributes window, as shown in Figure 3.6b.

You can now play up with the various attributes (eg., selecting normal plane) to obtain the desired visualization. The checkbox "Project to 2D" should be unchecked

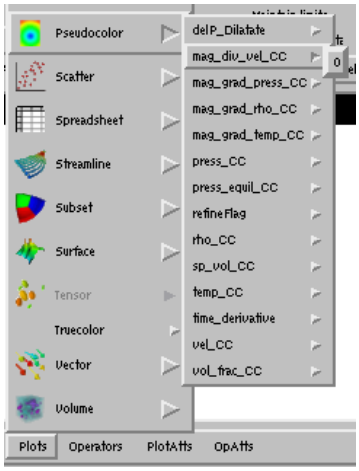

(a) Applying the Pseudocolor plot to a variable

(b) Applying an operator to a plot

Figure 3.5:

(a) Ordering of an operator and a plot

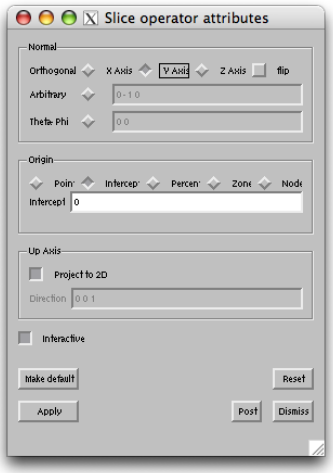

(b) Slice plot attributes in VisIt

Figure 3.6:

is you want to have the slice in 3D space.

3.4 Vectors

By default, VisIt reduces the number of vectors plotted (to 400) and this needs to be manually changed to the original number or something greater, only if required. This can be accomplished by changing the attributes of the Vector plot. In Figure 3.7, the number of vectors has been increased to 2000.

Also if you would like all the vectors to be visible, you would need to switch off both the options, `Scale by magnitude` and `Auto scale` under the Scale tab in the same window as shown in figure 3.8 describes this.

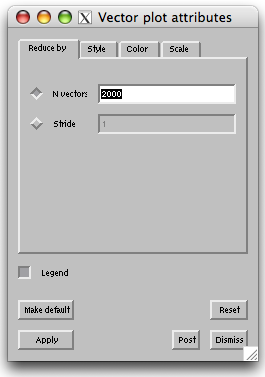

Figure 3.7: Increasing the number of Vectors

3.5 AMR datasets

AMR datasets are read the same way as single level datasets. Once you have it read, you can apply an plot/ operator on it. Since the dataset is organized as levels and patches, you now have the flexibility of visualizing each of them independently or as in a group. To achieve this (assuming that you have already selected a plot), click on the Subset button either on the Active Plots window in the gui or on the same option in the Controls menu. This is illustrated in Figures 3.9a and 3.9b.

Figure 3.8: Increasing the scale of Vectors

3.6 Examples

3.6.1 Volume visualization

1. Read in the uda by selecting the index.xml file. A list of timesteps should now appear on the gui.

(a) Clicking on this icon pops up the Subset window

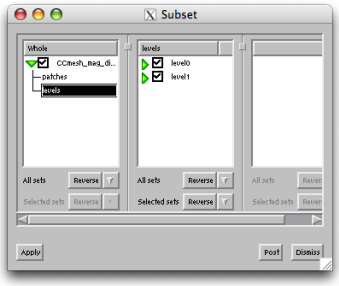

(b) The Subset window in VisIt

Figure 3.9:

2. The first timestep (cycle 0000) should be preselected. In case you are interested in plotting a different timestep, just double click on it. Alternatively you can type it in the small rectangular box (Figure 3.10a), just below the list of timesteps. This can also be done at a later period in time, when you are done plotting the variable associated with a specific timestep and want to traverse through the others.

3. Next we select a variable to plotted. We click on the Plots menu, select the Volume plot and then select the variable tempIN as shown in the Figure 3.10b. The number '1' refers to the material associated with the variable.

4. The variable tempIN/1 now appears on the Active plots window (Figure 3.10c). Select the variable and click Draw.

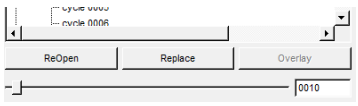

(a) The window on the gui lists all the timesteps

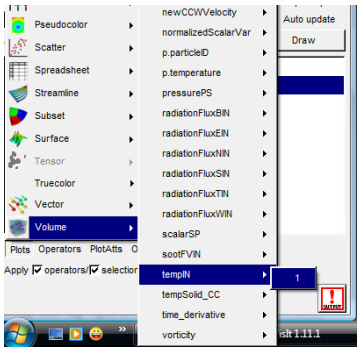

(b) Selecting a volume plot and an associated variable/ material

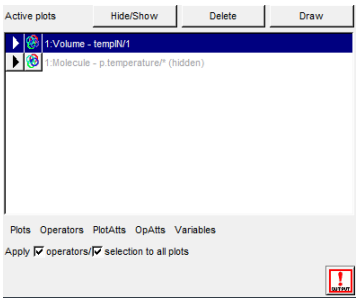

(c) The list of plots in the Active plots window

Figure 3.10:

5. A visualization now appears on the Viewer window, as shown in Figure 3.11a. You can interact with the visualization in terms of rotating it (holding the left mouse button and dragging it), zooming in/ out (scrolling the roller on the mouse and/ or selecting the magnifier at the top of the Viewer window) etc.

6. Once you have this basic volume visualization, you can change its attributes by double clicking on the Volume - tempIN/1 plot in the Active plots window. This pops up the Volume plot attributes window (Figure 3.11b and figure 3.11c).

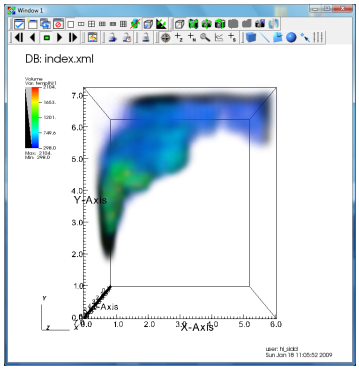

(a) Visualization of a volume on the viewer window

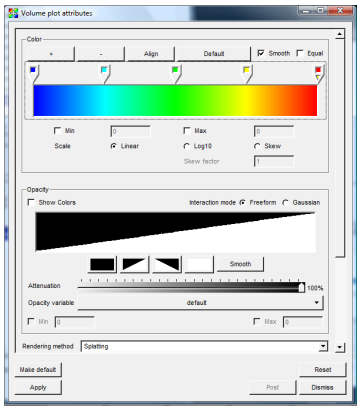

(b) Volume visualization attributes window

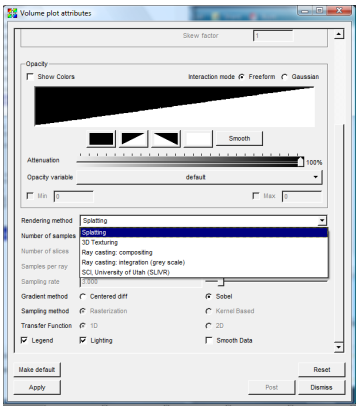

(c) Volume visualization attributes window

Figure 3.11:

The tab Color specifies the color table and the various options associated with it. The user can add/ remove control points by clicking on the + and - buttons. These can then be equally spaced by pressing the Align button.

A different color table can be selected by clicking on the Default button and then selecting an appropriate color table. The color(s) associated with the control points can be changed by right-clicking on the them and then selecting an appropriate color.

The user also has the option of specifying a Min and Max on the scalar value range by checking on the associated box(s) and entering in the values.

The second tab Opacity lets you specify a transfer function for the color table. Clicking on the check box Show Colors copies the colors from the color table onto this graph. Selecting the Interaction Mode as Gaussian lets you draw curves and specify a more accurate color table (Figure 3.12).

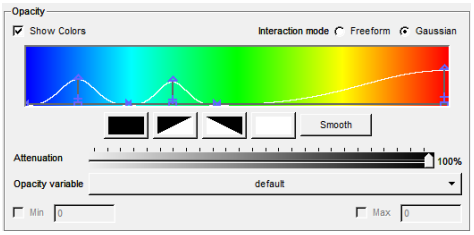

Figure 3.12: The opacity transfer function in the attributes window

You can add in as many curves on the graph by clicking on the left mouse button and then placing them accordingly. To delete an unwanted curve, just right click on it.

After specifying an opacity transfer function, one can select an appropriate rendering method, Splatting being the default. The related fields thereafter become active/ inactive as and when different rendering methods are selected.

3.6.2 Particle visualization

1. To add particles, we select the Molecule plot and then click on the variable p.temperature as shown in the Figure 3.13a. The asterisk '*' refers to all the materials associated with the variable.

2. The variable p.temperature/* now appears on the Active plots list. Select the variable and hit Draw. A container in the form of particles now appears on the Viewer window.

3. Now double click on the variable name in Active plots list. This brings up the Molecule plot attributes window as shown in Figure 3.13b.

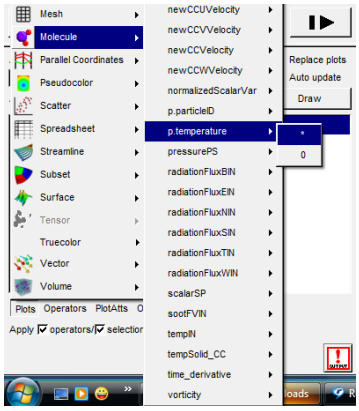

(a) Selecting a molecule plot and an associated variable/ material

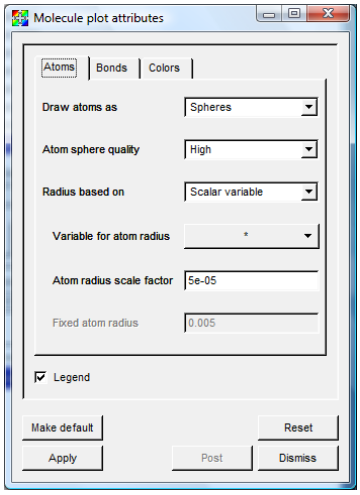

(b) Selecting a molecule plot and an associated variable/ material

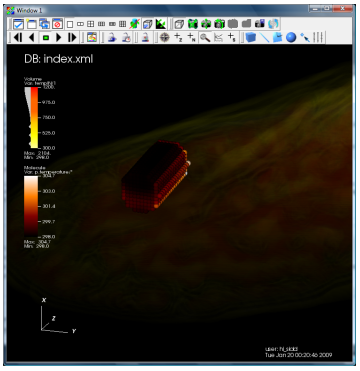

(c) Selecting a molecule plot and an associated variable/ material

Figure 3.13:

We choose to visualize the particles as Sphere Impostors (doesn't runs the GPU out of memory, drawing as Spheres does). We also choose to scale the sphere radius by a Scalar Variable and specify that variable to be p.temperature/* itself (therefore the * appears). Since the temperature values are too high, we scale them all by a factor of 5.e-05 (on the basis of trial and error). Finally in Colors tab, we set the Color map for scalars as orangehot. Combined with volume visualization, we get a visualization as shown in Figure 3.13c.

3.6.3 Visualizing patch boundaries

In order to visualize patch boundaries, we use the Subset plot. As with other variables, we select the Subset plot and an associated variable. The variables have a prefix 'level/

patch'. There is a level/ patch variable associated with every kind of variable (Cell Centered, Node Centered, Face Centered) present in the dataset. In the Figure 3.14a, we select one such variable. Next, we hit Draw. This produces a visualization as shown in Figure 3.14b.

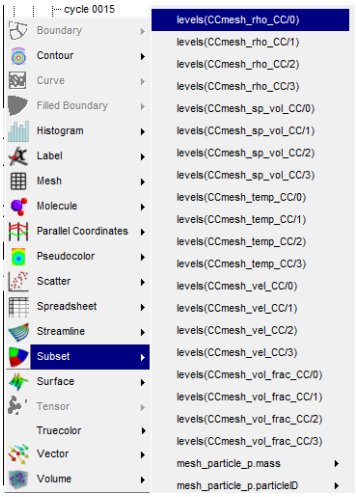

(a) A patch/ level variable, associated with every kind of variable

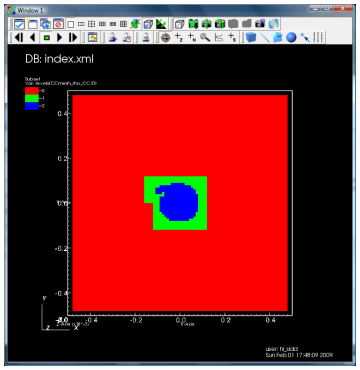

(b) The default visualization of patches

Figure 3.14:

To generate a wire-frame model, we double click on the Subset plot in the Active plots window. This pops up the Subset plot attributes window, where we check the Wireframe mode as shown in Figure‘3.15a. This would produce a visualization, similar to one shown in Figure 3.15b.

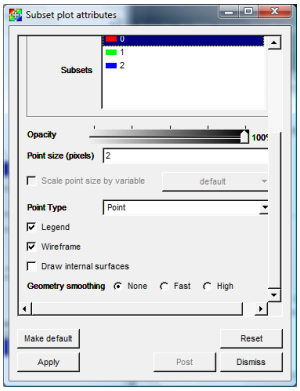

(a) Enabling the 'Wireframe' mode for visualizing patch boundaries

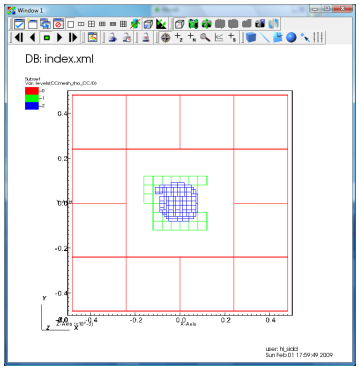

(b) The patch boundaries after enabling the wireframe mode

Figure 3.15:

3.6.4 Iso-surfaces

The easiest way to draw iso-surfaces is to use the 'Contour' Plot. As with other plots demonstrated above, the contour plot is selected on a regular 3D scalar variable. Figure 3.16 illustrates this.

Once the plot is selected, we hit 'Draw'. This would produce a visualization, similar to one shown in Figure 3.17a. You can then modify the plot attributes by double clicking on the plot in the 'Active plots' window. This would pop up the 'Contour plot attributes window', as shown in Figure 3.17b.

The 'Select by' option can be changed to 'Value(s)' and 'Percent(s)'. When specifying multiple values, they should be separated by a space.

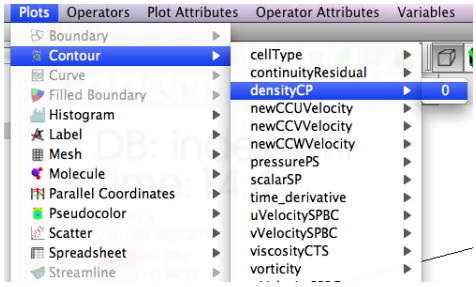

Figure 3.16: Selecting the 'Contour' plot on a regular 3D scalar variable

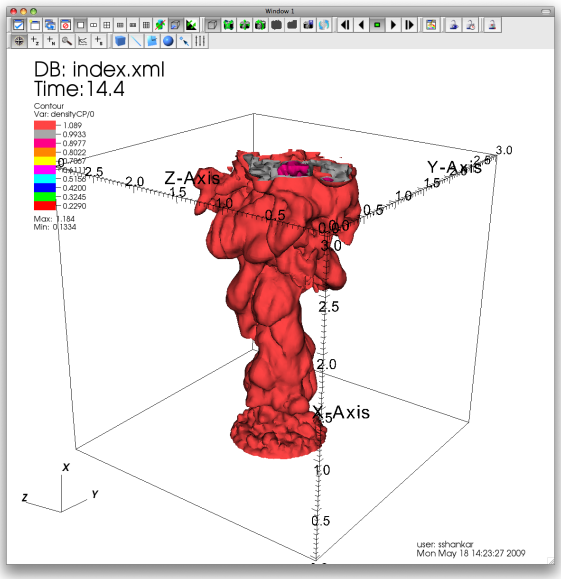

(a) Iso-surface visualization

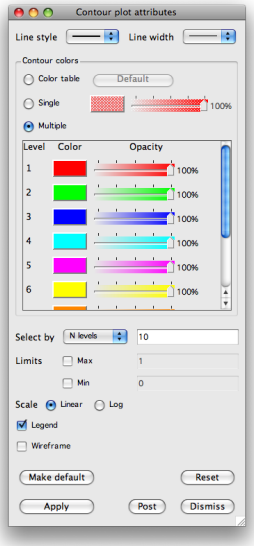

(b) The attributes window for the 'Contour' plot

Figure 3.17:

3.6.5 Streamlines

The 'Streamlines' plot has issues with the current version of VisIt (1.11.2 and older). However, these have been corrected in the trunk and should be out in version 2.0. The

controls remain the same in all these version and the example below was implemented on the trunk version.

As shown in Figure 3.18 we select the 'Streamlines' plot on a vector variable. We then double click on the plot itself, which pops up the 'Streamlines attributes window'.

We set the 'Distance' parameter such that it covers the entire computational domain. We set the 'Streamline direction' as forward. In the 'Source' tab, Figure 3.19a, we define the 'Source type' as 'Line'. We can select other options too, notably 'Single Point', 'Sphere' etc. We now define the line 'Start' and 'End' coordinates. In this specific case, we define them as [-0.1 -0.05 0] and [-0.1 0.05 0] respectively. This choice ensures that we cover the entire y axis and start at the leftmost corner of the computational domain.

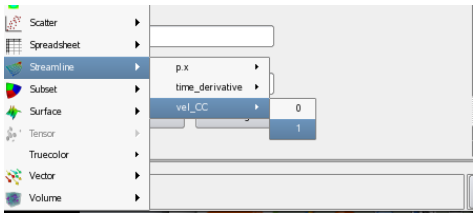

Figure 3.18: Selecting the 'Streamlines' plot on a vector variable

To ensure that our stream lines are smooth, we change the 'Maximum step length' in the in the 'Advanced' tab. In this case, we change it to 1.e-05. The thing to keep in mind is that this length should be order of magnitude smaller than the length of the computational domain. This is shown in Figure 3.19b.

Once these parameters are set, we hit 'Apply' and then click on the 'Draw' button on the gui. This produces a visualization similar to one shown in Figure 3.19c.

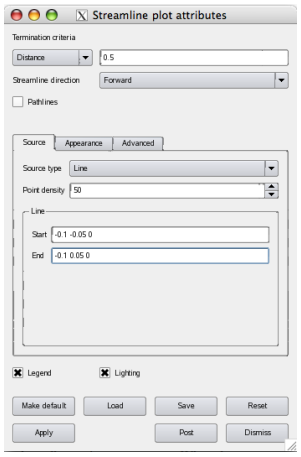

(a) Setting the 'Source' tab parameters

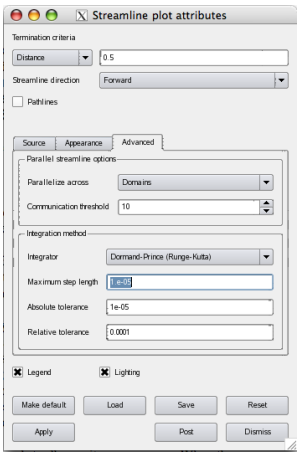

(b) Setting the 'Advanced' tab parameters

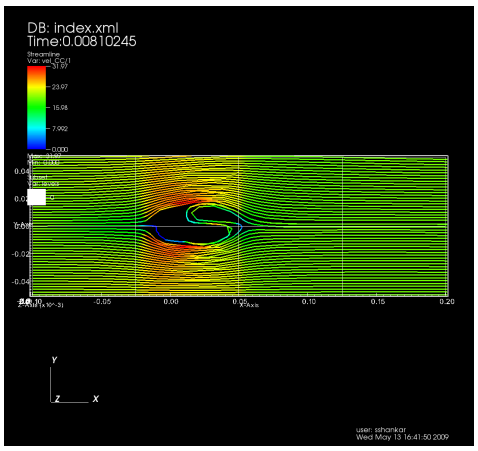

(c) Streamlines visualization

Figure 3.19:

3.6.6 Visualizing extra cells

For visualizing extra cells we use the 'Inverse Ghost Zone' operator 3.20a in conjunction with the 'Pseudocolor' plot. Since the plugin reads in extra cells as ghost cells, the usage of this operator make sense in this scenario.

After the operator is applied to the 'Pseudocolor' plot, we double click on the operator to change its attributes. We switch to 'Both ghost zones and real zones' in this window 3.20b and hit 'Apply'.

We then hit 'Draw'. When combined with the 'Mesh' plot we get a visualization similar to the one shown in Figure 3.20c. The pick operations on the viewer can then be used to investigate the value(s) in these extra cells.

(a) Selecting the Inverse Ghost Zone operator

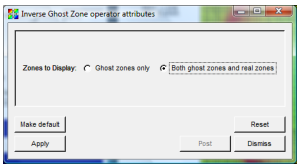

(b) The attributes window for the 'Inverse Ghost Zone' operator

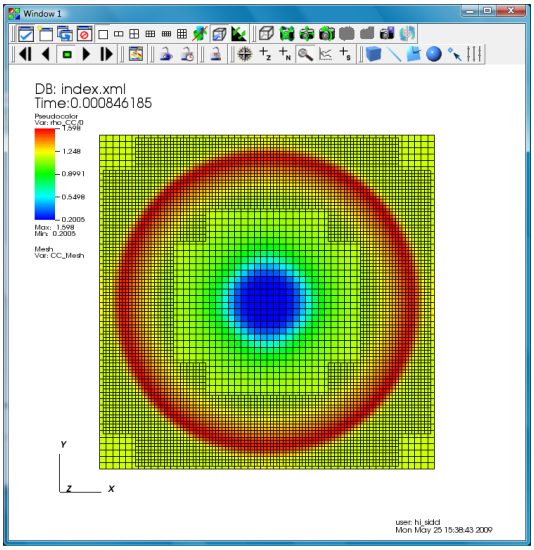

(c) Extra cells together with the 'Mesh' plot

Figure 3.20:

3.6.7 Picking on particles

The 'Node pick mode' on the visualization window can be used to pick particles and investigate particles attributes. After plotting particles using the 'Molecule' plot, the user can then select the 'Node pick mode' 3.21 and select particles (by clicking on them) of interest.

Once a particle is picked, the 'Pick' window pops up with the particle attributes. By default only the variable plotted is queried, if the user wants to query more variables per pick - they can be added by selecting additional variables from the 'Variables' menu and as shown in the Figure 3.22.

Figure 3.21: The 'Node pick mode' on the visualization window

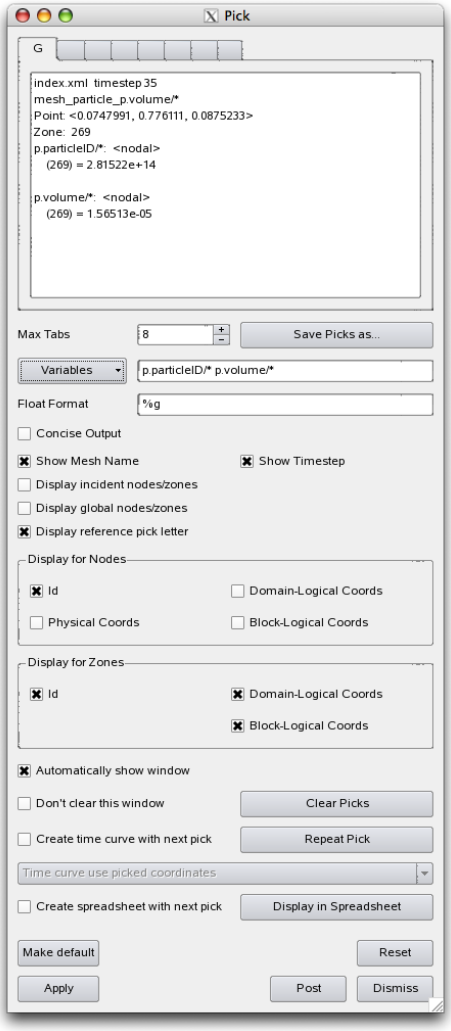

Figure 3.22: The 'Pick' window

Chapter 4

Data Extraction Tools

Uintah offers a number of tools for accessing data stored in Uintah Data Archives ("UDAs"). Because the format of Uintah data is specific to the framework, these tools allow a user to quickly extract data, which can then either be postprocessed within that tool (simple modification of the source code may be necessary), postprocessed with external software such as Matlab or Octave, or simply plotted with, e.g. gnuplot. These tools are not compiled automatically when "make sus" is issued. To compile them cd to "opt/StandAlone/tools" and issue "make". These tools are described below.

4.1 puda

The command line extraction utility `puda` (for "parse Uintah data archive") has a number of uses. For example, it may be used to extract a subset of particle data from a UDA. Once the extraction tools have been compiled, the puda executable will be located in `opt/StandAlone/tools/puda/`. If the executable is run with no additional command line arguments, the following usage information will be displayed:

```
Usage: puda [options] <archive file>

Valid options are:
  -h[elp]
  -timesteps
  -gridstats
  -listvariables
  -varsummary
  -jim1
  -jim2
  -partvar <variable name>
  -asci
  -tecplot <variable name>
  -no_extra_cells     (Excludes extra cells when iterating over cells.
                       Default is to include extra cells.)
  -cell_stresses
```

```
  -rtdata <output directory>
  -PTvar
  -ptonly             (prints out only the point location
  -patch              (outputs patch id with data)
  -material           (outputs material number with data)
  -NCvar <double | float | point | vector>
  -CCvar <double | float | point | vector>
  -verbose            (prints status of output)
  -timesteplow <int>  (only outputs timestep from int)
  -timestephigh <int> (only outputs timesteps up to int)
  -matl,mat <int>         (only outputs data for matl)
*NOTE* to use -PTvar or -NVvar -rtdata must be used
*NOTE* ptonly, patch, material, timesteplow, timestephigh are used in conjunction with -PTvar.
```

As an example of how to use `puda,` suppose that one wanted to know the locations of all particles at the last archived timestep for the `const_test_hypo.uda` First one may wish to know how many timesteps have been archived. This could be accomplished by:

```
puda -timesteps const_test_hypo.uda
```

The resulting terminal output would be:

```
Parsing const_test_hypo.uda/index.xml
There are 11 timesteps:
1: 1.8257001926347728e-05
548: 1.0012914931998474e-02
1094: 2.0005930425875382e-02
1640: 3.0015616802173569e-02
2184: 4.0005272397960444e-02
2728: 5.0011587657447343e-02
3271: 6.0016178181543284e-02
3812: 7.0000536667661845e-02
4353: 8.0001537138146825e-02
4893: 9.0000702723306208e-02
5433: 1.0001655973087024e-01
```

These represent all of the timesteps for which data has been archived. Suppose now that we wish to know what the stress state is for all particles (in this case two) at the final archived timestep. For this one could issue:

```
puda -partvar p.stress -timesteplow 10 -timestephigh 10 const_test_hypo.uda
```

The resulting output is:

```
Parsing const_test_hypo.uda/index.xml
1.00016560e-01 1 0 281474976710656 -2.72031498e-10 -1.05064208e-26 -2.53781271e-08 -1.05064208e-
1.00016560e-01 1 1 0 1.93256890e-13 6.56787331e-18 1.85514400e-14 6.56787331e-18 2.24310469e-13
```

The first column is the simulation time, the third column is the material number, the fourth column is the particle ID, and the remaining nine columns represent the components of the Cauchy stress tensor (σ_{11},σ_{12},σ_{13}, ..., σ_{32},σ_{33}). If desired, the terminal output can be redirected to a text file for further use.

4.2 partextract

The command-line utility `partextract` may be used to extract data from an individual particle. To do this you first need to know the ID number of the particle you are interested in. This may be done by using the puda utility, or the visualization tools. Once the extraction tools have been compiled, the partextract utility executable will be located in `/opt/StandAlone/tools/extractors/` . If the executable is run without any arguments the following usage guide will be displayed in the terminal:

```
No archive file specified
Usage: partextract [options] <archive file>

Valid options are:
  -mat <material id>
  -partvar <variable name>
  -partid <particleid>
  -part_stress [avg or equiv or all]
  -part_strain [avg/true/equiv/all/lagrangian/eulerian]
  -timesteplow [int] (only outputs timestep from int)
  -timestephigh [int] (only outputs timesteps upto int)
```

As an example of how to use the partextract utility, suppose we wanted to find the velocity at every archived timestep for the particle with ID 281474976710656 (found above using puda) in the "const_test_hypo.uda" file (src/StandAlone/inputs/MPM). The appropriate command to issue is:

```
partextract -partvar p.velocity -partid 281474976710656 const\_test\_hypo.uda
```

The output to the terminal is:

```
Parsing const_test_hypo.uda/index.xml
1.82570019e-05 1 0 281474976710656 0.00000000e+00 0.00000000e+00 -1.00000000e-02
1.00129149e-02 1 0 281474976710656 -1.03554318e-19 -1.03554318e-19 -1.00000000e-02
2.00059304e-02 1 0 281474976710656 -1.99388121e-19 -1.99388121e-19 -1.00000000e-02
        .
        .
        .
```

It is noted that if the stress tensor is output using the partextract utility, the output format is different than for the puda utility. The partextract utility only outputs the six independent components instead of all nine. For example, if we use partextract to get the stress tensor for the same particle as above at the last archived timestep only, the output is:

```
partextract -partvar p.stress -partid 281474976710656 -timesteplow 10 -timestephigh 10 const_tes
Parsing const_test_hypo.uda/index.xml
1.00016560e-01 1 0 281474976710656 -2.72031498e-10 -1.05064208e-26 -2.53781271e-08 -1.05064208e-
```

Compare this output with the output from puda above. Notice that the ordering of the six independent components of the stress tensor for partextract are σ_{11},σ_{22}, σ_{33}, σ_{23}, σ_{13} , σ_{12}.

4.3 lineextract

Lineextract is used to extract an array of data from a region of a computational domain. Data can be extracted from a point, along a line, or from a three dimensional region and then stored as a variable for ease of post processing.

Usage:

```
./lineextract [options] -uda <archive file>

Valid options are:
 -h,         --help
 -v,         --variable:      <variable name>
 -m,         --material:      <material number> [defaults to 0]
 -tlow,      --timesteplow:   [int] (sets start output timestep to int) [defaults to 0]
 -thigh,     --timestephigh:  [int] (sets end output timestep to int) [defaults to last timestep]
 -timestep, --timestep:       [int] (only outputs from timestep int) [defaults to 0]
 -istart,    --indexs:        <x> <y> <z> (cell index) [defaults to 0,0,0]
 -iend,      --indexe:        <x> <y> <z> (cell index) [defaults to 0,0,0]
 -l,         --level:         [int] (level index to query range from) [defaults to 0]
 -o,         --out:           <outputfilename> [defaults to stdout]
 -vv,        --verbose:       (prints status of output)
 -q,         --quiet:         (only print data values)
 -cellCoords:                 (prints the cell centered coordinates on that level)
 --cellIndexFile:              <filename> (file that contains a list of cell indices)
                                   [int 100, 43, 0]
                                   [int 101, 43, 0]
                                   [int 102, 44, 0]
```

The following example shows the usage of lineextract for extracting density data at the 60th computational cell in the x-direction, spanning the width of the domain in the y-direction (0 to 1000), at timestep, 7, (note "timestep" actually refers to the seventh data dump, not necessarily the seventh timestep in the simulation. The variable containing the density data within the uda is "rho_CC," and the output variable that will store the data for post processing is "rho."

```
./lineextract -v rho_CC  -timestep 7 -istart 60 0 0 -iend 60 1000 0 -m 1 -o rho -uda test01.uda.
```

4.4 compute_Lnorm_udas

`Compute_Lnorm_udas` computes the L_1, L_2 and L_∞ norms for each variable in two udas. This utility is useful in monitoring how the solution differs from small changes in either the solution tolerances, input parameters or algorithmic changes. You can also use it to test the domain size influence. The norms are computed using:

$$d[i] = |uda_1[i] - uda_2[i]| \tag{4.1}$$

$$L_1 = \frac{\sum_i^{\text{All Cells}} d[i]}{\text{number of cells}} \tag{4.2}$$

$$L_2 = \sqrt{\frac{\sum_i^{\text{All Cells}} d[i]^2}{\text{number of cells}}} \tag{4.3}$$

$$L_\infty = \max(d[i]) \tag{4.4}$$

These norms are computed for each `CC, NC, SFCX, SFCY, SFCZ` variable, on each level for each timestep. The output is displayed on the screen and is placed in a directory named 'Lnorm.' The directory structure is:

```
Lnorm/
  -- L-0
   |-- delP_Dilatate_0
   |-- mom_L_ME_CC_0
   |-- press_CC_0
   |-- press_equil_CC_0
   |-- variable
   |-- variable
   |--etc
```

and in each variable file is the physical time, L_1, L_2 and L_∞. These data can be plotted using `gnuplot` or another plotting program.

The command usage is

```
compute_Lnorm_udas <uda1> <uda2>
```

The utility allows for `udas` that have different computational domains and different patch distributions to be compared. The uda with the smallest computational domain should always be specified first. In order for the norms to be computed the physical times must satisfy

$$|\text{physical Time}_{uda_1} - \text{physical Time}_{uda_2}| < 1e^{-5}.$$

Chapter 5

Arches

5.1 Introduction

The ARCHES component was initially designed for predicting the potential hazard of an explosive device immersed in or near a pool fire of transportation fuel. Since then, this component has been extended to solve many industrially relevant problems such as industrial flares, oxy-coal combustion processes, and fuel gasification.

Given the wide range of length and time scales that are present in these examples, ARCHES utilizes models for bridging the molecular (micro) scales to the full, large (macro) scales. More to come....

The ARCHES component solves the conservative, finite volume, low-mach formulation of the Navier-Stokes equation with a pressure projection that includes the effect of variable density, reaction, and many modes of heat transfer including radiation.

5.2 Governing Equations

The essential governing equations for the Arches component, written in finite volume form, include the mass balance, momentum balance, mixture fraction balance, and energy balance equations. Using a bold-face symbol to represent a vector quantity, the equations are:

1. The mass balance,
$$\int_V \frac{\partial \rho}{\partial t} dV + \oint_S \rho \mathbf{u} \cdot d\mathbf{S} = 0 \ , \tag{5.1}$$
where ρ is density and $\mathbf{u}$ is the velocity vector.

2. The momentum balance,
$$\int_V \frac{\partial \rho \mathbf{u}}{\partial t} dV + \oint_S \rho \mathbf{u}\mathbf{u} \cdot d\mathbf{S} = \oint_S \tau \cdot d\mathbf{S} - \int_V \nabla p dV + \int_V \rho \mathbf{g} dV \ , \tag{5.2}$$

where τ is the deviatoric stress tensor defined as $\tau_{ij} = 2\mu S_{ij} - \frac{2}{3}\mu\frac{\partial u_k}{\partial x_k}\delta_{ij}$, the second isotropic term in τ_{ij} is absorbed into the pressure projection for the current low-Mach scheme, and $S_{ij} = \frac{1}{2}\left(\frac{\partial u_i}{\partial x_j} + \frac{\partial u_j}{\partial x_i}\right)$. Also in Equation 5.2, $\mathbf{g}$ is the gravitational body force and p is pressure.

3. The mixture fraction balance,

$$\int_V \frac{\partial \rho f}{\partial t} dV + \oint_S \rho \mathbf{u} f \cdot d\mathbf{S} = \oint_S D\nabla f \cdot d\mathbf{S} \,, \tag{5.3}$$

where f is the mixture fraction and a Fick's law form of the diffusion term assuming equal diffusivities results in a single diffusion coefficient, D.

4. The thermal energy balance,

$$\int_V \frac{\partial \rho h}{\partial t} dV + \oint_S \rho \mathbf{u} h \cdot d\mathbf{S} = \oint_S k\nabla h \cdot d\mathbf{S} - \oint_S q \cdot d\mathbf{S} \,, \tag{5.4}$$

where h is the sum of the chemical plus sensible enthalpy, q is the radiative flux, a Fourier's law form of the conduction term is used with a diffusion coefficient, k, and the pressure term is neglected.

These equations are solved in an LES context, meaning filters are applied to the equations. Here, we use Favre filtering, defined as

$$\overline{\phi} = \frac{\overline{\rho\phi}}{\overline{\rho}},$$

to isolate the density in the filtered equations. The filtering operations result in the classic turbulence closure problem and thus models are required.

Consider a control volume, V, with surface area S. Because the equations will be solved on a computational grid, one can safely assume that the the control volume has N faces, where unique faces are identified with their index, k. The discussion is further simplified by only considering cubic volumes with length h. Given the cubic control volume, a surface-filtered field for a variable ϕ is defined as $\overline{\phi}^{(j)}(\mathbf{x})$, where the variable is filtered on a plane in the x_j orthogonal direction. Then, for any surface, k, the field is sampled at the face centered location. For example, if $j = 1$, the surface-filtered quantity is

$$\overline{\phi}^{2d,(1)}(\mathbf{x}) = \frac{1}{h^2}\int_{x_2-h/2}^{x_2+h/2}\int_{x_3-h/2}^{x_3+h/2} \phi(\mathbf{x}')dx_2'dx_3' \,. \tag{5.5}$$

The volume average follows as

$$\overline{\phi}^{3d}(\mathbf{x}) = \frac{1}{h^3}\int_{x_1-h/2}^{x_1+h/2}\int_{x_2-h/2}^{x_2+h/2}\int_{x_3-h/2}^{x_3+h/2} \phi(\mathbf{x}')dx_1'dx_2'dx_3' \,. \tag{5.6}$$

The bars over the variable, ϕ, are labeled with '2d' and '3d' superscripts to distinguish between the two filters. Pope [7] identifies the proceeding definitions as using the "anisotropic box" filter kernel where the resultant variables are simply averages over the intervals $x_j - \frac{1}{2}h < x'_j < x_j + \frac{1}{2}h$.

For convenience in isolating density in the filtered equations, a Favre-filtered quantity is defined for an arbitrary variable, φ, as

$$\widetilde{\varphi}^{2d} \equiv \frac{\overline{\rho\varphi}^{2d}}{\overline{\rho}^{2d}} \ , \tag{5.7}$$

and

$$\widetilde{\varphi}^{3d} \equiv \frac{\overline{\rho\varphi}^{3d}}{\overline{\rho}^{3d}} \ . \tag{5.8}$$

Because the 2d and 3d filters are explicitly defined, this convention is slightly different than what is normally observed in the literature. Most literature, however, derives the filtered equations from the finite difference equations rather than the finite volume equations. Thus, using $\overline{\rho}^{2d}$ and $\overline{\rho}^{3d}$ in Equations 5.7 and 5.8 to stress surface and volume filtered densities are appropriate for the present discussion.

The previous definitions are applied to the integral forms of the governing equations to obtain the Favre-filtered LES equations. Nevertheless, there are terms in the Favre-filtered equations that cannot be solved. These include the surface filtered convection of momentum, $\widetilde{u_i u_j}^{2d}$, the surface filtered convection of mixture fraction, $\widetilde{u_j f}^{2d}$, and the surface filtered convection of enthalpy, $\widetilde{u_j h}^{2d}$.

For the filtered velocity product, $\overline{\rho}^{2d}\ \widetilde{u_i u_j}^{2d}$, a subgrid stress tensor is defined as,

$$\tau_{ij}^{sgs} = \widetilde{u_i u_j}^{2d} - \widetilde{u}_i^{2d}\widetilde{u}_j^{2d} \ . \tag{5.9}$$

Similarly, subgrid diffusion terms are defined for mixture fraction and enthalpy,

$$\mathcal{J}^f = \widetilde{u_j f}^{2d} - \widetilde{u}_j^{2d}\widetilde{f}^{2d} \ , \tag{5.10}$$

$$\mathcal{J}^h = \widetilde{u_j h}^{2d} - \widetilde{u}_j^{2d}\widetilde{h}^{2d} \ . \tag{5.11}$$

$$\tag{5.12}$$

Using these definitions, the final form of the Favre-filtered equations is

1. The filtered mass balance,

$$\frac{d}{dt}\left(\widetilde{\rho}^{3d}\right) + \frac{S_k}{V} n_{kj}\left(\overline{\rho}^{2d}\ \widetilde{u}_j^{2d}\right) = 0 \ . \tag{5.13}$$

2. The filtered momentum balance,

$$\frac{d}{dt}\left(\overline{\rho}^{3d}\ \widetilde{u}_i^{3d}\right) = \frac{S_k}{V} n_{kj}\left(-\overline{\rho}^{2d}\ \widetilde{u}_i^{2d}\widetilde{u}_j^{2d} + \overline{\tau}_{ij}^{2d} + \tau_{ij}^{sgs} - \overline{p}^{2d}\delta_{ij}\right) + \overline{\rho}^{3d}\ g_i \ . \tag{5.14}$$

3. The filtered mixture fraction balance,

$$\frac{d}{dt}\left(\overline{\rho}^{3d}\ \widetilde{f}^{3d}\right) = \frac{S_k}{V} n_{kj}\left(-\overline{\rho}^{2d}\ \widetilde{u}_j^{2d}\widetilde{f}^{2d} + D\nabla\overline{f}^{2d} + \mathcal{J}^f\right)\ . \tag{5.15}$$

4. The filtered thermal energy balance,

$$\frac{d}{dt}\left(\overline{\rho}^{3d}\ \widetilde{h}^{3d}\right) = \frac{S_k}{V} n_{kj}\left(-\overline{\rho}^{2d}\ \widetilde{u_j}^{2d}\widetilde{h}^{2d} + k\nabla\overline{h}^{2d} - \overline{q}^{2d} + \mathcal{J}^h\right)\ . \tag{5.16}$$

The subgrid momentum stress, τ_{ij}^{sgs}, the subgrid mixture fraction dissipation, $\mathcal{J}^f$, and the subgrid heat dissipation, $\mathcal{J}^h$, contain the unresolved or subgrid action of the turbulence on the transported quantities. Since these terms arise from definitions, models are introduced to include the subgrid effects that they represent. These models are discussed next.

5.2.1 Subgrid Turbulence Models

The construction of both $\mathcal{J}^f$ and $\mathcal{J}^h$ is relatively straight forward. Invoking an "eddy-viscosity" modeling concept, the subgrid transport due to turbulent advection is treated as an enhanced diffusion term for the unclosed terms listed above. That is, the subgrid mixture fraction dissipation and subgrid enthalpy dissipation are respectively written as,

$$\mathcal{J}^f = D_t \frac{\partial\overline{f}^{2d}}{\partial x_j}\ , \tag{5.17}$$

and

$$\mathcal{J}^h = k_t \frac{\partial\overline{h}^{2d}}{\partial x_j}\ . \tag{5.18}$$

To model D_t and k_t, constant turbulent Schmidt (Sc_t),

$$Sc_t = \frac{1}{\rho}\frac{\mu_t}{D_t}\ , \tag{5.19}$$

and Prandlt (Pr_t),

$$Pr_t = \frac{1}{\rho}\frac{\mu_t}{k_t}\ , \tag{5.20}$$

numbers are assumed with where μ_t is a turbulent viscosity. Following Pitsch and Steiner [6], the values of the turbulent Schmidt and Prandlt number are taken as $Sc_t = Pr_t = 0.4$, which is consistent with a unity Lewis number assumption.

For the subgrid scale stress tensor, τ_{ij}^{sgs}, two common LES turbulence closure models are the constant coefficient Smagorinsky model [8] and the dynamic coefficient

Smagorinsky model [4]. As with the scalar subgrid modeling terms, the eddy viscosity model is again invoked for τ_{ij}^{sgs}. Defining the deviatoric subgrid stress tensor as,

$$\tau_{ij}^{d,sgs} = \tau_{ij}^{sgs} - \frac{1}{3}\tau_{kk}^{sgs}\delta_{ij}, \tag{5.21}$$

the subgrid stress is taken as,

$$\tau_{ij}^{d,sgs} \approx -2\nu_t \overline{S}_{ij} = -2(C_s\Delta)^2|\overline{S}|\overline{S}_{ij} \ , \tag{5.22}$$

where Δ is the filter width, ν_t is the eddy viscosity and $|\overline{S}| \equiv (2\overline{S}_{ij}\overline{S}_{ij})^{1/2}$. For the Smagorinsky model, $C_s \approx 2$ depending on the filter type, numerical method, and flow configuration [7].

For the dynamic Smagorinsky model, C_s is computed by taking a least squares approach to determining the length scale [3],

$$(C_s\Delta)^2 = \frac{\langle \mathcal{L}_{ij} M_{ij} \rangle}{\langle M_{ij} M_{ij} \rangle} \ , \tag{5.23}$$

where

$$\mathcal{L}_{ij} = 2(C_s\Delta)^2 \widehat{|\overline{S}|\overline{S}}_{ij} - 2(C_s\widehat{\Delta})^2 \widehat{|\overline{S}|}\widehat{\overline{S}}_{ij} \ , \tag{5.24}$$

and

$$M_{ij} \equiv 2\left(\widehat{|\overline{S}|\overline{S}}_{ij} - \alpha^2 \widehat{|\overline{S}|}\widehat{\overline{S}}_{ij} \right) \ . \tag{5.25}$$

The hat defines an explicit test filter and the angled brackets in Equation 5.33 conceptually represent an averaging over a homogeneous region of space that, experience has shown, is necessary for stability. Experience has also shown that averaging over the test filter width is adequate and the filter width ratio, $\alpha = \widehat{\Delta}/\Delta$, is usually taken to be 2.

5.2.2 Subgrid Momentum Dissipation

Addressing the momentum closure involves finding a suitable model for the subgrid scale stress tensor, τ_{ij}^{sgs}. Two common LES turbulence closure models are examined: the constant coefficient Smagorinsky model and the dynamic coefficient Smagorinsky model. In LES modeling, field variables are decomposed into a spatially filtered field and a residual component, $u = \overline{u} + u'$. This decomposition is known as a Leonard decomposition. While seemingly similar to a Reynolds decomposition used in Reynolds Averaged Navier-Stokes (RANS) models, the Leonard decomposition has the property that the filtered residual component is generally not equal to zero, $\overline{u'} \neq 0$. As a result, the subgrid stress term contains several terms,

$$\begin{aligned} \tau_{ij}^{sgs} &= \overline{(\overline{u}_i + u_i')(\overline{u}_i + u_i')} - \overline{u}_i\overline{u}_j \ , \\ &= \underbrace{\overline{\overline{u}_i\overline{u}_j} - \overline{u}_i\overline{u}_j}_{L_{ij}} + \underbrace{\overline{\overline{u}_i u_j'} + \overline{u_i'\overline{u}_j}}_{C_{ij}} + \underbrace{\overline{u_i' + u_j'}}_{R_{ij}} \ , \end{aligned} \tag{5.26}$$

referred to as the Leonard stress, the cross stresses, and the Reynolds stress respectively.

It is useful to consider the physical interpretation of the various components of the stress. The Leonard term is responsible for filtering and projecting the nonlinear interactions of the resolved components back to the finite LES space. This is a correction to the resolved advective term in accordance with the stated explicit filter used to derive the LES equations. It does not account for aliasing errors. The first cross term represents advection of the resolved field by turbulent fluctuations. The second cross term represents the advection of subgrid scales by the resolved field. The Reynolds stress is familiar from RANS and represents the advection of subgrid scales by turbulent fluctuations.

As with the scalar subgrid modeling terms, the eddy viscosity model is again invoked for τ_{ij}^{sgs}. The most common eddy viscosity model in LES is the Smagorinsky model [8]. Defining the deviatoric subgrid stress tensor as,

$$\tau_{ij}^{d,sgs} = \tau_{ij}^{sgs} - \frac{1}{3}\tau_{kk}^{sgs}\delta_{ij}, \tag{5.27}$$

the subgrid stress is approximated by,

$$\tau_{ij}^{d,sgs} \approx -2\nu_t \overline{S}_{ij} = -2(C_s\Delta)^2|\overline{S}|\overline{S}_{ij} \ , \tag{5.28}$$

where, Δ is the filter width, ν_t is the eddy viscosity, $|\overline{S}| \equiv (2\overline{S}_{ij}\overline{S}_{ij})^{1/2}$, and typically $C_s \approx 2$ depending on the filter type, numerical method, and flow configuration [7]. This model is basically identical to Prandtl's mixing length model with $l = C_s\Delta$.

The dynamic procedure [1, 4] eliminates the need to specify the model constant, C_s, a priori, with the basic assumption that the constant is the same for two different filter scales. The smaller scale is historically referred to as the "grid scale" (though the filter width need not equal the grid spacing, $\Delta \geq h$)), and the larger scale is referred to as the "test scale". Implicit in this assumption is the requirement that both scales lie within the inertial subrange.

Defining the deviatoric residual stress tensor as,

$$T_{ij}^{d} = T_{ij} - \frac{1}{3}T_{kk}\delta_{ij} \ , \tag{5.29}$$

the residual stress at the test scale is given by,

$$T_{ij}^{d} \equiv \overline{\widehat{u_i u_j}} - \overline{\widehat{u}}_i\overline{\widehat{u}}_j \approx -2(C_s\widehat{\Delta})^2|\overline{\widehat{S}}|\overline{\widehat{S}}_{ij} \ . \tag{5.30}$$

where $\widehat{\Delta}$ is the test filter width and the hat defines an explicit test filter. By test filtering Equation 5.9 and combining this with 5.30, one can construct the Leonard term, $\mathcal{L}_{ij}$. This is also known as the "Germano identity",

$$\mathcal{L}_{ij} = T_{ij} - \widehat{\tau^{sgs}}_{ij} = \overline{\widehat{u_i u_j}} - \overline{\widehat{u}}_i\overline{\widehat{u}}_j \ . \tag{5.31}$$

Notice that the Leonard term is directly computable from resolved LES quantities. By restating the Smagorinsky model in terms of the Germano identity, one ends up with an over-determined system of equations for the unknown, C_s,

$$\mathcal{L}_{ij} = 2(C_s\Delta)^2\widehat{|\overline{S}|\overline{S}}_{ij} - 2(C_s\widehat{\Delta})^2\widehat{|\overline{S}|}\widehat{\overline{S}}_{ij} \ . \tag{5.32}$$

Although we have pulled C_s out of the test filtering operation of the subgrid stress, this approximation yields acceptable results. In practice, one takes a least squares approach to determining the length scale [3],

$$(C_s\Delta)^2 = \frac{\langle \mathcal{L}_{ij}M_{ij}\rangle}{\langle M_{ij}M_{ij}\rangle} \ , \tag{5.33}$$

where

$$M_{ij} \equiv 2\left(\widehat{|\overline{S}|\overline{S}}_{ij} - \alpha^2\widehat{|\overline{S}|}\widehat{\overline{S}}_{ij}\right) \ . \tag{5.34}$$

The only model parameter, then, is the filter width ratio, $\alpha = \widehat{\Delta}/\Delta$, usually taken to be 2.

The angled brackets in Equation 5.33 conceptually represent averaging over a homogeneous region of space which, experience has shown, is necessary for stability. We have found that averaging over the test filter width is adequate. With these implementation practices, the dynamic model is generally robust. The implementation can be made more efficient by computing the constant roughly every 10 time steps (based on the advective CFL), and only for the first Runge-Kutta step.

5.2.3 LES Algorithm

The set of filtered equations (Equations 5.13-5.16) are discretized in space and time and solved on a staggered, finite volume mesh. The staggering scheme consists of four offset grids. One grid stores the scalar quantities and the remaining three grids store each component of the velocity vector. The velocity components are situated so that the center of their control volume is located on the face centers of the scalar grid in their respective direction. Figure 5.1 shows an example of a two-dimensional grid and the staggering arrangement.

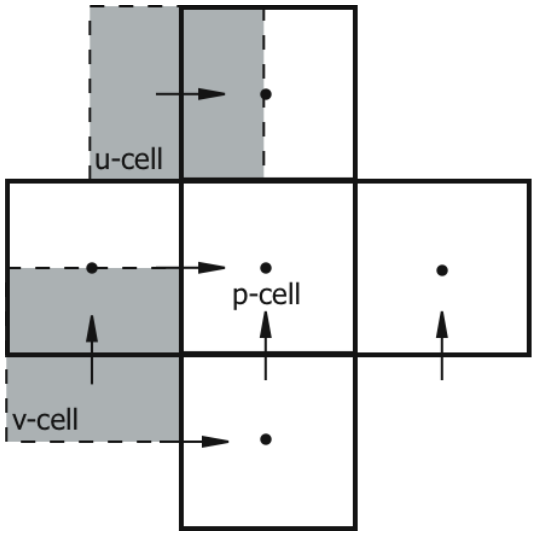

Figure 5.1: Staggered grid arrangement in two dimensions with u and v velocity cell centers located on the face centers of the scalar cells.

The staggering arrangement is advantageous for computing low-Mach LES reacting flows. First, since a pressure projection algorithm is used, the velocities

are exactly projected without interpolation error because the location of the pressure gradient coincides directly with the location of the velocity storage location. Second, Morinishi et al. [5] showed that kinetic energy is exactly conserved when using a central differencing scheme on the convection and diffusion terms without a subgrid model and in combination with a staggered grid. Having a spatial scheme that conserves kinetic energy is advantageous because it limits artificial dissipation that arises from the differencing scheme. These conservation properties make the staggered grid a prime choice for LES reacting flow simulation.

For the spatial discretization of the LES scalar equations, flux limiting and upwind schemes for the convection operator are used. These schemes are advantageous for ensuring that scalar values remain bounded. For the momentum equation, a central differencing scheme for the convection operator is used. All diffusion terms are computed with a second order approximation of the gradient.

When computing the 2d surface filtered field on the faces of the control volume, one is forced to use an interpolation from the 3d volume filtered field. This approximation is tolerated because computing the 2d surface field is simply not possible with the given grid scheme.

An explicit time stepping scheme is chosen. A general, multistep explicit update for a variable, ϕ, may be written as,

$$\begin{aligned} \phi^0 &= \phi^n \ , \\ \phi^{(i)} = V \sum_{k=0}^{m-1} \left(\alpha_{i,k} \phi^{(k)} + \Delta t \beta_{i,k} L(\phi^{(k)}) \right) \ , &\quad i = 1, ..., m \\ \phi^{(m)} &= \phi^{n+1} \ , \end{aligned} \tag{5.35}$$

where n is the time level, m is the substep between n and $n+1$, α and β are integration coefficients, and L is a linearization operator on the the convective flux and source terms. Letting $m = 1$ and $\alpha = \beta = 1$ the forward-Euler time integration scheme is determined,

$$(\phi)^{n+1} = (\phi)^n + \Delta t (L(\phi)^n) \ . \tag{5.36}$$

A higher order, multistep method is derived by letting $m > 1$ and choosing appropriate constants for α and β. For this study, two step and three step, strong stability preserving (SSP) coefficients were chosen from Gottlieb et al. [2].

Using the coefficients given by Gottlieb et al., the SSP-RK 2 stepping scheme is

$$\begin{aligned} (\phi)^{(1)} &= (\phi)^n + \Delta t (L(\phi)^n) \\ (\phi)^{n+1} &= \frac{1}{2}(\phi)^n + \frac{1}{2}(\phi)^1 + \frac{1}{2}\Delta t (L(\phi)^{(1)}) \ . \end{aligned} \tag{5.37}$$

SSP-RK 3 time stepping scheme is,

$$
\begin{aligned}
(\phi)^{(1)} &= (\phi)^n + \Delta t(L(\phi)^n) \\
(\phi)^{(2)} &= \frac{3}{4}(\phi)^n + \frac{1}{4}(\phi)^{(1)} + \frac{1}{4}\Delta t(L(\phi)^{(1)}) \\
(\phi)^{(n+1)} &= \frac{1}{3}(\phi)^n + \frac{2}{3}(\phi)^{(2)} + \frac{1}{4}\Delta t(L(\phi)^{(2)}) \ .
\end{aligned}
\tag{5.38}
$$

The time step is limited by

$$
\Delta t \leq c\Delta t_{F.E.} \tag{5.39}
$$

where $\Delta t_{F.E.}$ is the forward-Euler time step limited by the Courant-Friedrichs-Levy condition and c is a constant less than or equal to one.

A higher order, multistep method is derived by letting $m > 1$ and choosing appropriate constants for α and β. For this study, two step and three step, strong stability preserving (SSP) coefficients were chosen from Gottlieb et al. [2]. The coefficients for SSP-RK 2 and SSP-RK 3 are optimal in the sense that the scheme is stable when $c = 1$ if the forward-Euler time step is stable for hyperbolic problems. In practice, for the Navier-Stokes equations, the value of c is taken less than one.

Choosing an explicit time stepping scheme, rather than an implict one, creates a challenge for solving the set of equations. The density at the $n + 1$ timestep, which is required to determine the cardinal variables, requires an estimation. Taking the estimated density for $\overline{\rho}^{n+1}$ to be $\overline{\rho}^*$, the estimation can be as simple as $\overline{\rho}^* = \overline{\rho}^n$. Note that the 2d and 3d filter distinction is dropped for the remainder of this discussion for the sake of simplicity. A slightly more complicated procedure involves a forward-Euler step of the continuity equation to obtain $\overline{\rho}^*$. This is written as,

$$
\overline{\rho}^* = \overline{\rho}^n - \Delta t \frac{S_k}{V} n_{kj} \left(\overline{\rho}\widetilde{u_j}\right) \ . \tag{5.40}
$$

Ideally, one would like to know $\overline{\rho}^{n+1}$ rather than an estimate. While more details will be discussed in Section **??**, one recognizes that ρ is a function of the same variables that are being updated in time, namely, the mixture fraction, f, and enthalpy, h. This quandary is a result of the explicit time stepping method will not be resolved for variable density flows without using a fully implicit method. Explicit methods, however, do have advantages, especially for large scale parallel computations. Specifically, explicit methods are easier to load balance because the amount of work required for each processor is readily determined a priori, which makes for an efficient parallel computation. Explicit methods are also easier to code into a computer and to debug. For these reasons, the current algorithm discussion is limited to explicit methods only.

The explicit algorithm for solving the set of filtered equations is shown in Algorithm 5.1.

Listing 5.1: Explicit LES algorithm

```
for t:=t_{min} to t_{max} do
fill in later..
for $RK_{step}$:=1 to $N$
end;
end;
```

5.3 Uintah Specification

5.3.1 Basic Inputs

In order to run the the Arches component, the correct specification must be made for the simulation controller using the *SimulationComponent* tag. In this case (similar to the other Uintah components) the Arches component is specified as

```
<SimulationComponent type="arches" />
```

as a child of the *Uintah_specification* section.

Most other Arches specifications are located in the *CFD→ARCHES* section of the input file. Unless otherwise specified, the system of units for all Arches input parameters are SGI.

5.3.2 Time Integrator

Explicit Time Integrator

Arches is commonly run in a fully explicit time-stepping mode. That is, the update in time for any variable ϕ is expressed as

$$\phi^{t+\Delta t} = \frac{1}{\rho^*}\left((\rho\phi)^t + \Delta t RHS^t)\right) \ , \tag{5.41}$$

where RHS represents all forcing terms in the transport equation for ϕ at time level t. For the purposes of this discussion, we have dealt with the implicit nature of the density term by simply assuming we have a density approximation, called ρ^*, that suits the current update (for details of the ρ issue, see Section 5.2.3).

The explicit time integrator is activated (as a child node of *CFD→ARCHES*) by simply inserting the <ExplicitIntegrator> node. Within this node, the other solvers for the various transport equations will be defined along with a few parameters. The general structure will look something like this:

```
<ExplicitSolver>
          <!--Solver Options-->
          <option-1/>
```

```
            <option-2/>
            ....
            <!--Transport Equations-->
         <MomentumSolver>
         ...
         </MomentumSolver>

         <PressureSolver>
         ...
         </PressureSolver>

         <MixtureFractionSolver>
         ...
         </MixtureFractionSolver>

         <EnthalpySolver>
         ...
         </EnthalpySolver>
</ExplicitSolver>
```

The options for each transport equation will be described in Section 5.3.3.

Options for the <ExplicitSolver> section include:

1. **Initial time step**: <initial_dt>
   Input type: *Required, double*
   Default: *NA*
   Description: The explicit solver can be stepped forward in time by using a fixed time step or letting the code estimate a time step via a CFL condition (see Section 5.2.3). In either case, an initial time step must be specified.

2. **Variable time step**: <variable_dt>
   Input type: *Required, boolean*
   Default: *NA*
   Description: One may either step at a fixed time step with Δt equal to the *intial_dt* tag or let the code guess a stable time step according to a CFL condition. It is recommended that one sets the *variable_dt* to *true* as it helps maintain stability during the time integration.

3. **Time integration order**: <timeIntegratorType>
   Input type: *Required, string*
   Default: *FE*
   Description: Current options include one of the following:

   - FE, 1st order Forward-Euler
   - RK2SSP, Second Order, Strong-Stability Preserving Runge-Kutta

- RK3SSP, Third Order, Strong-Stability Preserving Runge-Kutta

See Section 5.2.3 for full details.

4. **Stability option for the density guess**: <restartOnNegativeDensityGuess>
   Input type: *Optional, boolean*
   Default: *false*
   Description: This parameter restarts a time step, regardless of the time integrator order, if the predicted density guess (see Section 5.2.3) from the continuity equation is negative and therefore unphysical. If this option is true, the time step is reduced by half and the time step is restarted with the new, smaller time step. The process with repeat until a) the density guess is physical or b) the code goes unstable. Instability usually will occur in the implicit pressure projection. If b) occurs, it is advised to set this option to *false*. By default this option is *false* and is not required. Note that in cases where this parameter is *false* and a negative density guess occurs, the density from the previous time step is used.

5. **Message control on density guess**: <NoisyDensityGuess>
   Input type: *Optional, boolean*
   Default: *true*
   Description : The negative density guess warning prints for every cell with a negative density guess. One may want to suppress the warning and can do so with this option. When used, a warning is printed for every patch rather than every cell.

6. **Turbulence model calculation frequency**: <turbModelCalcFreq>
   Input type: *Optional, integer*
   Default: *1*
   Description: This parameter allows one to control the frequency of the execution of the turbulence model. One may want to decrease the frequency for efficiency reasons.

7. **Turbulence model calculation frequency on time integrator sub-steps**: <turbModelCalcForAllRKSteps>
   Input type: *Optional, boolean*
   Default: *true*
   Description: If *false*, the turbulence closure will only be computed for the first time sub-step and then applied for all subsequent time sub-steps. By default, this parameter is *true*.

8. **Additional time step constraint**: <scalarUnderflowCheck>
   Input type: *Optional, boolean*
   Default: *false*
   Description: Guaranteeing stability for a problem with large length and time

scales is difficult. As previously mentioned, a guess at a stable time step is made using a CFL condition. The scalar underflow check option uses additional information about the local flow information to compute an additional time step guess. The minimum of this estimation and the CFL condition is used to step the equations forward in time. Here, a time step is computed from the inverse of the continuity equation by considering outward mass fluxes only. In other words, given the local velocity state, there is a limit to the amount of mass that can leave any given cell. This limit is computed from

$$\frac{\partial \rho}{\partial t} = -\nabla \cdot (\rho U)|_{+}$$

when only outward facing fluxes are considered (as indicated by the $|_{+}$ symbol). Thus one can rearrange this equation to give an estimate for Δt as,

$$\Delta t \approx \partial t = \frac{\partial \rho}{\nabla \cdot (\rho U)|_{+}}$$

This option is often helpful in helping with stability if your simulation is experiencing underflow (< 1.0) or overflow (> 1.0) errors from the mixture fraction scalar.

9. **Extra pressure projection option**: <extraProjection>
   Input type: *Optional, boolean*
   Default: *false*
   Description: This option performs a second pressure solve and projection step. In general, this option is not needed. By default the value is *false*.

Implicit Time Integrator

Currently the implicit time integrator is not supported. Please check back in subsequent releases.

5.3.3 Transport Equation Options

In the current configuration of Arches, transport equations are activated by specifying the option for each equation in a equation-specific node under the *ExplicitSolver* node. Currently, all equation nodes are required except for the enthalpy solver node.

Momentum Solver

The moment solver refers to solution of $\rho\mathbf{U}$, where $\mathbf{U}$ is the vector quantity of velocity. As mentioned above, the components are solved in a staggered, finite volume configuration. By default, the required <MomentumSolver> node must be present in the <ExplicitSolver> node.

The options for the moment solver include:

1. **The order of the convection scheme**: <convection_scheme>
   Input type: *Required, string*
   Default: *NA*
   Description: The two options that currently are implemented for the convection term in the moment equation are first-order upwind (set as *upwind*) and second-order central difference (set as *central*). Both types of discretization can be found in any common CFD text. It is recommended that one use the *central* option as it has desirable energy conservation properties (see Moronishi [add reference]).

2. **Filter the divergence of ρU**: <filter_divergence_constraint>
   Input type: *Optional, boolean*
   Default: *false*
   Description: This options turns on the filtering of the divergence constraint used in the pressure solver. When false, the divergence is unfiltered.

Pressure Solver

Arches is solved in an incompressible manner, in the sense that there is a degree of pressure-velocity decoupling which is resolved through an implicit pressure projection. This results in the classic Poisson equation for pressure than requires solution. By default, the required <PressureSolver> node must be present in the <ExplicitSolver> node.

The options for the pressure solver include:

1. **Perform only the last projection**: <do_only_last_projection>
   Input type: *Optional, boolean*
   Default: *false*
   Description: For multi-step time schemes, only perform the projection on the last time sub-step. The result is that intermediate time steps do not conserve mass.

2. **Normalize the pressure with the reference pressure**: <normalize_pressure>
   Input type: *Optional, boolean*
   Default: *false*
   Description: When true, this option subtracts the reference pressure, set in <PhysicalProperties>, from the current value of pressure for each time step.

3. **Solver choice for the pressure Poisson equation**: <linear_solver>
   Input type: *Required, string*
   Default: *NA*
   Description: Arches uses external linear solver packages to solve the pressure Poisson equation. Currently, there are two solver that have an interface to the pressure equation; *hypre* or *petsc*. A solver must be specified and specifics of the solver follow in the <parameter> section (detailed next).

4. **Solver parameters for the pressure Poisson equation**: <parameters>
   Input type: *Required, NA*
   Default: *NA*
   Description: The solver parameters, as children of the *parameters* node, include the following:

   - <solver>, Required solver parameter. Options include: *cg*.
   - <max_iter>, Required maximum iterations for the solver.
   - <preconditioner>, Required preconditioner. Options include: *jacobi*, *pfmg*.
   - <res_tol>, Required tolerance of the residual ($res = b - Ax$).

Mixture Fraction Solver

Arches has identified specific scalar variables that require specification, the mixture fraction being one of them. The mixture fraction equation is a conserved scalar equation that is used as a parameter to map the thermo-chemical state of the gas. By default, the required <MixtureFractionSolver> node must be present in the <ExplicitSolver> node.

1. **Initial value of of the mixture fraction in the domian**: <initial_value>
   Input type: *Optional, double*
   Default: *0.0*
   Description: One may set the mixture fraction everywhere inside the domain to a constant value. Boundary condition values are set elsewhere.

2. **Convection scheme**: <convection_scheme>
   Input type: *Required, string*
   Default: *central-upwind, flux-limited*
   Description:

Enthalpy Solver

5.3.4 Initial and Boundary Conditions

5.3.5 Turbulence Models

5.3.6 Properties, Reaction and Sub-Grid Mixing

5.3.7 Extra Scalar Solvers

This section and all options will soon be replaced with Section 5.3.8.

5.3.8 Additional Transport Equations

5.3.9 Direct Quadrature Method of Moments (DQMOM)

5.4 Examples

The following ARCHES examples illustrate the diverse set of problems that can be solved using the ARCHES component of Uintah code. The first two examples exemplify techniques used to verify various ARCHES algorithms that were implemented in the code. The following three [or more] examples illustrate the kinds of problems that ARCHES can solve. The input files used here can be used as templates to build similar input files for similar problems. Due to the complexity of ARCHES simulations, exact solutions (with the exception of MMS) do not exist. Hence the emphasis on model validation, or the comparison of simulation with experimental results. Model validation provides a framework that allows the simulation scientist to be confident in his or her results in the absence of analytical solutions. All modeling should be accompanied by some form of validation analysis.

Almgren MMS

Problem Description

Methods of Manufactured Solutions (MMS) are verification tools that are used with computer codes such as ARCHES that seek to solve the Navier-Stokes Equations. They are extremely useful for finding programming errors and ensuring expected behavior of the computer code. The Almgren MMS is especially easy to implement because of the absence of source terms that must be added to the transport equations. ARCHES uses a second-order spatial discretization scheme and a first-order scheme in the temporal direction. Therefore, if the Almgren MMS problem is run in Arches at different mesh resolutions and the normalized error plotted on a semilog plot, the slope of the line should be 2. To facilitate this exercise, a shell script has been written to perform this analysis [**not done yet....**]

Simulation Specifics

Component used: **ARCHES**

Input file name: `almgrenMMS.ups`

Command used to run input file:

`./runAlmgren.sh`

If you examine the shell script you will see the following line of code: `mpirun -np 1 sus inputs/UintahRelease/ARCHES/almgrenMMS.ups` This is call to run the ARCHES via sus.

Simulation Domain: 1.0 x 1.0 x 3.0 m

Cell Spacing:
0.3125 x 0.3125 x 0.275 m

Example Runtimes:
113.2 seconds (1 processor, 2.4 GHz Intel Core 2)

Physical time simulated: 1.0 sec.

Periodic Box Problem

Problem Description

The Periodic Box Problem indicates how well ARCHES is modeling the kinetic energy contained in the turbulence modeled on the grid and at a sub-grid level. The LES algorithm transfers kinetic energy from cell to cell in the ARCHES structured grid. Turbulence models such as "compdynamicprocedure," "dynamicprocedure," and "smagorinsky" are used to model kinetic energy at the sub-grid level. Ideally, there would be a seamless transition between the resolved turbulence and sub-grid models at the Nyquist limit. **SHOW SAMPLE PLOT** Experience has shown that this is not normally the case. By plotting the kinetic energy as a function of the wave number, it is possible to determine how well the kinetic energy dissipation is being modeled by the code. The Periodic Box problem is initialized with a kinetic energy (turbulence) profile from Direct Numerical Simulation (DNS). As the simulation proceeds that energy is dissipated.

Simulation Specifics

Component used: ARCHES

Input file name: `periodic.ups`

Command used to run input file:
This simulation, like many ARCHES simulations, requires another file, in addition to the input file called by sus. That file is the initial condition called upon in periodic.ups by

```
mpirun -np 1 sus inputs/UintahRelease/ARCHES/periodic.ups
```

Simulation Domain: 0.565 x 0.565 x 0.565 m

Cell Spacing:
0.0177 x 0.0177 x 0.0177 m

Example Runtimes:
2 minutes (1 processor, 2.4 GHz Intel Core 2)

Physical time simulated: 0.1 sec.

Helium Plume

Problem Description

Helium plumes are classical experiments that allow for the easy capture of turbulent mixing data that can be used to validate the turbulent mixing models used in LES algorithms such as Arches. The non-reacting nature of the plume makes it easy to capture experimental data without damaging expensive equipment. Reacting flows require special mixing tables that contain temperature, pressure and composition as a function of the transported scalars in Arches. The coldFlowMixingModel is used to determine the mixing of **isothermal? streams.** After the mixing model is specific in the .ups file, the temperature and densities of the two mixing streams are specified.

Simulation Specifics

Component used: ARCHES

Input file name: `helium_1m.ups`

Command used to run input file:

```
mpirun -np 8 sus inputs/UintahRelease/ARCHES/helium_1m.ups
```

Simulation Domain: 3.0 x 3.0 x 3.0 m

Cell Spacing:
0.06 x 0.06 x 0.0.6 m

Example Runtimes:
54 minutes (8 processors, 2.8 GHz Xeon)

Physical time simulated: 5.0 sec.

Results

Methane Plume

Problem Description

This methane plume is geometrically identical to the Helium Plume problem. The difference is the addition of chemistry. Instead of unreacting, isothermal fluids mixing, a fuel is reacting to combustion products inside of the computational domain. This chemistry is captured via a mixing table. The input file is pointed to the mixing table which contains state variables and species mass fractions as a function of mixture fraction, heat loss, and mixture fraction variance.

Simulation Specifics

Component used: ARCHES

Input file name: `helium_1m.ups`

Note that the input file is pointed to the mixing table (inputs/UintahRelease/ARCHES/CH4_equil_clipped.mx

Command used to run input file:

```
mpirun -np 8 sus inputs/UintahRelease/ARCHES/helium_1m.ups
```

Simulation Domain: 3.0 x 3.0 x 3.0 m

Cell Spacing:

0.06 x 0.06 x 0.0.6 m

Example Runtimes:

2 hours 10 minutes (8 processors, 2.8 GHz Xeon)

Physical time simulated: 5.0 sec.

Results

Fast Cookoff

Problem Description

The Fast Cookoff test is a procedure used for hazard classification of energetic materials. The object is immersed over a jet fuel pool fire and the reaction, if any, is observed. Current protocol requires that the full size article must be subjected to this test, making such procedures prohibitively expensive and unfeasible for articles such as solid rocket motors. An alternative procedure has been proposed, combining sub-scale experiments with computer simulation. Through validation and uncertainty quantification procedures, the computer simulation tool (ARCHES) can be used as a surrogate for full-scale experimental testing. This Fast Cookoff problem includes a reacting flow as well as an MPMARCHES object. After performing the simulation, the incident heat flux to the cylinder can be extracted.

Simulation Specifics

Component used: MPMARCHES

Input file name: `fastcookoff.ups`

Command used to run input file:

Note that the input file is pointed to the mixing table (inputs/UintahRelease/ARCHES/sandia_jp8_flmlt_cg.mxn)

`mpirun -np 64 sus inputs/UintahRelease/ARCHES/fastcookoff.ups` To extract the incident heat flux to the cylinder, use the faceextract and timeextract utilities. ¡How to do this¿

Simulation Domain: 24.0 x 24.0 x 24.0 m

Cell Spacing:

0.24 x 0.24 x 0.24 m

Example Runtimes:

7 hours 27 minutes (64 processors, 2.8 GHz Xeon)

Physical time simulated: 10.0 sec.

Results

Bibliography

[1] M. Germano, U. Piomelli, P. Moin, and W. H. Cabot. A dynamic subgrid-scale eddy viscosity model. *Physics of Fluids A:Fluid Dynamics*, 3(7):1760–1765, 1991.

[2] S. Gottlieb, C.-W. Shu, and E. Tadmor. Strong stability-preserving high-order time discretization methods. *SIAM Review*, 43(1):89–112, 2001.

[3] D. K. Lilly. A proposed modifcation of the Germano subgrid-scale closure method. *Physics of Fluids A*, 4:633–635, 1992.

[4] P. Moin, K. Squires, W. Cabot, and S. Lee. A dynamic subgrid-scale model for compressible turbulence and scalar transport. *Physics of Fluids A*, 3(11):2746–2757, 1991.

[5] Y. Morinishi, T.S. Lund, O.V. Vasilyev, and P. Moin. Fully conservatice higher order finite difference schemes for incompressible flow. *Journal of Computational Physics*, 143:90–124, 1998.

[6] H. Pitsch and H. Steiner. Large-eddy simulation of a turbulent piloted methane/air diffusion flame (Sandia flame D). *Physics of Fluids*, 12(10):2541–2544, 2000.

[7] S. B. Pope. *Turbulent Flows*. Cambridge University Press, Cambridge, UK, 2000.

[8] J. Smagorinsky. General circulation experiments with the primitive equations. *Monthly Weather Review*, 91(3):99–106, 1963.

Chapter 6

ICE

6.1 Introduction

The work presented here describes a multi-material CFD approach designed to solve "full physics" simulations of dynamic fluid structure interactions involving large deformations and material transformations (e.g., phase change). "Full physics" refers to problems involving strong interactions between the fluid field and solid field temperatures and velocities, with a full Navier Stokes representation of fluid materials and the transient, nonlinear response of solid materials. These interactions may include chemical or physical transformation between the solid and fluid fields.

The theoretical and algorithmic basis for the multi-material CFD algorithm presented here is based on a body of work of several investigators at Los Alamos National Laboratory, primarily Bryan Kashiwa, Rick Rauenzahn and Matt Lewis. Several reports by these researchers are publicly available and are cited herein. It is largely through our personal interactions that we have been able to bring these ideas to bear on the simulations described herein.

An exposition of the governing equations is given in the next section, followed by an algorithmic description of the solution of those equations. This description is first done separately for the materials in the Eulerian and Lagrangian frames of reference, before details associated with the integrated approach are given.

6.1.1 Governing Equations

The governing multi-material model equations are stated and described, but not developed, here. Their development can be found in [6]. Here, our intent is to identify the quantities of interest, of which there are eight, as well as those equations (or closure models) which govern their behavior. Consider a collection of N materials, and let the subscript r signify one of the materials, such that $\mathrm{r} = 1, 2, 3, \ldots, N$. In an arbitary volume of space $V(\mathbf{x}, t)$, the averaged thermodynamic state of a material is given by the vector $[M_\mathrm{r}, \mathbf{u}_\mathrm{r}, e_\mathrm{r}, T_\mathrm{r}, v_\mathrm{r}, \theta_\mathrm{r}, \boldsymbol{\sigma}_\mathrm{r}, p]$, the elements of which are the r-material mass,

velocity, internal energy, temperature, specific volume, volume fraction, stress, and the equilibration pressure. The r-material averaged density is $\rho_{\rm r} = M_{\rm r}/V$. The rate of change of the state in a volume moving with the velocity of r-material is:

$$\frac{1}{V}\frac{D_{\rm r}M_{\rm r}}{Dt} = \sum_{s=1}^{N}\Gamma_{\rm rs} \tag{6.1}$$

$$\frac{1}{V}\frac{D_{\rm r}(M_{\rm r}\mathbf{u}_{\rm r})}{Dt} = \theta_{\rm r}\boldsymbol{\nabla}\cdot\boldsymbol{\sigma} + \boldsymbol{\nabla}\cdot\theta_{\rm r}(\boldsymbol{\sigma}_{\rm r} - \boldsymbol{\sigma}) + \rho_{\rm r}\mathbf{g} + \sum_{s=1}^{N}\mathbf{f}_{\rm rs} + \sum_{s=1}^{N}\mathbf{u}_{\rm rs}^{+}\Gamma_{\rm rs} \tag{6.2}$$

$$\frac{1}{V}\frac{D_{\rm r}(M_{\rm r}e_{\rm r})}{Dt} = -\rho_{\rm r}p\frac{D_{\rm r}v_{\rm r}}{Dt} + \theta_{\rm r}\boldsymbol{\tau}_{\rm r} : \nabla\mathbf{u}_{\rm r} - \boldsymbol{\nabla}\cdot\mathbf{j}_{\rm r} + \sum_{s=1}^{N}q_{\rm rs} + \sum_{s=1}^{N}h_{\rm rs}^{+}\Gamma_{\rm rs} \tag{6.3}$$

Equations (6.1-6.3) are the averaged model equations for mass, momentum, and internal energy of r-material, in which $\boldsymbol{\sigma}$ is the mean mixture stress, taken here to be isotropic, so that $\boldsymbol{\sigma} = -p\mathbf{I}$ in terms of the hydrodynamic pressure p. The effects of turbulence have been explicitly omitted from these equations, and the subsequent solution, for the sake of simplicity. However, including the effects of turbulence is not precluded by either the model or the solution method used here.

In Eq. (6.2) the term $\sum_{s=1}^{N}\mathbf{f}_{\rm rs}$ signifies a model for the momentum exchange among materials. This term results from the deviation of the r-field stress from the mean stress, averaged, and is typically modeled as a function of the relative velocity between materials at a point. (For a two material problem this term might look like $\mathbf{f}_{12} = K_{12}\theta_1\theta_2(\mathbf{u}_1 - \mathbf{u}_2)$ where the coefficient K_{12} determines the rate at which momentum is transferred between materials). Likewise, in Eq. (6.3), $\sum_{\rm s=1}^{N} q_{\rm rs}$ represents an exchange of heat energy among materials. For a two material problem $q_{12} = H_{12}\theta_1\theta_2(T_2 - T_1)$ where $T_{\rm r}$ is the r-material temperature and the coefficient $H_{\rm rs}$ is analogous to a convective heat transfer rate coefficient. The heat flux is $\mathbf{j}_{\rm r} = -\rho_{\rm r}b_{\rm r}\boldsymbol{\nabla}T_{\rm r}$ where the thermal diffusion coefficient $b_{\rm r}$ includes both molecular and turbulent effects (when the turbulence is included).

In Eqs. (6.1-6.3) the term $\Gamma_{\rm rs}$ is the rate of mass conversion from s-material into r-material, for example, the burning of a solid or liquid reactant into gaseous products. The rate at which mass conversion occurs is governed by a reaction model. In Eqs. (6.2) and (6.3), the velocity $\mathbf{u}_{\rm rs}^{+}$ and the enthalpy $h_{\rm rs}^{+}$ are those of the s-material that is converted into r-material. These are simply the mean values associated with the donor material.

The temperature $T_{\rm r}$, specific volume $v_{\rm r}$, volume fraction $\theta_{\rm r}$, and hydrodynamic pressure p are related to the r-material mass density, $\rho_{\rm r}$, and specific internal energy, $e_{\rm r}$, by way of equations of state. The four relations for the four quantites $(T_{\rm r}, v_{\rm r}, \theta_{\rm r}, p)$ are:

$$
\begin{aligned}
e_{\mathrm{r}} &= e_{\mathrm{r}}(v_{\mathrm{r}}, T_{\mathrm{r}}) && (6.4)\\
v_{\mathrm{r}} &= v_{\mathrm{r}}(p, T_{\mathrm{r}}) && (6.5)\\
\theta_{\mathrm{r}} &= \rho_{\mathrm{r}} v_{\mathrm{r}} && (6.6)\\
0 &= 1 - \textstyle\sum_{s=1}^{N} \rho_{\mathrm{s}} v_{\mathrm{s}} && (6.7)
\end{aligned}
$$

Equations (6.4) and (6.5) are, respectively, the caloric and thermal equations of state. Equation (6.6) defines the volume fraction, θ, as the volume of r-material per total material volume, and with that definition, Equation (6.7), referred to as the multi-material equation of state, follows. It defines the unique value of the hydrodynamic pressure p that allows arbitrary masses of the multiple materials to identically fill the volume V. This pressure is called the "equilibration" pressure [8].

A closure relation is still needed for the material stress $\boldsymbol{\sigma}_{\mathrm{r}}$. For a fluid $\boldsymbol{\sigma}_{\mathrm{r}} = -p\mathbf{I} + \boldsymbol{\tau}_{\mathrm{r}}$ where the deviatoric stress is well known for Newtonian fluids. For a solid, the material stress is the Cauchy stress. The Cauchy stress is computed using a solid constitutive model and may depend on the the rate of deformation, the current state of deformation ($\mathbf{E}$), the temperature, and possibly a number of history variables. Such a relationship may be expressed as:

$$
\boldsymbol{\sigma}_{\mathrm{r}} \equiv \boldsymbol{\sigma}_{\mathrm{r}}(\boldsymbol{\nabla}\mathbf{u}_{\mathrm{r}}, \mathbf{E}_{\mathrm{r}}, T_{\mathrm{r}}, \ \ldots) \tag{6.8}
$$

The approach described here imposes no restrictions on the types of constitutive relations that can be considered. More specific discussion of some of the models used in this work is found in Sec. **??**

Equations (6.1-6.8) form a set of eight equations for the eight-element state vector, $[M_{\mathrm{r}}, \mathbf{u}_{\mathrm{r}}, e_{\mathrm{r}}, T_{\mathrm{r}}, v_{\mathrm{r}}, \theta_{\mathrm{r}}, \boldsymbol{\sigma}_{\mathrm{r}}, p]$, for any arbitrary volume of space V moving with the r-material velocity. The approach described here uses the reference frame most suitable for a particular material type. As such, there is no guarantee that arbitrary volumes will remain coincident for materials described in different reference frames. This problem is addressed by treating the specific volume as a dynamic variable of the material state which is integrated forward in time from initial conditions. In so doing, at any time, the total volume associated with all of the materials is given by:

$$
V_t = \textstyle\sum_{r=1}^{N} M_{\mathrm{r}} v_{\mathrm{r}} \tag{6.9}
$$

so the volume fraction is $\theta_{\mathrm{r}} = M_{\mathrm{r}} v_{\mathrm{r}} / V_t$ (which sums to one by definition). An evolution equation for the r-material specific volume, derived from the time variation of Eqs. (6.4-6.7), has been developed in [6]. It is stated here as:

$$
\begin{aligned}
\frac{1}{V}\frac{D_{\mathrm{r}}(M_{\mathrm{r}} v_{\mathrm{r}})}{Dt} = f_{\mathrm{r}}^{\theta} \boldsymbol{\nabla}\cdot\mathbf{u} \ &+ \ \left[v_{\mathrm{r}}\Gamma_{\mathrm{r}} - f_{\mathrm{r}}^{\theta} \textstyle\sum_{s=1}^{N} v_{\mathrm{s}}\Gamma_{\mathrm{s}}\right] \\
&+ \ \left[\theta_{\mathrm{r}}\beta_{\mathrm{r}}\frac{D_{\mathrm{r}} T_{\mathrm{r}}}{Dt} - f_{\mathrm{r}}^{\theta} \textstyle\sum_{s=1}^{N} \theta_{\mathrm{s}}\beta_{\mathrm{s}}\frac{D_{\mathrm{s}} T_{\mathrm{s}}}{Dt}\right] . \qquad (6.10)
\end{aligned}
$$

where $f_{\rm r}^{\theta} = \frac{\theta_{\rm r}\kappa_{\rm r}}{\sum_{\rm s=1}^{N}\theta_{\rm s}\kappa_{\rm s}}$, and $\kappa_{\rm r}$ is the r-material bulk compressibility.

The evaluation of the multi-material equation of state (Eq. (6.7)) is still required in order to determine an equilibrium pressure that results in a common value for the pressure, as well as specific volumes that fill the total volume identically.

A description of the means by which numerical solutions to the equations in Section 6.2 are found is presented next. This begins with separate, brief overviews of the methodologies used for the Eulerian and Lagrangian reference frames. The algorithmic details necesssary for integrating them to achieve a tightly coupled fluid-structure interaction capability is provided in Sec. **??**.

6.2 Algorithm Description

The Eulerian method implemented here is a cell-centered, finite volume, multi-material version of the ICE (for Implicit, Continuous fluid, Eulerian) method [5] developed by Kashiwa and others at Los Alamos National Laboratory [7]. "Cell-centered" means that all elements of the state are colocated at the grid cell-center (in contrast to a staggered grid, in which velocity components may be centered at the faces of grid cells, for example). This colocation is particularly important in regions where a material mass is vanishing. By using the same control volume for mass and momentum it can be assured that as the material mass goes to zero, the mass and momentum also go to zero at the same rate, leaving a well-defined velocity. The technique is fully compressible, allowing wide generality in the types of problems that can be addressed.

Our use of the cell-centered ICE method employs time splitting: first, a Lagrangian step updates the state due to the physics of the conservation laws (i.e., right hand side of Eqs. 6.1-6.3); this is followed by an Eulerian step, in which the change due to advection is evaluated. For solution in the Eulerian frame, the method is well developed and described in [7].

In the mixed frame approach used here, a modification to the multi-material equation of state is needed. Equation (6.7) is unambiguous when all materials are fluids or in cases of a flow consisting of dispersed solid grains in a carrier fluid. However in fluid-structure problems the stress state of a submerged structure may be strongly directional, and the isotropic part of the stress has nothing to do with the hydrodynamic (equilibration) pressure p. The equilibrium that typically exists between a fluid and a solid is at the interface between the two materials: there the normal part of the traction equals the pressure exerted by the fluid on the solid over the interface. Because the orientation of the interface is not explicitly known at any point (it is effectively lost in the averaging) such an equilibrium cannot be computed.

The difficulty, and the modification that resolves it, can be understood by considering a solid material in tension coexisting with a gas. For solid materials, the equation of state is the bulk part of the constitutive response (that is, the isotropic part of the Cauchy stress versus specific volume and temperature). If one attempts to equate

the isotropic part of the stress with the fluid pressure, there exist regions in pressure-volume space for which Eq. (6.7) has no physical solutions (because the gas pressure is only positive). This can be seen schematically in Fig. **??**, which sketches equations of state for a gas and a solid, at an arbitrary temperature.

Recall that the isothermal compressiblity is the negative slope of the specific volume versus pressure. Embedded structures considered here are solids and, at low pressure, possess a much smaller compressibility than the gasses in which they are submerged. Nevertheless the variation of condensed phase specific volume can be important at very high pressures, where the compressibilities of the gas and condensed phase materials can become comparable (as in a detonation wave, for example). Because the speed of shock waves in materials is determined by their equations of state, obtaining accurate high pressure behavior is an important goal of our FSI studies.

To compensate for the lack of directional information for the embedded surfaces, we evaluate the solid phase equations of state in two parts. Above a specified postive threshold pressure (typically 1 atmosphere), the full equation of state is respected; below that threshold pressure, the solid phase pressure follows a polynomial chosen to be C^1 continuous at the threshold value and which approaches zero as the specific volume becomes large. The effect is to decouple the solid phase specific volume from the stress when the isotropic part of the stress falls below a threshold value. In regions of coexistence at states below the threshold pressure, p tends to behave according to the fluid equation of state (due to the greater compressibility) while in regions of pure condensed phase material p tends rapidly toward zero and the full material stress dominates the dynamics as it should.

6.3 Uintah Specification

6.3.1 Basic Inputs

Each Uintah component is invoked using a single executable called *sus* , which chooses the type of simulation to execute based on the *SimulationComponent* tag in the input file. In the case of ICE simulations, this looks like:

```
<SimulationComponent type="ice" />
```

near the top of the inputfile. The system of units **must** be consistent (mks, cgs) and the majority of input files will be in Meter-Kilogram-Sec system.

6.3.2 Semi-Implicit Pressure Solve

The equation for the change in the pressure field ΔP during a given timestep is given by

$$\frac{dP}{dt} = \frac{\sum_{m=1}^{N} \frac{\dot{m}}{V\rho_m^o} - \sum_{m=1}^{N} \nabla \cdot \widehat{\theta_m \vec{U}_m}^{*f}}{\sum_{m=1}^{N} \frac{\theta_m}{\rho_m^o c_m^2}} \tag{6.11}$$

which can be written in matrix form $Ax = b$ and solved with a linear solver. Details on the notation, discretization of Eq. 6.11 and the formation of A and b can be found in

```
src/CCA/Components/ICE/Docs/implicitPressSolve.pdf
```

The linear system $Ax = b$ can be solved using the default Uintah:conjugate gradient solver (cg) (slow) or one of the many that are available through the scalable linear solvers and preconditioner package hypre [3]. Experience has shown that the most efficient hypre preconditioner and solver are the pfmg and cg respectively. Below are typical values for both the Uintah:cg and hypre:cg solver

```
<ImplicitSolver>
   <max_outer_iterations>         20    </max_outer_iterations>
   <outer_iteration_tolerance>    1e-8  </outer_iteration_tolerance>
   <iters_before_timestep_restart> 5    </iters_before_timestep_restart>
   <Parameters variable="implicitPressure">

    <tolerance>     1.e-10  </tolerance>

    <!-- CGSolver options -->
    <norm>     LInfinity  </norm>
    <criteria> Absolute   </criteria>

    <!-- Hypre options -->
    <solver>         cg      </solver>
    <preconditioner> pfmg    </preconditioner>
    <maxiterations>  7500    </maxiterations>
    <npre>           1       </npre>
    <npost>          1       </npost>
    <skip>           0       </skip>
    <jump>           0       </jump>
   </Parameters>
</ImplicitSolver>
```

If the user is interested in altering the tolerance to which the equations are solved they should look at

```
<tolerance> and <outer_iteration_tolerance>
```

XML tag	Description
max_outer_iterations	maximum number of iterations in the outer loop of the pressure solve.
outer_iteration_tolerance	tolerance XXXXDX
iters_before_timestep_restart	number of outer iterations before a timestep is restarted
tolerance	XXXX

6.3.3 Physical Constants

The gravitational constant and a reference pressure are specified in:

```
<PhysicalConstants>
   <gravity>            [0,0,0]   </gravity>
   <reference_pressure> 101325.0  </reference_pressure>
</PhysicalConstants>
```

6.3.4 Material Properties

For each ICE material the thermodynamic and transport properties must be specified, in addition to the initial conditions of the fluid inside of each geom_object. Below is the an example of how to specify an invisid ideal gas over square region with dimensions $6mX6mX6m$. The initial conditions of the gas in that region are $T = 300, \rho = 1.179, v_x = 1, v_y = 2, v_z = 3$ (Note, the pressure XML tag is not used as an initial condition and is simply there to make the user aware of what the pressure would be at that thermodynamic state.)

```
<MaterialProperties>
   <ICE>
     <material>
       <EOS type = "ideal_gas">                 </EOS>
       <dynamic_viscosity>   0.0                </dynamic_viscosity>
       <thermal_conductivity>0.0                </thermal_conductivity>
       <specific_heat>      716.0               </specific_heat>
       <gamma>               1.4                </gamma>
       <geom_object>
           <box label="wholeDomain">
               <min>       [ 0.0, 0.0, 0.0 ]  </min>
               <max>       [ 6.0, 6.0, 6.0 ]  </max>
           </box>
           <res>                 [2,2,2]      </res>
           <velocity>      [1.,2.,3.]         </velocity>
           <density>       1.1792946927374306 </density>
           <pressure>      101325.0           </pressure>
           <temperature>   300.0              </temperature>
       </geom_object>
     </material>
```

```
  </ICE>
</MaterialProperties>
```

6.3.5 Equation of State

Below is a list of the various equations of state, along with the user defined constants, that are available. The reader should consult the literature for the theoretical development and applicability of the equations of state to the problem being solved. The most commonly used EOS is the ideal gas law

$$p = (\gamma - 1)c_v \rho T \tag{6.12}$$

and is specified in the input file with:

```
<EOS type="ideal_gas"/>
```

The Thomsen Hartka EOS for cold liquid water (1-100 atm pressure range) is specified with [15, 1]

```
<EOS type="Thomsen_Hartka_water">
  <a>  2.0e-7     </a>    <!-- (K/Pa)     -->
  <b>  2.6        </b>    <!-- (J/kg K^2) -->
  <co> 4205.7     </co>   <!-- (J/Kg K)   -->
  <ko> 5.0e-10    </ko>   <!-- (1/Pa)     -->
  <To> 277.0      </To>   <!-- (K)        -->
  <L>  8.0e-6     </L>    <!-- (1/K^2)    -->
  <vo> 1.00008e-3 </vo>   <!-- (m^3/kg)   -->
</EOS>
```

The input specification for the "JWLC", "JWL++" and "Murnahan" equations of state from [11] are:

```
<EOS type = "JWLC">
  <A>   2.9867e11   </A>
  <B>   4.11706e9   </B>
  <C>   7.206147e8  </C>
  <R1>    4.95      </R1>
  <R2>    1.15      </R2>
  <om>    0.35      </om>
  <rho0>  1160.0    </rho0>
</EOS>

<EOS type = "JWL">
  <A>     1.6689e12 </A>
  <B>     5.969e10  </B>
  <R1>      5.9     </R1>
  <R2>      2.1     </R2>
  <om>      0.45    </om>
  <rho0>  1835.0    </rho0>
</EOS>
```

```
<EOS type = "Murnahan">
  <n>     7.4       </n>
  <K>     39.0e-11  </K>
  <rho0>  1160.0    </rho0>
  <P0>    101325.0  </P0>
</EOS>
```

The "hard sphere" or "Abel" equation of state for dense gases is

$$p(v - b) = RT \tag{6.13}$$

where b corresponds to the volume occupied by the molecules themselves [14]. Input parameters are specified using:

```
<EOS type="hard_sphere_gas">
   <b> 1.4e-3 </b>
</EOS>
```

Non-idea gas equation of state used in HMX combustion simulations the Twu-Sim-Tassone(TST) EOS is

$$p = \frac{(\gamma - 1)c_v T}{v - b} - \frac{a}{(v + 3.0b)(v - 0.5b)} \tag{6.14}$$

Input parameters are specified using:

```
<EOS type="TST">
  <a>       -260.1385968     </a>
  <b>       7.955153678e-4   </b>
  <u>       -0.5             </u>
  <w>       3.0              </w>
  <Gamma>   1.63             </Gamma>
</EOS>
```

The input parameters for the Tillotson equation of state [4] for soils :

```
<EOS type = "Tillotson">
  <a>       .5      </a>
  <b>       1.3     </b>
  <A>       4.5e9   </A>
  <B>       3.0e9   </B>
  <E0>      6.e6    </E0>
  <Es>      3.2e6   </Es>
  <Esp>     18.0e6  </Esp>
  <alpha>   5.0     </alpha>
  <beta>    5.0     </beta>
  <rho0>    1700.0  </rho0>
</EOS>
```

6.3.6 Exchange Properties

The heat and momentum exchange coefficients K_{rs} and H_{rs}, which determine the rate at which momentum and heat are transferred between materials, and are specified in the following format.

```
0->1,   0->2,  0->3
        1->2,  1->3
               2->3
```

For a two material problem the coefficients would be:

```
<exchange_properties>
   <exchange_coefficients>
      <momentum>  [0, 1e15, 1e15 ]     </momentum>
      <heat>      [0, 1e10, 1e10 ]     </heat>
   </exchange_coefficients>
</exchange_properties>
```

6.3.7 BoundaryConditions

Boundary conditions must be specified on each face of the computational domain $(x^-, x^+, y^-, y^+, z^-, z^+)$ for the variables $P, \mathbf{u}, \mathbf{T}, \rho, \mathbf{v}$ for each material. The three main types of numerical boundary conditions that can be applied are "Neumann", "Dirichlet" and "Symmetric". A Neumann boundary condition is used to set the gradient or $\frac{\partial q}{\partial n}|_{surface} = value$ at the boundary. The value of the primative variable in the boundary cell is given by,

$$q[\text{boundary cell}] = q[\text{interior cell}] - value * dn; \tag{6.15}$$

if we use a first order upwind discretization of the gradient. Dirichlet boundary conditions set the value of primative variable in the boundary cell using

$$q[\text{boundary cell}] = value; \tag{6.16}$$

```
<Grid>
  <BoundaryConditions>
    <Face side = "x-">
      <BCType id = "0"   label = "Pressure"     var = "Neumann">
                            <value> 0. </value>
      </BCType>
      <BCType id = "all" label = "Velocity"     var = "Neumann">
                            <value> [0.,0.,0.] </value>
      </BCType>
      <BCType id = "all" label = "Temperature"  var = "Neumann">
                            <value> 0.0 </value>
      </BCType>
      <BCType id = "all" label = "Density"      var = "Neumann">
                            <value> 0.0 </value>
```

```
      </BCType>
      <BCType id = "all" label = "SpecificVol"  var = "computeFromDensity">
                              <value> 0.0  </value>
      </BCType>
    </Face>
      .
      [other faces]
      .
  </BoundaryConditions>
</Grid>
```

There is also the field tag `id = "all"`. In principal, one could set different boundary condition types for different materials. In practice, this is rarely used, so the usage illustrated here should be used. Note that pressure field id is always 0. Symmetric boundary conditions are set using:

```
<Face side = "y-">
    <BCType id = "all" label = "Symmetric" var = "symmetry"> </BCType>
</Face>
```

In addition to "Dirichlet", "Neumann", and "Symmetric" type boundary conditions ICE has several custom or experimental boundary conditions the user can access. The "Sine" boundary condition was designed to impose a pulsating pressure wave in the boundary cells by applying

$$p = p_{reference} + Asin(\omega t) \tag{6.17}$$

The input file parameters that control the frequency and magnitude of the wave are:

```
<SINE_BC>
  <omega>    1000 </omega>
  <A>        800 </A>
</SINE_BC>
```

and to specify them add

```
<BCType id = "0"   label = "Pressure"     var = "Sine">
                      <value> 0.0 </value>
</BCType>
<BCType id = "0"   label = "Temperature"  var = "Sine">
                      <value> 0.0 </value>
</BCType>
```

to the input file. For non-reflective boundary conditions the user should specify the "LODI" or locally one-dimensional invisid type [13]

```
<LODI>
  <press_infinity> 1.0132500000010138e+05  </press_infinity>
  <sigma>          0.27                    </sigma>
  <ice_material_index> 0                   </ice_material_index>
</LODI>
```

and

```
<Face side = "x+">
  <BCType id = "0"   label = "Pressure"     var = "LODI">
                        <value> 0. </value>
  </BCType>
  <BCType id = "0"   label = "Velocity"     var = "LODI">
                        <value> [0.,0.,0.] </value>
  </BCType>
  <BCType id = "0"   label = "Temperature"  var = "LODI">
                        <value> 0.0 </value>
  </BCType>
  <BCType id = "0"   label = "Density"      var = "LODI">
                        <value> 0.0 </value>
  </BCType>
  <BCType id = '0' label = "SpecificVol" var = "computeFromDensity">
                        <value> 0.0 </value>
  </BCType>
</Face>
```

This boundary condition is designed to suppress all the unwanted effects of an artifical boundary. **This BC is computationally expensive, not entirely effective and should be used with caution**. In flow fields where there are no passing through the outlet of the domain it reduces the reflected pressure waves significantly.

6.3.8 Output Variable Names

There are numerous variables that can be saved during a simulation. The table below is a list of the most commonly saved variables. To see the entire list ICE specfic variables available to the user run

```
inputs/labelNames ice
```

Dimensions are given in mass (M), length (L), time (t) and tempertare (T). Bold face label names signify vectors quantities. The location of the variable on the grid is denoted by (CC) for the cell-centered or (FC) for face-centered. Conserved quantities that are summed over all cells, every timestep, and written to a "dat" file inside of the `uda` directory are denoted with (dat).

LabelName		Description
delP_Dilatate	M/Lt^2	change in pressure during the, (CC).
delP_MassX	M/Lt^2	change in pressure due to mass addition, (CC).
eng_adv	ML^2/t^2	energy of a material after the advection task, (CC).
eng_exch_error	ML^2/t^2	$\sum_{i=1}^{\text{AllCells}}$ Internal Energy After Exchange Process− $\sum_{i=1}^{\text{AllCells}}$ Internal Energy Before Exchange Process, (dat).
eng_L_ME_CC	ML^2/t^2	Energy of a material after the exchange task and just before the advection task, (CC).
imp_delP	M/Lt^2	(CC).
KineticEnergy	ML^2/t^2	$\sum_{i=1}^{\text{AllCells}}(0.5m\vec{(v)}^2)_i$, (dat).
mach		Mach number, (CC).
mag_div_vel_CC		Magnitude of the divergence of the velocity, (CC).
mag_grad_press_CC		Magnitude of the gradient of the pressure, (CC).
mag_grad_rho_CC		Magnitude of the gradient of the density, (CC).
mag_grad_temp_CC		Magnitude of the gradient of the temperature, (CC).
mag_grad_vol_frac_CC		Magnitude of the gradient of the volume fraction, (CC).
mass_adv	M	Mass of a material after the advection task, (CC).
mass_L_CC	M	Mass of a material just before the advection task, (CC).
modelEng_src	ML^2/t^2	Energy source term, computed from a reaction model, (CC).
modelMass_src	M	Mass source term, computed from a reaction model, (CC).
modelMom_src	ML/t	Momentum source term, computed from a reaction model, (CC).
modelVol_src		Volume source term, computed from a reaction model, (CC).
mom_exch_error	ML/t	$\sum_{i=1}^{\text{AllCells}}$ Momemtum After Exchange Process− $\sum_{i=1}^{\text{AllCells}}$ Momentum Before Exchange Process, (dat).
mom_L_CC	ML/t	Momemtum before momentum exchange task, (CC).
mom_L_ME_CC	ML/t	Momentum after momentum exchange task, (CC).
mom_source_CC	ML/t	All sources of momentum,(CC).
press_CC	M/Lt^2	Pressure $P = P_{\text{equilibration}} + \Delta P$, (CC).
press_equil_CC	M/Lt^2	Pressure after the compute equilibration task, (CC).
pressX_FC	M/Lt^2	Pressure on the $x^{-,+}$ cell faces, (FC).
pressY_FC	M/Lt^2	Pressure on the $y^{-,+}$ cell faces, (FC).
pressZ_FC	M/Lt^2	Pressure on the $z^{-,+}$ cell faces, (FC).
rho_CC	M/L^3	Density of each material, (CC).
rho_micro_CC	M/L^3	Microscopic or intensive density, (CC).
specific_heat	L^2/t^2T	Constant Specific Heat, (CC).
speedSound_CC	L/t	Speed of sound of each material, (CC).
sp_vol_adv		
sp_vol_CC	$L3/M$	Specific volume of each material, (CC).
temp_CC	T	Temperature of each material, (CC).
TempX_FC	T	temperature on the $x^{-,+}$ cell faces, (FC).
TempY_FC	T	temperature on the $y^{-,+}$ cell faces, (FC).
TempZ_FC	T	temperature on the $z^{-,+}$ cell faces, (FC).
thermalCond	ML/t^3T	Thermal conductivity, (CC).
TotalIntEng	ML^2/t^2	$\sum_{i=1}^{\text{AllCells}}(mc_vT)_i$, (dat).
TotalMass	M	$\sum_{i=1}^{\text{AllCells}} m_i$, (dat).
TotalMomentum	ML/t	$\sum_{i=1}^{\text{AllCells}}(m\vec{v})_i$, (dat).
uvel_FC	L/t	x-component of velocity, before momentum exchange, (FC).
uvel_FCME	L/t	x-component of velocity, after momentum exchange task, (FC).
vel_CC	L/t	Velocity at the end of a timestep, (CC).
viscosity	M/Lt	Dynamic viscosity, (CC).
vol_frac_CC		Volume fraction of each material, (CC).
vol_fracX_FC		Volume fraction on the $x^{-,+}$ cell faces, (FC).
vol_fracY_FC		Volume fraction on the $y^{-,+}$ cell faces, (FC).
vol_fracZ_FC		Volume fraction on the $z^{-,+}$ cell faces, (FC).
vvel_FC	L/t	y-component of velocity, before momentum exchange task, (FC).
vvel_FCME	L/t	y-component of velocity, after momentum exchange task, (FC).
wvel_FC	L/t	z-component of velocity, before momentum exchange, (FC).
wvel_FCME	L/t	z-component of velocity, after momentum exchange task, (FC).

The variables, `mag_div_vel_CC, mag_grad_press_CC, mag_grad_rho_CC, mag_grad_temp_CC, mag_grad_vol_frac_CC,` are the magnitude of the gradient or divergence of the respec-

tive primative variable. If the user visual To are large and based on this information the adaptive mesh cell refinement criteria can be set.

Below is a list of the `XML` tags pertaining specifically to `ICE` problems.

6.3.9 XML tag description

XML tag	Type	Dimensions	Description
cfl	double		Courant Number.
gravity	Vector	$[L/t^2]$	gravitational acceleration, $\vec{g}$.
global material properties			
dynamic_viscosity	double	$[M/Lt]$	viscosity, μ.
thermal_conditucivity	double	$[ML/t^3T]$	thermal conductivity, k
specific_heat	double	$[L^2/t^2T]$	c_p
gamma	double		ratio of specific heats, γ.
geometry object related			
res	vector		resolution used for defining geometry objects.
velocity	vector	$[L/t]$	initial velocity, $\vec{u}$.
density	double	$[M/L^3]$	initial density, ρ.
temperature	double	$[T]$	initial temperature, T.
pressure	double		Not used.
AMR Parameters			
orderOfInterpolation	integer		Order of interpolation at the coarse/fine interfaces.
do_Refluxing	boolean		on/off switch for correcting the flux of mass, momentum, and energy at the course/fine interfaces.

6.4 Examples

Below are several example problems that illustrate the wide range of problems that can be solved using the ICE algorithm. Where possible simulation results are compared to exact solutions or high fidelity numerical results. Note in order to run the post processing scripts the user should have a recent version of Octave installed. To visualize the results the visualization package VisIT should be used. VisIT session files are included.

Poiseuille Flow

Problem Description

The Poiseuille flow problem is classical viscous flow problem in which flow is driven through two parallel plates from fixed pressure gradient. The pressure gradient is balanced by the diffusion x momentum in the y direction.

Simulation Specifics

Component used: ICE

Input file name: `CouettePoiseuille.ups`

Edit this file and set the boundary condition for the velocity on the y+ = 0.0. Change:

```
<BCType id = "0"   label = "Velocity"     var = "Dirichlet">
                       <value> [1.25,0.,0.] </value>
[to]
<BCType id = "0"   label = "Velocity"     var = "Dirichlet">
                      <value> [0,0.,0.] </value>
```

Command used to run input file:

```
mpirun -np 1 sus -solver hypre inputs/UintahRelease/ICE/CouettePoiseuille.ups
```

Postprocessing command:

`inputs/UintahRelease/ICE/compare_CouettePoiseuille.m -uda Couette-Poiseuille.uda`
You must edit `compare_CouettePoiseuille.m` and set `wallVel = 0` . This will generate a postscript file CouettePoiseuille.ps

Simulation Domain: 1 x .01 x .01 m

Cell Spacing:

10 x 5 x 10 mm (Level 0)

Example Runtimes:

8ish minutes (1 processor, 2.66 GHz Xeon)

Physical time simulated: 15 sec.

Results

Figure 6.1 shows a comparison of the exact and simulated u velocity at time $t = 15sec$, 5 cells from the end of the domain. The lower plot shows the difference of the velocity $\|u - u_{exact}\|$.

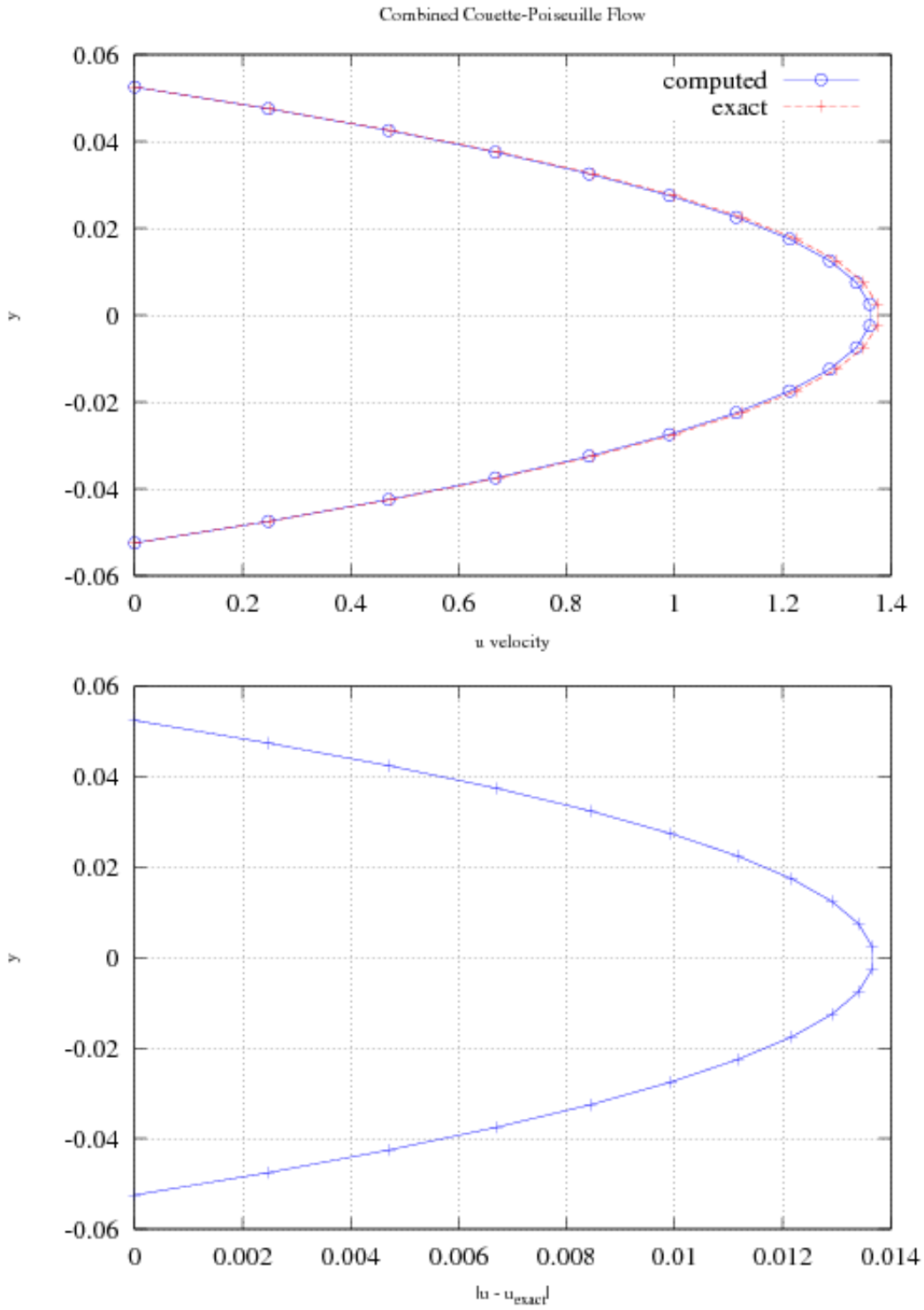

Figure 6.1: Comparison of u velocity $t = 15sec$

Combined Couette-Poiseuille Flow

Problem Description

The combined Couette-Poiseuille flow problem is another classical viscous flow problem in which flow is driven through a channel by a pressure gradient and a wall moving. The reduced x momentum equation differential is

$$\mu \frac{d^2u}{dy^2} = \frac{dp}{dx} = \text{constant} \tag{6.18}$$

subject to the no slip boundary condition $u(\pm h)$ = wall velocity, where h is half the height of the channel [17].

Simulation Specifics

Component used: ICE

Input file name: `CouettePoiseuille.ups`

Command used to run input file:

```
mpirun -np 1 sus -solver hypre inputs/UintahRelease/ICE/CouettePoiseuille.ups
```

Postprocessing command:

`inputs/UintahRelease/ICE/compare_CouettePoiseuille.m -uda Couette-Poiseuille.uda`
This Octave script will generate a postscript file CouettePoiseuille.ps

Simulation Domain: 1 x .01 x .01 m

Cell Spacing:
10 x 5 x 10 mm (Level 0)

Example Runtimes:
8ish minutes (1 processor, 2.66 GHz Xeon)

Physical time simulated: 15 sec.

Results

Figure 6.2 shows a comparison of the exact and simulated u velocity at time $t = 15sec$, 5 cells from the end of the domain. The lower plot shows the difference of the velocity $\|u - u_{exact}\|$.

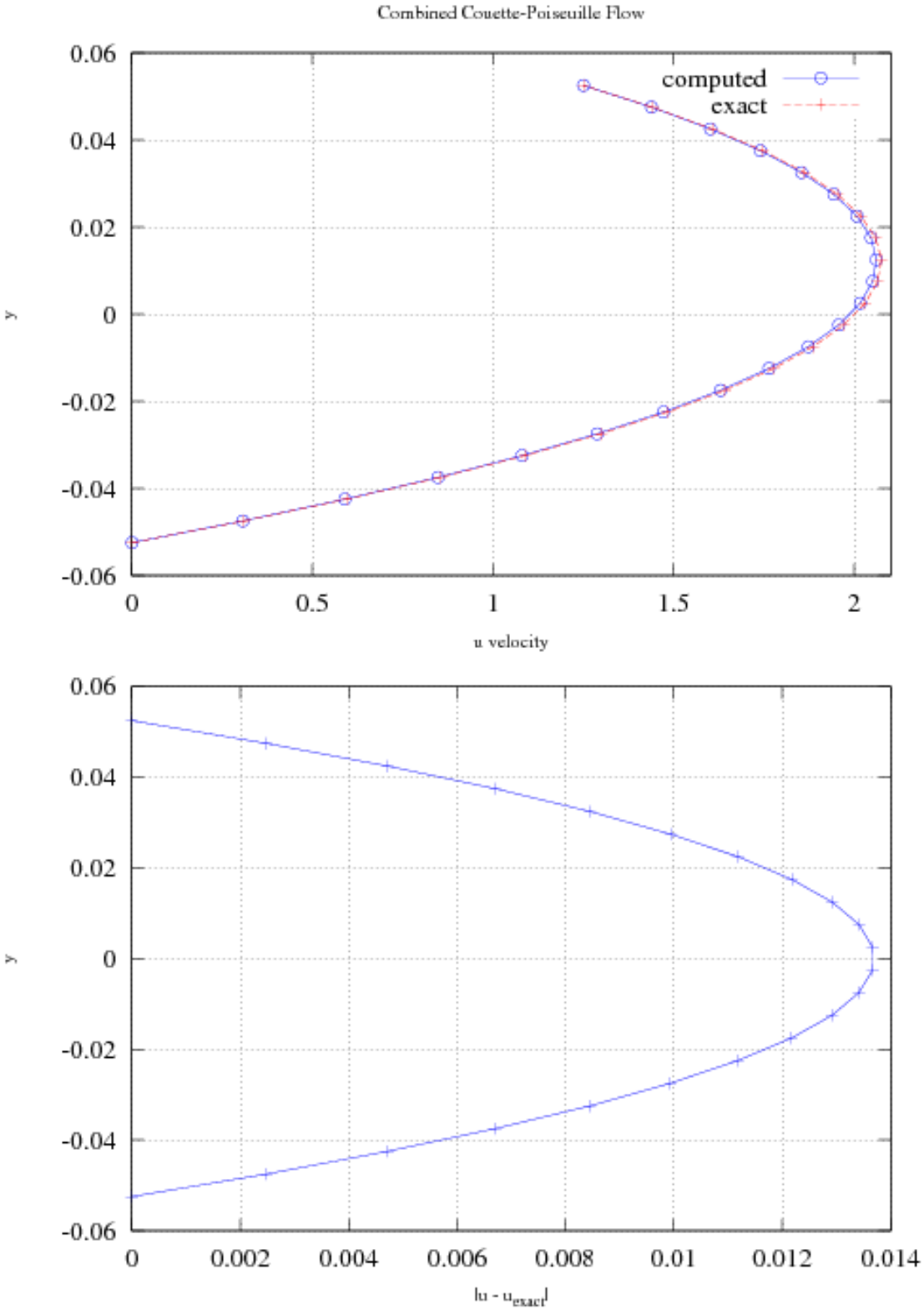

Figure 6.2: Comparison of u velocity $t = 15sec$

Shock Tube

Problem Description

The shock tube problem is a standard 1D compressible flow problem that has been used by many as a validation test case [9, 12, 16]. At time $t = 0$ the computational domain is divided into two separate regions of space by a diaphram, with each region at a different density and pressure. The separated regions are at rest with a uniform temperature $= 300K$. The initial pressure ratio is $\frac{P_R}{P_L} = 10$ and density ratio is $\frac{\rho_R}{\rho_L} = 0.1$ The diaphram is instantly removed and a traveling shockwave, discontinutity and expansion fan form. The expansion fan moves towards the left while the shockwave and contact discontinutity move to the right. This problem tests the algorithm's ability to capture steep gradients and solve Eulers equations.

Simulation Specifics

Component used: ICE

Input file name: `rieman_sm.ups`

Command used to run input file: `sus inputs/UintahRelease/ICE/shockTube.ups`

Postprocessing command:
`inputs/UintahRelease/ICE/plot_shockTube_1L shockTube.uda y`
This Octave script will generate a postscript file shockTube.ps

Simulation Domain: 1 x .001 x .001 m

Cell Spacing:
1 x 1 x 1 mm (Level 0)

Example Runtimes:
1 minute (1 processor, 2.66 GHz Xeon)

Physical time simulated: 0.005 sec.

Results

Figure 6.3 shows a comparison of the exact versus simulated results at time $t = 5msec$.

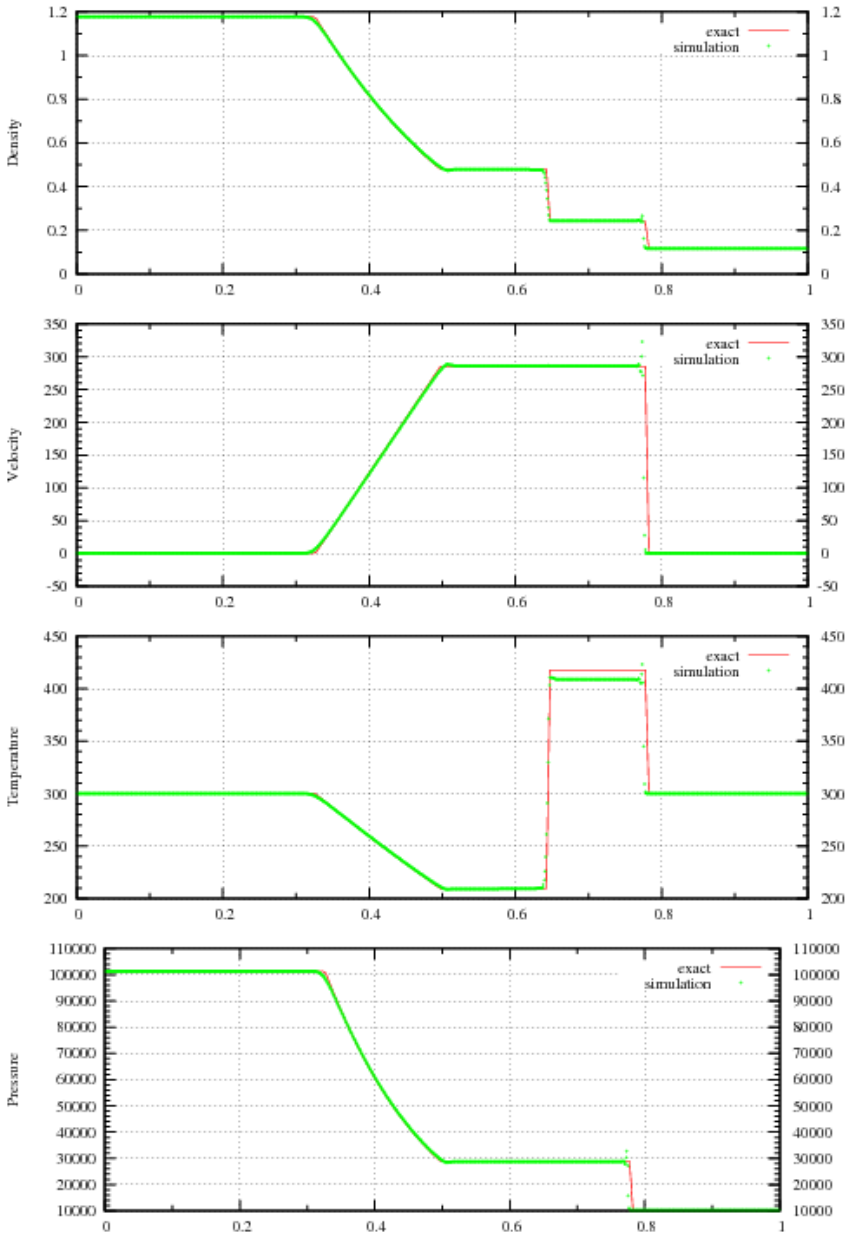

Figure 6.3: Shock tube results at time $t = 5msec$

Shock Tube with Adaptive Mesh Refinement

Simulation Specifics

Component used: ICE

Input file name: `shocktube_AMR.ups`

Command used to run input file:

`sus inputs/UintahRelease/ICE/shocktube_AMR.ups`

Postprocessing command:

`inputs/UintahRelease/ICE/plot_shockTube_AMR shockTube_AMR.uda y`

This Octave script will generate a postscript file shockTube_AMR.ps

Simulation Domain: 1 x .001 x .001 m

Cell Spacing:

10 x 1 x 1 mm (Level 0)
2.5 x 1 x1 mm (Level 1)
0.625 x1 x1 mm (Level 2)

Example Runtimes:

2ish minutes (1 processor, 2.66 GHz Xeon)

Physical time simulated: 0.005 sec.

Results

Figure 6.4 shows a comparison of the exact versus simulated results at time $t = 5msec$.

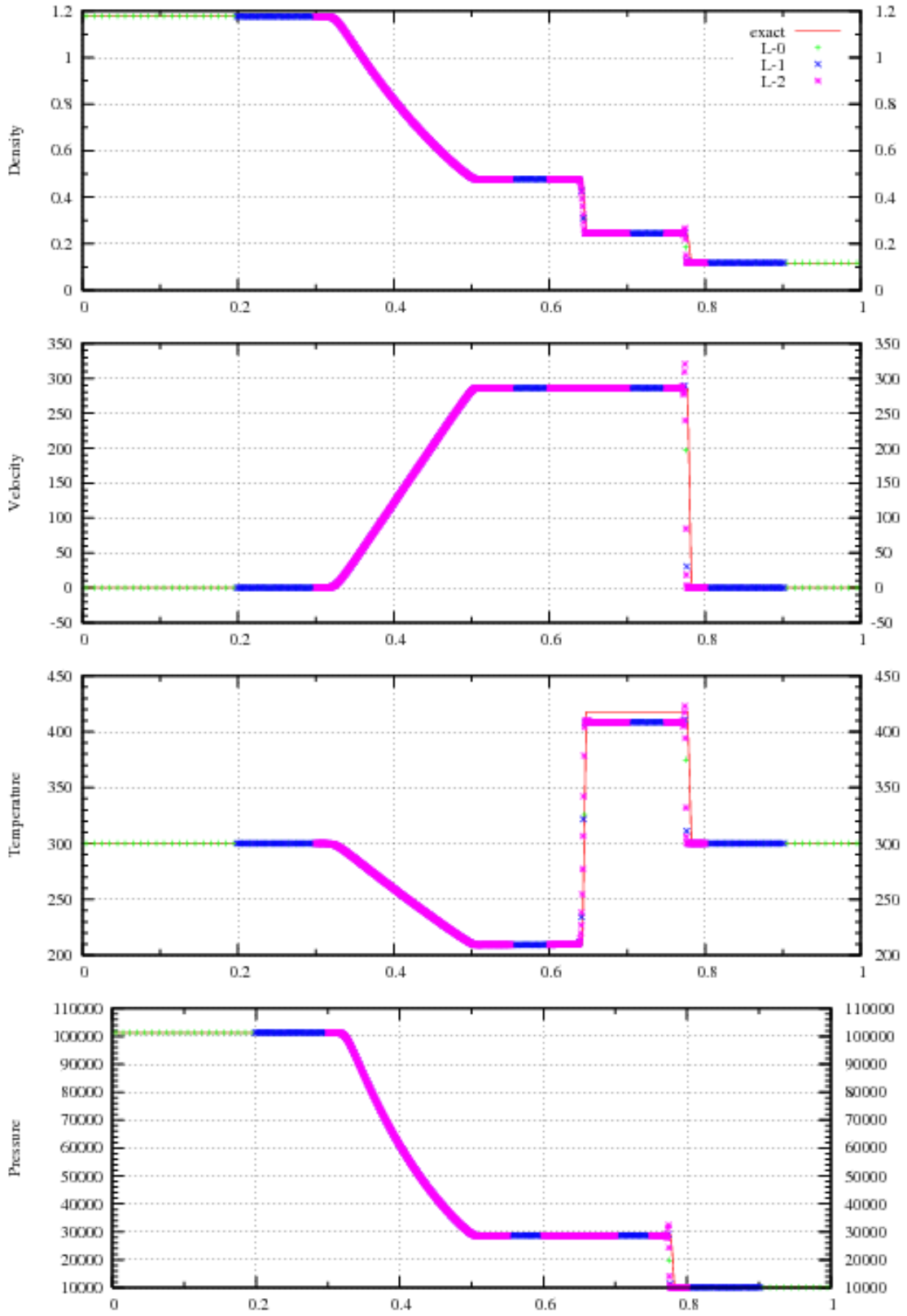

Figure 6.4: Shock tube results at time $t = 5msec$

2D Riemann Problem with Adaptive Mesh Refinement

Problem Description

In two-dimensional Riemann problems there 15 different solutions that combine rarefaction waves, shock waves and a slip line or contact discontinuities [2, 10]. Here we simulate 4 slip lines that form a symmetrical single vortex turning counter clockwise. At time $t = 0$ the computational domain is divided into four quadrants by the lines $x = 1/2, y = 1/2$ The initial condition for $V = (p, \rho, u, v)$ in the four quadrants are $V_{ll} = (1, 1, -0.75, 0.5), V_{lr} = (1, 3, -0.75, -0.5), V_{ul} = (1, 2, 0.75, 0.5), V_{ur} = (1, 1, 0.75, -0.5)$ where, p is pressure, ρ is the density of the polytropic gas, u and v are the x and y component of velocity.

Simulation Specifics

Component used: ICE

Input file name: `riemann2D_AMR.ups`

Command used to run input file:

```
mpirun -np 5 sus inputs/UintahRelease/ICE/riemann2D_AMR.ups
```

VisIT session file: `inputs/UintahRelease/ICE/riemann2D.session`

Simulation Domain: 0.96 x 0.96m x 0.1 m

Cell Spacing:

40 x 40 x 1 mm (Level 0)
10 x 10 x 1 mm (Level 1)
2.5 x 2.5 x 1 mm (Level 2)

Example Runtimes:

5ish minutes (5 processors, 2.66 GHz Xeon)

Physical time simulated: 0.3 sec.

Results

Figure 6.5 shows a flood and line contour plot(s) of the density of the gas at 0.03sec.

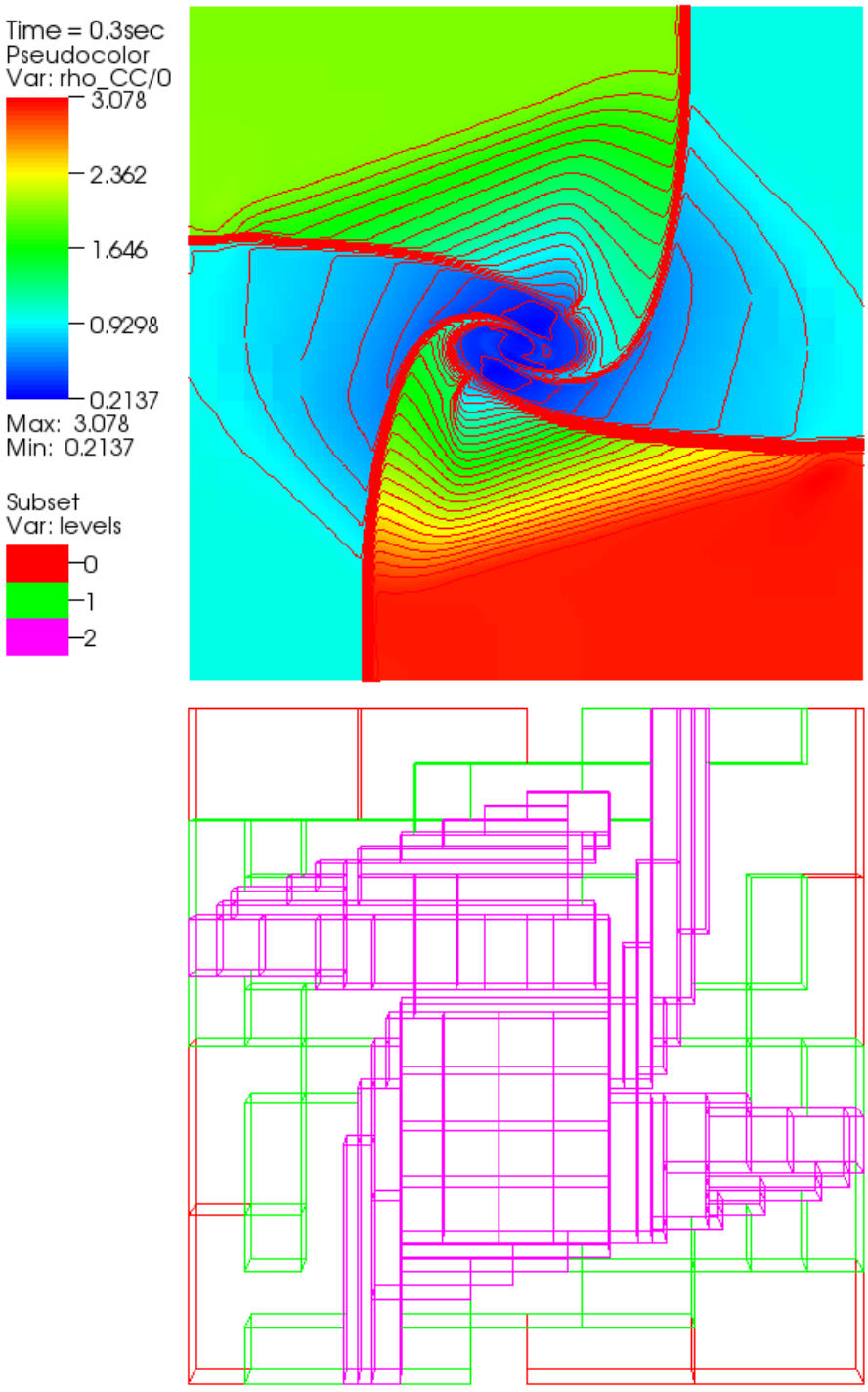

Figure 6.5: Contour plot of density for the 2D Riemann problem at time $t = 0.3sec$. Bottom plot shows the outline of the patches on the 3 levels.

Explosion 2D

Problem Description

For the multidimensional blast wave orexplosion test is a standard compressible flow problem that has been used by many as a validation test case. At time $t = 0$ there is a circular region of gas at the center of the domain at a relatively high pressure and density. The expansion of high pressure gas forms a circular shock wave and contact surface that expands into surrounding atmosphere. At the same time a circular rarefaction travels towards the origin. As the shock wave and contact surface move outwards they become weaker and at some point the contact reverses direction and travels inward. The rarefraction reflects from the center and forms an overexpanded region, creating a shock that travels inward [16]. At time $t = 0$ the computational domain is divided into two region, circular high pressure region with a radius $R = 0.4$ and the surrounding box 2x2x0.1. The initial condition inside of the circular region were $(p = 1, \rho = 1, u = 0, v = 0)$ and outside $(p = 0.1, \rho = 0.125, u = 0, v = 0)$. The fluid was an ideal, inviscid, polytropic gas.

Simulation Specifics

Component used: ICE

Input file name: `Explosion.ups`

Command used to run input file:

```
mpirun -np 4 sus inputs/UintahRelease/ICE/Explosion.ups
```

Visualization net file: `inputs/UintahRelease/ICE/Explosion.session`

Postprocessing command:

`inputs/ICE/Scripts/plot_explosion_AMR Explosion_AMR.uda y`
This Octave script will generate a postscript file explosion_AMR.ps

Simulation Domain: 2 x 2 x .1

Cell Spacing:

62.5 x 62.5 x 10 (Level 0)
15.625 x 15.625 x 10 (Level 1)
3.9 x 3.9 x 10 (Level 2)

Example Runtimes:

20 minutes (4 processor, 2.66 GHz Xeon)

Physical time simulated: 0.25 (non-dimensional).

Results

Figures 6.6 and 6.7 shows surface plots of the pressure and density at $t = 0.25$. Since this test is symetrical we can use results from the equivalent 1 dimensional problem to compare against

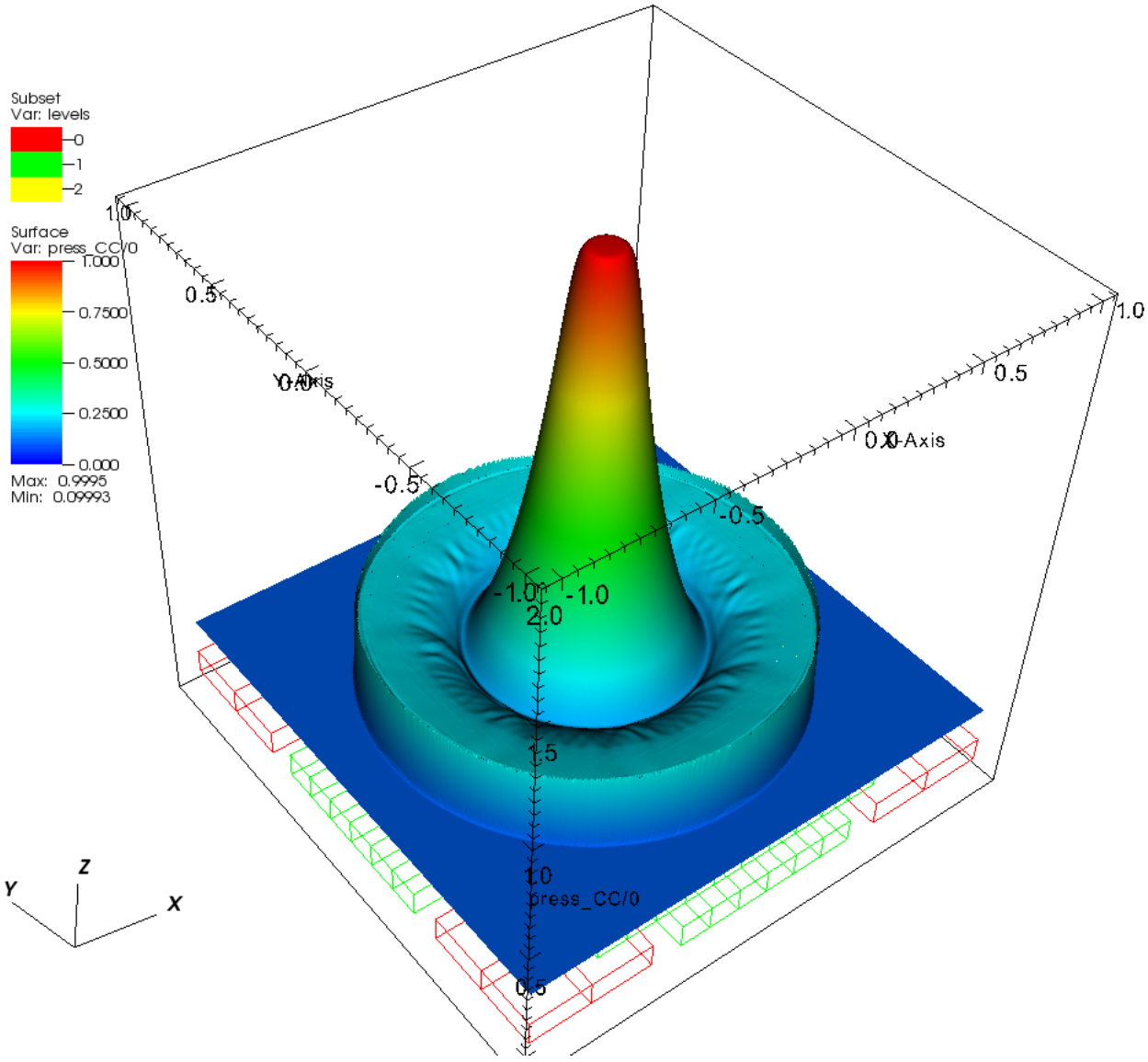

Figure 6.6: Pressure field at $t = 0.25$

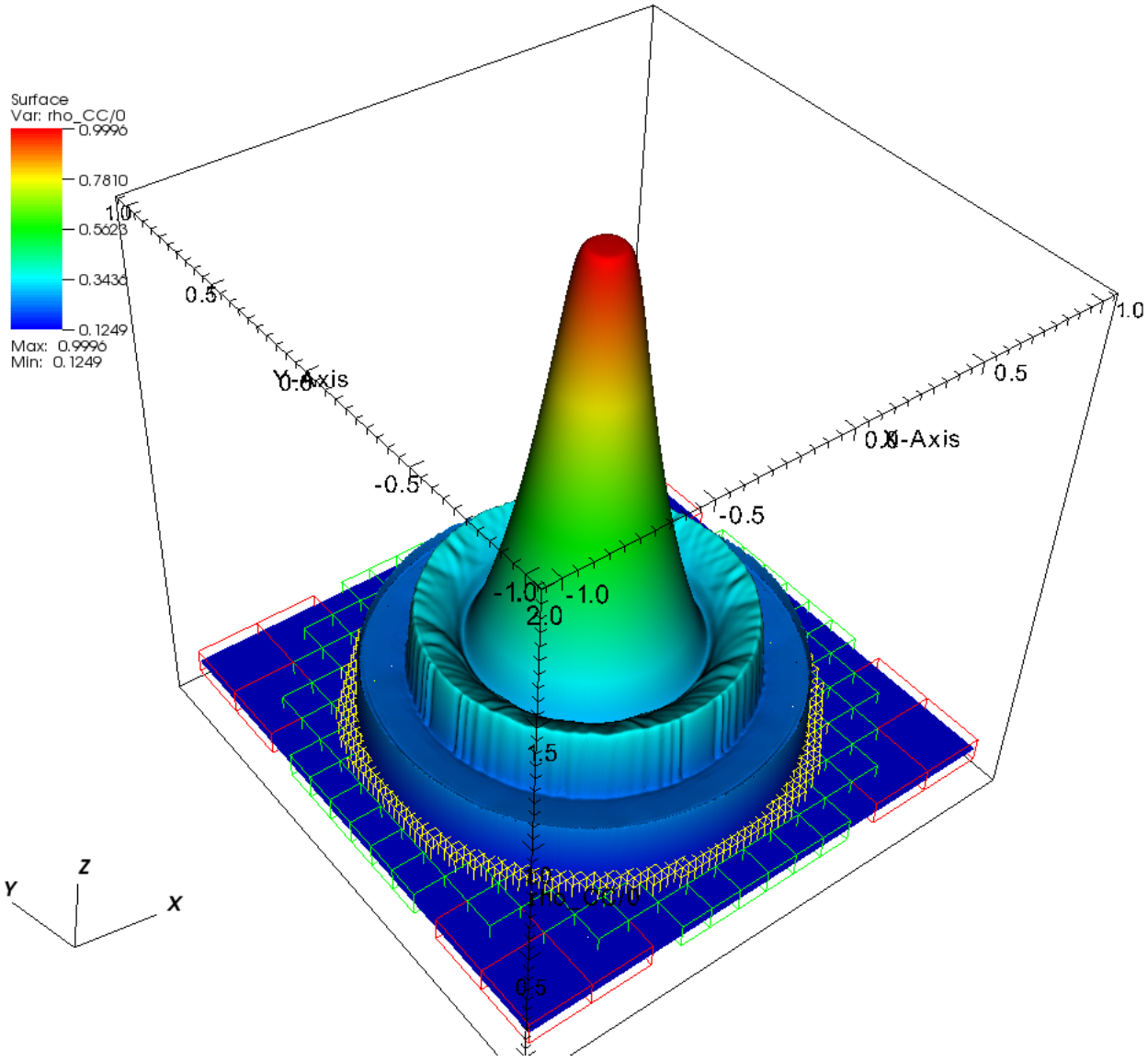

Figure 6.7: Density field at time $t = 0.25$

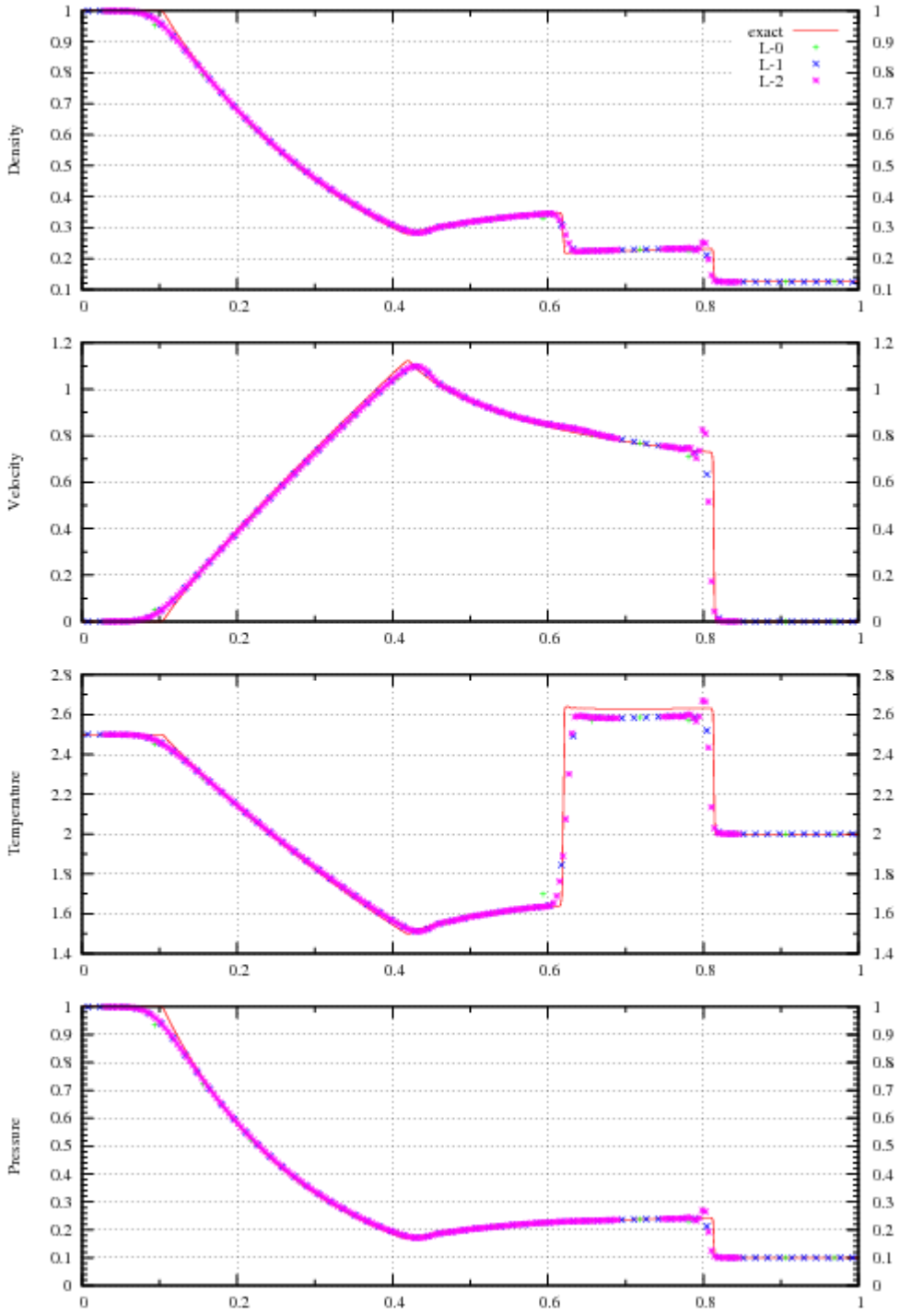

Figure 6.8: $t = 0.25$

ANFO Rate Stick

Problem Description

A cylindrical stick ($r = 8mm$) of Ammonium Nitrate Fuel Oil (ANFO) given an initial velocity of $90m/s$. As it strikes the domain boundary, pressure is generated sufficient to reach the initial pressure required to activate the JWL++ [11] detonation model. This empirically based model results in a steady state detonation that traverses the stick, consuming the solid explosive and generating high pressure gas. The experimentally observed curvature is generated at the detonation front, a feature that will not develop in programmed burn models. By running this simulation at a variety of cylinder radii, one can observe the "size effect", namely that cylinders of larger radii will reach a higher steady state detonation velocity, due to the increased effective confinement. An infinite radius case can be simulated by shrinking the computational domain to one cell in each of the transverse directions.

Simulation Specifics

Component used: ICE

Input file name: `JWLpp8mmRS.ups`

Command used to run input file:

```
mpirun -np 4 sus inputs/UintahRelease/ICE/JWLpp8mmRS.ups
```

Visualization net file: `inputs/UintahRelease/ICE/RateStick.session`

Simulation Domain: 0.1 m x 0.015 m x 0.015 m

Cell Spacing:
0.0005 x 0.0005 x 0.0005 (Level 0)

Example Runtimes:
1.5 hours (4 processor, 3.16 GHz Xeon)

Physical time simulated: 20.0 μseconds

Results

Figure 6.9 shows a volume rendering of the density of the reactant. Note the curvature of the reaction zone.

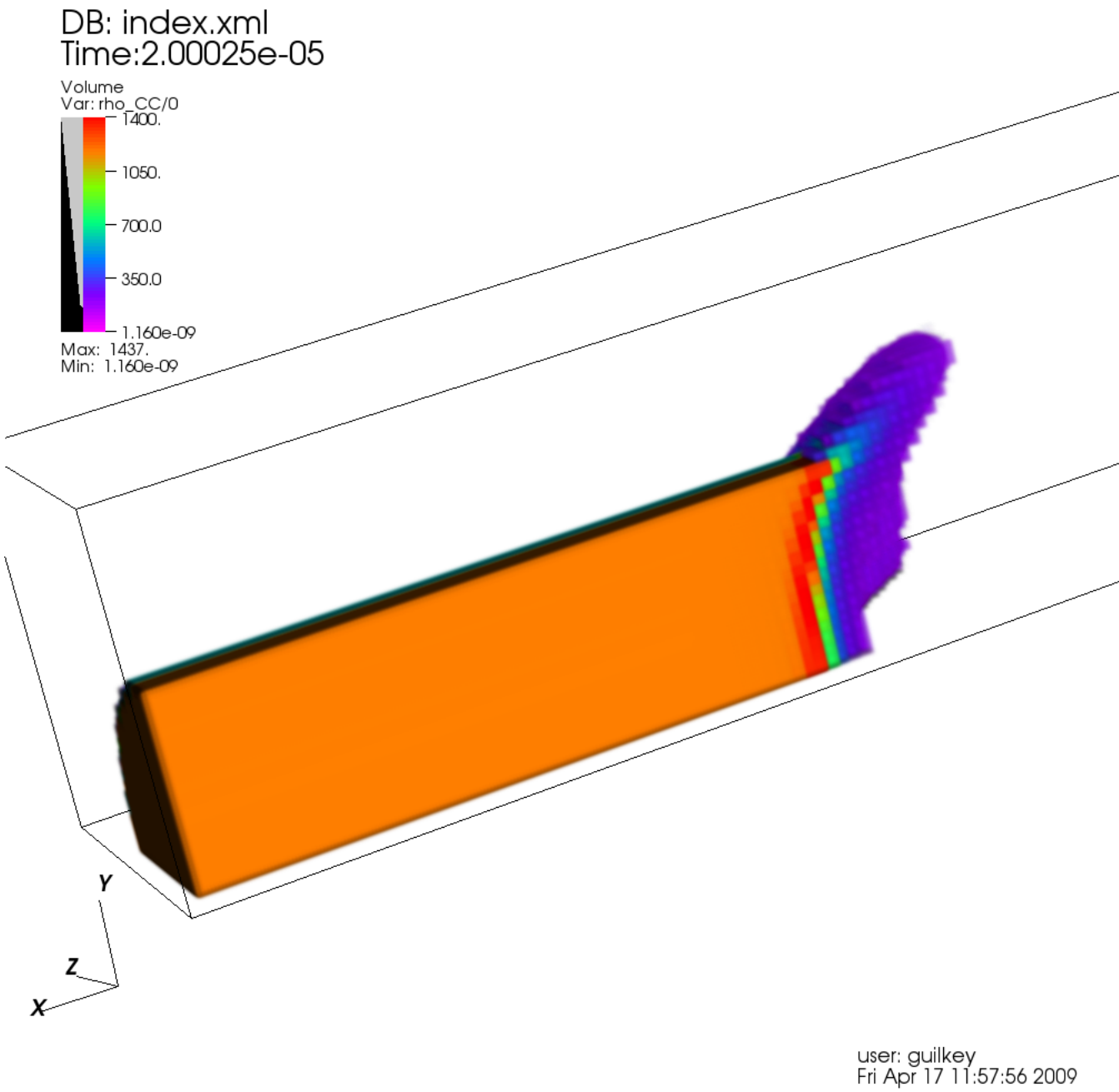

Figure 6.9: Density of reactant material.

Bibliography

[1] A. Bejan. *Advanced Engineering Thermodynamics*. John Wiley and Sons, USA, 1988.

[2] J. P. Collins C. W. Schulz-Rinne and H. M. Glaz. Numerical solution of the riemann problem for two-dimensional gas dynamics. *J. Comput. Phys*, 14:1394–1414, 1993.

[3] R.D. Falgout, J.E. Jones, and U.M. Yang. The design and implementation of hypre, a library of parallel high performance preconditioners. In A.M. Bruaset and A. Tveito, editors, *Numerical Solution of Partial Differential Equations on Parallel Computers*, Lecture Notes in Computational Science and Engineering. Springer-Verlag, 2006.

[4] G. R. Gathers. *Selected Topics in Shock Wave Physics and Equation of State Modeling*. World Scientific, River Edge, NJ, 1994.

[5] F.H. Harlow and A.A. Amsden. Numerical calculation of almost incompressible flow. *J. Comp. Phys.*, 3:80–93, 1968.

[6] B.A. Kashiwa. A multifield model and method for fluid-structure interaction dynamics. Technical Report LA-UR-01-1136, Los Alamos National Laboratory, Los Alamos, 2001.

[7] B.A. Kashiwa and R.M. Rauenzahn. A cell-centered ICE method for multiphase flow simulations. Technical Report LA-UR-93-3922, Los Alamos National Laboratory, Los Alamos, 1994.

[8] B.A. Kashiwa and R.M. Rauenzahn. A multimaterial formalism. Technical Report LA-UR-94-771, Los Alamos National Laboratory, Los Alamos, 1994.

[9] C. B. Laney. *Computational Gasdynamics*. Cambridge University Press, Cambridge, 1998.

[10] R. Liska and B. Wendroff. Comparison of several difference schemes on 1d and 2d test problems for the euler equations. *J. Comput. Phys*, 25:995–1017, 2003.

[11] P. C. Souers S. Anderson J. Mercer E. McGuire and P. Vitello. Jwl++: A simple reactive flow code package for detonation. *Propellants, Explosives, Pyrotechnics*, 25:54–58, 2000.

[12] G. A. Sod. A survey of several finite difference methods for systems of nonlinear hyperbolic conservation laws. *J. Comput. Phys*, 27:1–31, 1978.

[13] J. C. Sutherland and Kenndey C.A. Improved boundary conditions for viscous, reacting compressible flows. *Journal of Computational Physics*, 191:502–524, 2003.

[14] P. A. Thompson. *Compressible-Fluid Dynamics*. McGraw-Hill, New York, 1988.

[15] J. S. Thomsen and T. J. Hartka. Strange carnot cycles; thermodynamics fo a system with a density extremum. *Am. J. Phys.*, 30:26–33, 1962.

[16] E. F. Toro. *Riemann Solvers and Numerical Methods for Fluid Dynamics*. Springer, Berlin Heidelberg, 1997.

[17] F. M. White. *Viscous Fluid Flow, 2nd Edition*. McGraw-Hill, 1991.

Chapter 7

MPM

7.1 Introduction

The material point method (MPM) was described by Sulsky et al. [50, 52] as an extension to the FLIP (Fluid-Implicit Particle) method of Brackbill [11], which itself is an extension of the particle-in-cell (PIC) method of Harlow [26]. Interestingly, the name "material point method" first appeared in the literature two years later in a description of an axisymmetric form of the method [51]. In both FLIP and MPM, the basic idea is the same: objects are discretized into particles, or material points, each of which contains all state data for the small region of material that it represents. This includes the position, mass, volume, velocity, stress and state of deformation of that material. MPM differs from other so called "mesh-free" particle methods in that, while each object is primarily represented by a collection of particles, a computational mesh is also an important part of the calculation. Particles do not interact with each other directly, rather the particle information is accumulated to the grid, where the equations of motion are integrated forward in time. This time advanced solution is then used to update the particle state.

The method usually uses a regular structured grid as a computational mesh. While this grid, in principle, deforms as the material that it is representing deforms, at the end of each timestep, it is reset to its original undeformed position, in effect providing a new computational grid for each timestep. The use of a regular structured grid for each time step has a number of computational advantages. Computation of spatial gradients is simplified. Mesh entanglement, which can plague fully Lagrangian techniques, such as the Finite Element Method (FEM), is avoided. MPM has also been successful in solving problems involving contact between colliding objects, having an advantage over FEM in that the use of the regular grid eliminates the need for doing costly searches for contact surfaces[6].

In addition to the advantages that MPM brings, as with any numerical technique, it has its own set of shortcomings. It is computationally more expensive than a comparable FEM code. Accuracy for MPM is typically lower than FEM, and errors associated

with particles moving around the computational grid can introduce non-physical oscillations into the solution. Finally, numerical difficulties can still arise in simulations involving large deformation that will prematurely terminate the simulation. The severity of all of these issues (except for the expense) has been significantly reduced with the introduction of the Generalized Interpolation Material Point Method, or GIMP[8]. The basic concepts associated with GIMP will be described below. Throughout this document, MPM (which ends up being a special case of GIMP) will frequently be referred to interchangably with GIMP.

In addition, MPM can be incorporated with a multi-material CFD algorithm as the structural component in a fluid-structure interaction formulation. This capability was first demonstrated in the CFDLIB codes from Los Alamos by Bryan Kashiwa and co-workers[32]. There, as in the Uintah-MPMICE component, MPM serves as the Lagrangian description of the solid material in a multimaterial CFD code. Certain elements of the solution procedure are based in the Eulerian CFD algorithm, including intermaterial heat and momentum transfer as well as satisfaction of a multimaterial equation of state. The use of a Lagrangian method such as MPM to advance the solution of the solid material eliminates the diffusion typically associated with Eulerian methods. The Uintah-MPM component will be described in later chapter of this manual.

Subsequent sections of this chapter will first give a relatively brief description of the MPM and GIMP algorithms. This will, of course, be focused mainly on describing the capabilities of the Uintah-MPM component. This is followed by a section that attempts to relate the information in Section 7.2 to the implementation in Uintah. Following that is a description of the information that goes into an input file. Finally, a number of examples are provided, along with representative results.

7.2 Algorithm Description

Time and space prohibit an exhaustive description of the theoretical underpinnings of the Material Point Method. Here we will concentrate on the discrete equations that result from applying a weak form analysis to the governing equations. The interested reader should consult [50, 52] for the development of these discrete equations in MPM, and [8] for the development of the equations for the GIMP method. These end up being very similar, the differences in how the two developments affect implementation will be described in Section 7.3.

In solving a structural mechanics problem with MPM, one begins by discretizing the object of interest into a suitable number of particles, or "material points". (**Aside:** What constitutes a suitable number is something of an open question, but it is typically advisable to use at least two particles in each computational cell in each direction, i.e. 4 particles per cell (PPC) in 2-D, 8 PPC in 3-D. In choosing the resolution of the computational grid, similar considerations apply as for any computational method

(trade-off between time to solution and accuracy, use of resolution studies to ensure convergence in results, etc.).) Each of these particles will carry, minimally, the following variables:

- position - $\mathbf{x}_p$
- mass - m_p
- volume - v_p
- velocity - $\mathbf{v}_p$
- stress - $\boldsymbol{\sigma}_p$
- deformation gradient - $\mathbf{F}_p$

The description that follows is a recipe for advancing each of these variables from the current (discrete) time n to the subsequent time $n+1$. Note that particle mass, m_p, typically remains constant throughout a simulation unless solid phase reaction models are utilized, a feature that is not present in Uintah-MPM. (Such models are available in MPMICE, see Section 8.) It is also important to point out that the algorithm for advancing the timestep is based on the so-called Update Stress Last (USL) algorithm. The superiority of this approach over the Update Stress First (USF) approach was clearly demonstrated by Wallstedt and Guilkey [56]. USF was the formulation used in Uintah until mid-2008.

The discrete momentum equation that results from the weak form is given as:

$$\mathbf{ma} \quad = \quad \mathbf{F}^{\text{ext}} - \mathbf{F}^{\text{int}} \tag{7.1}$$

where $\mathbf{m}$ is the mass matrix, $\mathbf{a}$ is the acceleration vector, $\mathbf{F}^{\text{ext}}$ is the external force vector (sum of the body forces and tractions), and $\mathbf{F}^{\text{int}}$ is the internal force vector resulting from the divergence of the material stresses. The construction of each of these quantities, which are based at the nodes of the computational grid, will be described below.

The solution begins by accumulating the particle state on the nodes of the computational grid, to form the mass matrix $\mathbf{m}$ and to find the nodal external forces $\mathbf{F}^{\text{ext}}$, and velocities, $\mathbf{v}$. In practice, a lumped mass matrix is used to avoid the need to invert a system of equations to solve Eq. 7.1 for acceleration. These quantities are calculated at individual nodes by the following equations, where the $\sum_p$ represents a summation over all particles:

$$m_i = \sum_p S_{ip} m_p, \qquad \mathbf{v}_i = \frac{\sum_p S_{ip} m_p \mathbf{v}_p}{m_i}, \qquad \mathbf{F}_i^{\text{ext}} \quad = \quad \sum_p S_{ip} \mathbf{F}_p^{\text{ext}} \tag{7.2}$$

and i refers to individual nodes of the grid. m_p is the particle mass, $\mathbf{v}_p$ is the particle velocity, and $\mathbf{F}_p^{\text{ext}}$ is the external force on the particle. The external forces that start on the particles typically the result of tractions, the application of which will be discussed in Section 7.5. S_{ip} is the shape function of the ith node evaluated at $\mathbf{x}_p$. The functional form of the shape functions differs between MPM and GIMP. This difference is discussed in Section 7.3.

Following the operations in Eq. 7.2, $\mathbf{F}^{\text{int}}$ is still required in order to solve for acceleration at the nodes. This is computed at the nodes as a volume integral of the divergence of the stress on the particles, specifically:

$$\mathbf{F}_i^{\text{int}} = \sum_p \mathbf{G}_{ip}\boldsymbol{\sigma}_p v_p, \tag{7.3}$$

where $\mathbf{G}_{ip}$ is the gradient of the shape function of the ith node evaluated at $\mathbf{x}_p$, and $\boldsymbol{\sigma}_p$ and v_p are the time n values of particle stress and volume respectively.

Equation 7.1 can then be solved for $\mathbf{a}$.

$$\mathbf{a}_i = \frac{\mathbf{F}_i^{\text{ext}} - \mathbf{F}_i^{\text{int}}}{m_i} \tag{7.4}$$

An explicit forward Euler method is used for the time integration:

$$\mathbf{v}_i^L = \mathbf{v}_i + \mathbf{a}_i \Delta t \tag{7.5}$$

The time advanced grid velocity, $\mathbf{v}^L$ is used to compute a velocity gradient at each particle according to:

$$\nabla \mathbf{v}_p = \sum_i \mathbf{G}_{ip}\mathbf{v}_i^L \tag{7.6}$$

This velocity gradient is used to update the particle's deformation gradient, volume and stress. First, an incremental deformation gradient is computed using the velocity gradient:

$$\mathbf{dF}_p^{n+1} = (\mathbf{I} + \nabla \mathbf{v}_p \Delta t) \tag{7.7}$$

Particle volume and deformation gradient are updated by:

$$v_p^{n+1} = \text{Det}(\mathbf{dF}_{\text{p}}^{\text{n+1}})\text{v}_{\text{p}}^{\text{n}}, \qquad \mathbf{F}_{\text{p}}^{\text{n+1}} = \mathbf{dF}_{\text{p}}^{\text{n+1}}\mathbf{F}_{\text{p}}^{\text{n}} \tag{7.8}$$

Finally, the velocity gradient, and/or the deformation gradient are provided to a constitutive model, which outputs a time advanced stress at the particles. Specifics of this operation will be further discussed in Section 7.5

At this point in the timestep, the particle position and velocity are explicitly updated by:

$$\mathbf{v}_p(t+\Delta t) = \mathbf{v}_p(t) + \sum_i S_{ip}\mathbf{a}_i\Delta t \tag{7.9}$$

$$\mathbf{x}_p(t+\Delta t) = \mathbf{x}_p(t) + \sum_i S_{ip}\mathbf{v}_i^L\Delta t \tag{7.10}$$

This completes one timestep, in that the update of all six of the variables enumerated above (with the exception of mass, which is assumed to remain constant) has been accomplished. Conceptually, one can imagine that, since an acceleration and velocity were computed at the grid, and an interval of time has passed, the grid nodes also experienced a displacement. This displacement also moved the particles in an isoparametric fashion. In practice, particle motion is accomplished by Equation 7.10, and the grid never deforms. So, while the MPM literature will often refer to resetting the grid to its original configuration, in fact, this isn't necessary as the grid nodes never leave that configuration. Regardless, at this point, one is ready to advance to the next timestep.

The algorithm described above is the core of the Uintah-MPM implementation. However, it neglects a number of important considerations. The first is kinematic boundary conditions on the grid for velocity and acceleration. The manner in which these are handled will be described in Section 7.4. Next, is the use of advanced contact algorithms. By default, MPM enforces no-slip, no-interpenetration contact. This feature is extremely useful, but it also means that two bodies initially in "contact" (meaning that they both contain particles whose data are accumulated to common nodes) behave as if they are a single body. To enable multi-field simulations with frictional contact, or to impose displacement based boundary conditions, e.g. a rigid piston, additional steps must be taken. These steps implement contact formulations such as that described by Bardenhagen, et al.[7]. The *use* of the contact algorithms is described in Section 7.5, but the reader will be referred to the relevant literature for their development. Lastly, heat conduction is also available in the explicit MPM code, although it may be neglected via a run time option in the input file. Explicit MPM is typically used for high rate simulations in which heat conduction is negligible.

7.3 Shape functions for MPM and GIMP

In both MPM and GIMP, the basic idea is the same: objects are discretized into particles, or material points, each of which contains all state data for the small region of material that it represents. In MPM, these particles are spatially Dirac delta functions, meaning that the material that each represents is assumed to exist at a single point in space, namely the position of the particle. Interactions between the particles and the

grid take place using weighting functions, also known as shape functions or interpolation functions. These are typically, but not necessarily, linear, bilinear or trilinear in one, two and three dimensions, respectively.

More recently, Bardenhagen and Kober [8] generalized the development that gives rise to MPM, and suggested that MPM may be thought of as a subset of their "Generalized Interpolation Material Point" (GIMP) method. In the family of GIMP methods one chooses a characteristic function χ_p to represent the particles and a shape function S_i as a basis of support on the computational nodes. An effective shape function $\bar{S}_{ip}$ is found by the convolution of the χ_p and S_i which is written as:

$$\bar{S}_{ip}(\mathbf{x}_p) = \frac{1}{V_p} \int_{\Omega_p \cap \Omega} \chi_p(\mathbf{x} - \mathbf{x}_p) S_i(\mathbf{x}) \, \mathrm{d}\mathbf{x}. \tag{7.11}$$

While the user has significant latitude in choosing these two functions, in practice, the choice of S_i is usually given (in one-dimension) as,

$$S_i(x) = \begin{cases} 1 + (x - x_i)/h & -h < x - x_i \leq 0 \\ 1 - (x - x_i)/h & 0 < x - x_i \leq h \\ 0 & \text{otherwise,} \end{cases} \tag{7.12}$$

where x_i is the vertex location, and h is the cell width, assumed to be constant in this formulation, although this is not a general restriction on the method. Multi-dimensional versions are constructed by forming tensor products of the one-dimensional version in the orthogonal directions.

When the choice of characteristic function is the Dirac delta,

$$\chi_p(\mathbf{x}) = \delta(\mathbf{x} - \mathbf{x}_p) V_p, \tag{7.13}$$

where $\mathbf{x}_p$ is the particle position, and V_p is the particle volume, then traditional MPM is recovered. In that case, the effective shape function is still that given by Equation 7.12. Its gradient is given by:

$$G_i(x) = \begin{cases} 1/h & -h < x - x_i \leq 0 \\ -1/h & 0 < x - x_i \leq h \\ 0 & \text{otherwise,} \end{cases} \tag{7.14}$$

Plots of Equations 7.12 and 7.14 are shown below. The discontinuity in the gradient gives rise to poor accuracy and stability properties.

Typically, when an analyst indicates that they are "using GIMP" this implies use of the linear grid basis function given in Eq. 7.12 and a "top-hat" characteristic function, given by (in one-dimension),

$$\chi_p(x) = H(x - (x_p - l_p)) - H(x - (x_p + l_p)), \tag{7.15}$$

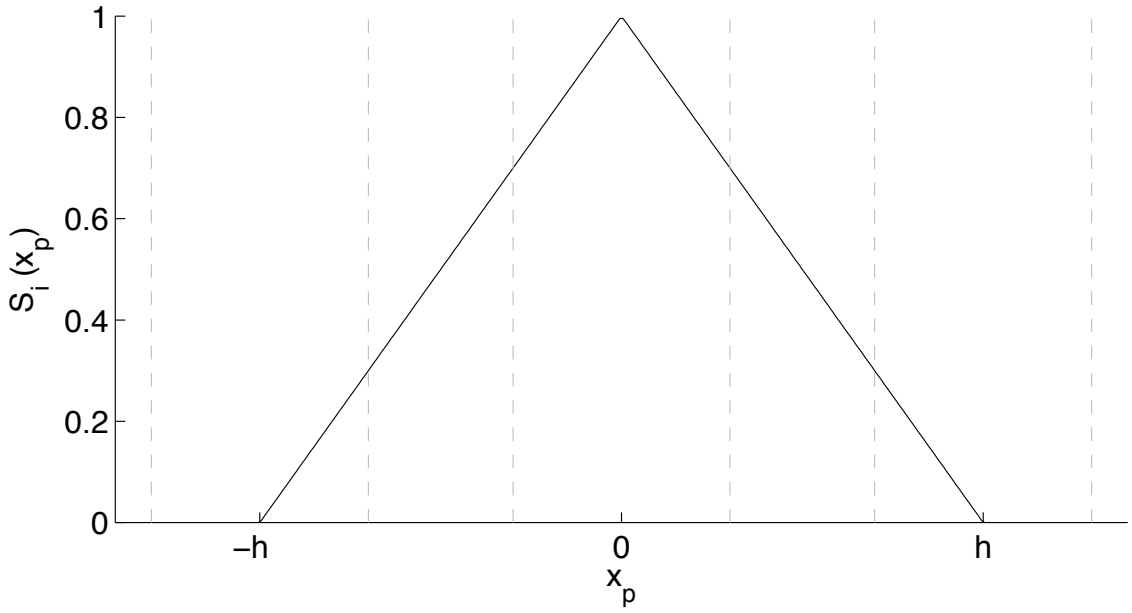

Figure 7.1: Effective shape function when using traditional MPM.

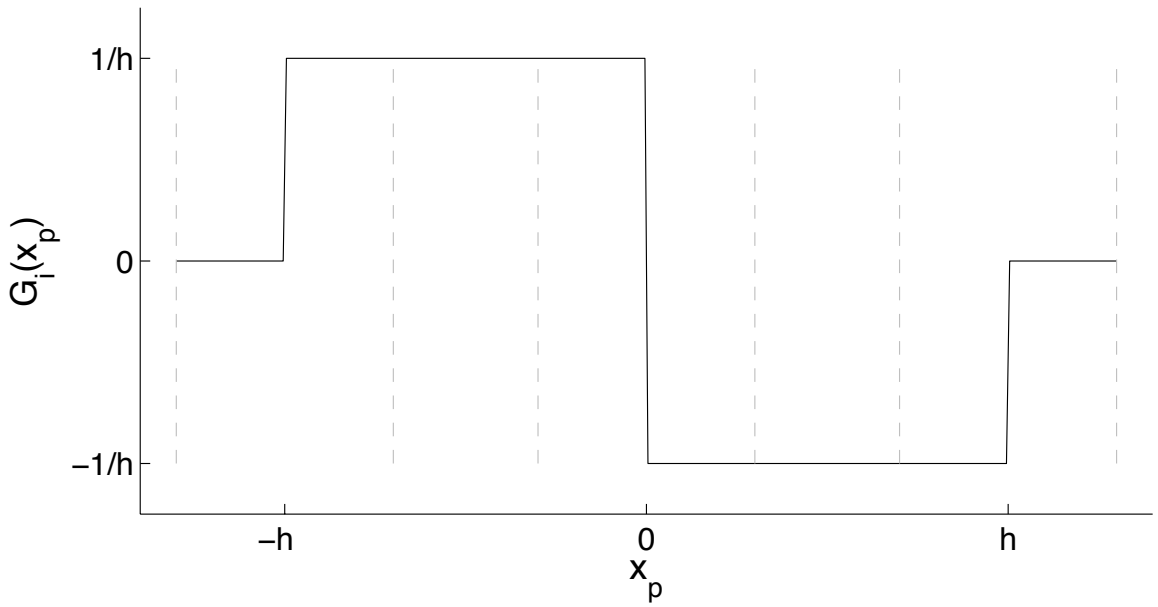

Figure 7.2: Gradient of the effective shape function when using traditional MPM.

where $H(x)$ is the Heaviside function ($H(x) = 0$ if $x < 0$ and $H(x) = 1$ if $x \geq 0$) and l_p is the half-length of the particle. When the convolution indicated in Eq. 7.11 is carried out using the expressions in Eqns. 7.12 and 7.15, a closed form for the effective shape function can be written as:

$$S_i(x_p) = \begin{cases} \frac{(h+l_p+(x_p-x_i))^2}{4hl_p} & -h-l_p < x_p - x_i \leq -h+l_p \\ 1 + \frac{(x_p-x_i)}{h} & -h+l_p < x_p - x_i \leq -l_p \\ 1 - \frac{(x_p-x_i)^2+l_p^2}{2hl_p} & -l_p < x_p - x_i \leq l_p \\ 1 - \frac{(x_p-x_i)}{h} & l_p < x_p - x_i \leq h-l_p \\ \frac{(h+l_p-(x_p-x_i))^2}{4hl_p} & h-l_p < x_p - x_i \leq h+l_p \\ 0 & \text{otherwise,} \end{cases} \tag{7.16}$$

The gradient of which is:

$$G_i(x_p) = \begin{cases} \frac{h+l_p+(x_p-x_i)}{2hl_p} & -h-l_p < x_p - x_i \leq -h+l_p \\ \frac{1}{h} & -h+l_p < x_p - x_i \leq -l_p \\ -\frac{(x_p-x_i)}{hl_p} & -l_p < x_p - x_i \leq l_p \\ -\frac{1}{h} & l_p < x_p - x_i \leq h-l_p \\ -\frac{h+l_p-(x_p-x_i)}{2hl_p} & h-l_p < x_p - x_i \leq h+l_p \\ 0 & \text{otherwise,} \end{cases} \tag{7.17}$$

Plots of Equations 7.16 and 7.17 are shown below. The continuous nature of the gradients are largely responsible for the improved robustness and accuracy of GIMP over MPM.

There is one further consideration in defining the effective shape function, and that is whether or not the size (length in 1-D) of the particle is kept fixed (denoted as "UGIMP" here) or is allowed to evolve due to material deformations ("Finite GIMP" or "Contiguous GIMP" in (1) and "cpGIMP" here). In one-dimensional simulations, evolution of the particle (half-)length is straightforward,

$$l_p^n = F_p^n l_p^0, \tag{7.18}$$

where F_p^n is the deformation gradient at time n. In multi-dimensional simulations, a similar approach can be used, assuming an initially rectangular or cuboid particle, to find the current particle shape. The difficulty arises in evaluating Eq. 7.11 for these general shapes. One approach, apparently effective, has been to create a cuboid that circumscribes the deformed particle shape [35]. Alternatively, one can assume that the particle size remains constant (insofar as it applies to the effective shape function evaluations only). This is the approach currently implemented in Uintah.

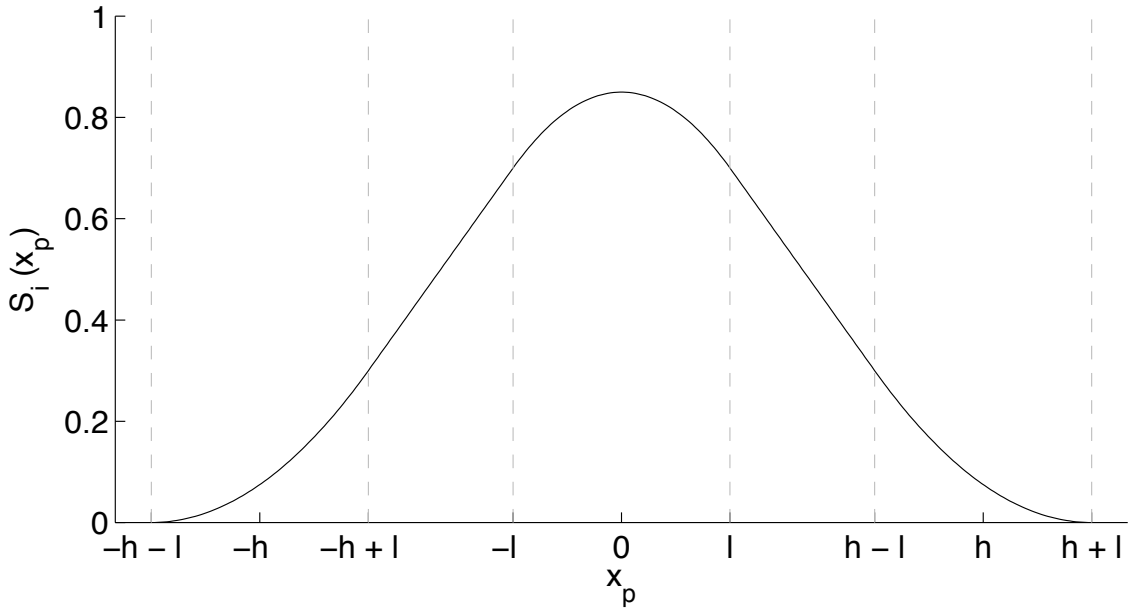

Figure 7.3: Effective shape function when using GIMP.

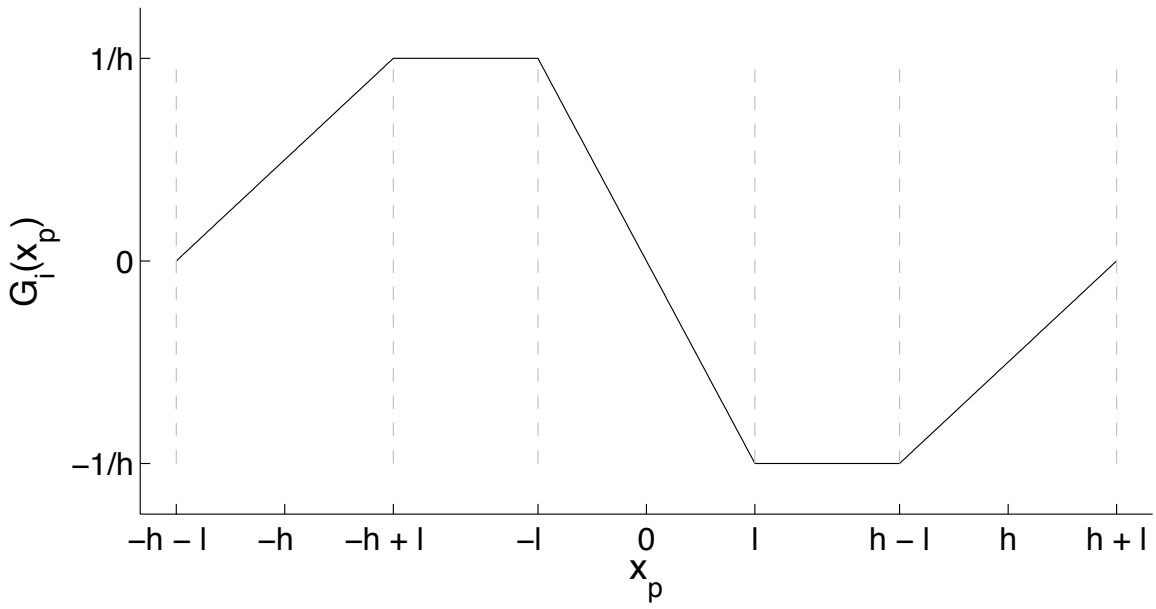

Figure 7.4: Gradient of the effective shape function when using GIMP.

7.4 Uintah Implementation

Users of Uintah-MPM needn't necessarily bother themselves with the implementation in code of the algorithm described above. This section is intended to serve as a reference for users who find themselves needing to modify the source code, or those who are simply interested. Anyone just wishing to run MPM simulations may skip ahead to Sections 7.5 and 7.6. The goal of this section is to provide a mapping from the the algorithm described above to the software that carries it out. This won't be exhaustive, but will be a good starting point for the motivated reader.

The source code for the Uintah-MPM implementation can be found in

```
src/CCA/Components/MPM
```

Within that directory are a number of files and subdirectories, these will be discussed as needed. For the moment, consider the various files that end in "MPM.cc":

```
AMRMPM.cc  FractureMPM.cc  ImpMPM.cc  RigidMPM.cc  SerialMPM.cc  ShellMPM.cc
```

`AMRMPM.cc` is the nascent beginnings of an AMR implementation of MPM. It is far from complete and should be ignored. `FractureMPM.cc` is an implementation of the work of Guo and Nairn [22], and while it is viable, it is undocumented and unsupported. `ShellMPM.cc` is a treatment of MPM particles as shell and membrane elements, developed by Biswajit Bannerjee. It is also viable, but also undocumented and unsupported. `ImpMPM.cc` is an implicit time integration form of MPM based on the work of Guilkey and Weiss [21]. It is also viable, and future releases of Uintah will include documentation of its capabilities and uses. For now, interested readers should contact Jim Guilkey directly for more information. `RigidMPM.cc` contains a very reduced level of functionality, and is used solely in conjunction with the MPMArches component.

This leaves `SerialMPM.cc`. This contains, despite its name, the parallel implementation of the algorithm described above in Section 7.2. For now, we will skip over the initialization procedures such as:

```
SerialMPM::problemSetup
SerialMPM::scheduleInitialize
SerialMPM::actuallyInitialize
```

and focus mainly on the timestepping algorithm described above. Reference will be made back to these functions as needed in Section 7.5.

Each of the Uintah components contains a function called `scheduleTimeAdvance`. The algorithms implemented in these components are broken into a number of steps. The implementation of these steps in Uintah take place in "tasks". Each task is responsible for performing the calculations needed to accomplish that step in the algorithm. Thus, each task requires some data upon which to operate, and it also creates some data, either as a final result, or as input to a subsequent task. Before

individual tasks are executed, each is first "scheduled". The scheduling of tasks describes the dataflow and data dependencies for a given algorithm. By describing the data dependencies, both temporally and spatially, each task can be executed in the proper order, and communication tasks can automatically be generated by the Uintah infrastructure to achieve parallelism. Thus, scheduleTimeAdvance calls a series of functions, each of which schedules the individual tasks. Let's begin by looking at the `scheduleTimeAdvance` for `SerialMPM,` pasted below.

```
void
SerialMPM::scheduleTimeAdvance(const LevelP & level,
                               SchedulerP   & sched)
{
  MALLOC_TRACE_TAG_SCOPE("SerialMPM::scheduleTimeAdvance()");
  if (!flags->doMPMOnLevel(level->getIndex(), level->getGrid()->numLevels()))
    return;

  const PatchSet* patches = level->eachPatch();
  const MaterialSet* matls = d_sharedState->allMPMMaterials();

  scheduleApplyExternalLoads(             sched, patches, matls);
  scheduleInterpolateParticlesToGrid(     sched, patches, matls);
  scheduleExMomInterpolated(              sched, patches, matls);
  scheduleComputeContactArea(             sched, patches, matls);
  scheduleComputeInternalForce(           sched, patches, matls);

  scheduleComputeAndIntegrateAcceleration(sched, patches, matls);
  scheduleExMomIntegrated(                sched, patches, matls);
  scheduleSetGridBoundaryConditions(      sched, patches, matls);
  scheduleSetPrescribedMotion(            sched, patches, matls);
  scheduleComputeStressTensor(            sched, patches, matls);
  if(flags->d_doExplicitHeatConduction){
    scheduleComputeHeatExchange(          sched, patches, matls);
    scheduleComputeInternalHeatRate(      sched, patches, matls);
    scheduleComputeNodalHeatFlux(         sched, patches, matls);
    scheduleSolveHeatEquations(           sched, patches, matls);
    scheduleIntegrateTemperatureRate(     sched, patches, matls);
  }
  scheduleAddNewParticles(                sched, patches, matls);
  scheduleConvertLocalizedParticles(      sched, patches, matls);
  scheduleInterpolateToParticlesAndUpdate(sched, patches, matls);

  if(flags->d_canAddMPMMaterial){
    //  This checks to see if the model on THIS patch says that it's
    //  time to add a new material
    scheduleCheckNeedAddMPMMaterial(         sched, patches, matls);

    //  This one checks to see if the model on ANY patch says that it's
    //  time to add a new material
    scheduleSetNeedAddMaterialFlag(         sched, level,   matls);
  }
```

```
  sched->scheduleParticleRelocation(level, lb->pXLabel_preReloc,
                                    d_sharedState->d_particleState_preReloc,
                                    lb->pXLabel,
                                    d_sharedState->d_particleState,
                                    lb->pParticleIDLabel, matls);
  if(d_analysisModule){
    d_analysisModule->scheduleDoAnalysis( sched, level);
  }
}
```

The preceding includes scheduling for a number of rarely used features. For now, let's condense the preceding to the essential tasks:

```
void
SerialMPM::scheduleTimeAdvance(const LevelP & level,
                               SchedulerP   & sched)
{
  if (!flags->doMPMOnLevel(level->getIndex(), level->getGrid()->numLevels()))
    return;

  const PatchSet* patches = level->eachPatch();
  const MaterialSet* matls = d_sharedState->allMPMMaterials();

  scheduleApplyExternalLoads(             sched, patches, matls);
  scheduleInterpolateParticlesToGrid(     sched, patches, matls);
  scheduleExMomInterpolated(              sched, patches, matls);
  scheduleComputeInternalForce(           sched, patches, matls);

  scheduleComputeAndIntegrateAcceleration(sched, patches, matls);
  scheduleExMomIntegrated(                sched, patches, matls);
  scheduleSetGridBoundaryConditions(      sched, patches, matls);
  scheduleComputeStressTensor(            sched, patches, matls);
  scheduleInterpolateToParticlesAndUpdate(sched, patches, matls);

  sched->scheduleParticleRelocation(level, lb->pXLabel_preReloc,
                                    d_sharedState->d_particleState_preReloc,
                                    lb->pXLabel,
                                    d_sharedState->d_particleState,
                                    lb->pParticleIDLabel, matls);
}
```

As described above, each of the "schedule" functions describes dataflow, and it also calls the function that actually executes the task. The naming convention is illustrated by an example, `scheduleComputeAndIntegrateAcceleration` calls `computeAndIntegrateAccele` Let's examine this particular task, which executes Equations 7.4 and 7.5, more carefully. First, the scheduling of the task:

```
void SerialMPM::scheduleComputeAndIntegrateAcceleration(SchedulerP& sched,
                                                        const PatchSet* patches,
```

```
                                                    const MaterialSet* matls)
{
  if (!flags->doMPMOnLevel(getLevel(patches)->getIndex(),
                           getLevel(patches)->getGrid()->numLevels()))
    return;

  printSchedule(patches,cout_doing,"MPM::scheduleComputeAndIntegrateAcceleration\t\t\t\t");

  Task* t = scinew Task("MPM::computeAndIntegrateAcceleration",
                        this, &SerialMPM::computeAndIntegrateAcceleration);

  t->requires(Task::OldDW, d_sharedState->get_delt_label() );

  t->requires(Task::NewDW, lb->gMassLabel,          Ghost::None);
  t->requires(Task::NewDW, lb->gInternalForceLabel, Ghost::None);
  t->requires(Task::NewDW, lb->gExternalForceLabel, Ghost::None);
  t->requires(Task::NewDW, lb->gVelocityLabel,      Ghost::None);

  t->computes(lb->gVelocityStarLabel);
  t->computes(lb->gAccelerationLabel);

  sched->addTask(t, patches, matls);
}
```

The `if` statement basically directs the schedule to only do this task on the finest level (MPM can be used in AMR simulations, but only at the finest level.) The `printSchedule` command is in place for debugging purposes, this type of print statement can be turned on by setting an environmental variable. The real business of this task begins with the declaration of the Task. In the task declaration, the function associated with that task is identified. Subsequent to that is a description of the data dependencies. Namely, this task `requires` the mass, internal and external forces as well as velocity on the grid. No ghost data are required as this task is a node by node calculation. It also requires the timestep size. Note also that most of the required data are needed from the `NewDW` where `DW` refers to DataWarehouse. This simply means that these data were calculated by an earlier task in the current timestep. The timestep size for this step was computed in the previous timestep, and thus is required from the `OldDW.` Finally, this task `computes` the acceleration and time advanced velocity at each node.

The code to execute this task is as follows:

```
void SerialMPM::computeAndIntegrateAcceleration(const ProcessorGroup*,
                                                const PatchSubset* patches,
                                                const MaterialSubset*,
                                                DataWarehouse* old_dw,
                                                DataWarehouse* new_dw)
{
  for(int p=0;p<patches->size();p++){
    const Patch* patch = patches->get(p);
```

```
    printTask(patches, patch,cout_doing,"Doing computeAndIntegrateAcceleration\t\t\t\t");

    Ghost::GhostType  gnone = Ghost::None;
    Vector gravity = d_sharedState->getGravity();
    for(int m = 0; m < d_sharedState->getNumMPMMatls(); m++){
      MPMMaterial* mpm_matl = d_sharedState->getMPMMaterial( m );
      int dwi = mpm_matl->getDWIndex();

      // Get required variables for this patch
      constNCVariable<Vector> internalforce, externalforce, velocity;
      constNCVariable<double> mass;

      delt_vartype delT;
      old_dw->get(delT, d_sharedState->get_delt_label(), getLevel(patches) );

      new_dw->get(internalforce,lb->gInternalForceLabel, dwi, patch, gnone, 0);
      new_dw->get(externalforce,lb->gExternalForceLabel, dwi, patch, gnone, 0);
      new_dw->get(mass,         lb->gMassLabel,          dwi, patch, gnone, 0);
      new_dw->get(velocity,     lb->gVelocityLabel,      dwi, patch, gnone, 0);

      // Create variables for the results
      NCVariable<Vector> velocity_star,acceleration;
      new_dw->allocateAndPut(velocity_star, lb->gVelocityStarLabel, dwi, patch);
      new_dw->allocateAndPut(acceleration,  lb->gAccelerationLabel, dwi, patch);

      acceleration.initialize(Vector(0.,0.,0.));
      double damp_coef = flags->d_artificialDampCoeff;

      for(NodeIterator iter=patch->getExtraNodeIterator__New();
                       !iter.done();iter++){
        IntVector c = *iter;
        Vector acc(0.,0.,0.);
        if (mass[c] > flags->d_min_mass_for_acceleration){
          acc  = (internalforce[c] + externalforce[c])/mass[c];
          acc -= damp_coef*velocity[c];
        }
        acceleration[c] = acc +  gravity;
        velocity_star[c] = velocity[c] + acceleration[c] * delT;
      }
    }    // matls
  }
}
```

This task contains three nested for loops. First, is a loop over all of the "patches" that the processor executing this task is responsible for. Next is a loop over all materials (imagine a simulation involving the interaction between, say, tungsten and copper). Within this loop, the required data are retrieved from the `new_dw` (New DataWarehouse) and space for the data to be created is allocated. The final loop is over all of the nodes on the current patch, and the calculations described by Equations 7.4 and 7.5 are carried out. (This also includes a linear damping term not described above.)

Let's consider each task in turn. The remaining tasks will be described in much less detail, but the preceding dissection of a fairly simple task, along with a description of what the remaining tasks are intended to accomplish, should allow interested individuals to follow the remainder of the Uintah-MPM implementation.

1. `scheduleApplyExternalLoads` This task is mainly responsible for applying traction boundary conditions described in the input file. This is done by assigning external force vectors to the particles. If the user wishes to apply a load that is not possible to acheive via the input file options, it is straightforward to modify the code here to do "one-off" tests.

2. `scheduleInterpolateParticlesToGrid` The name of this task was poorly chosen, but has persisted. This task carries out the operations given in Equation 7.2. It also sets boundary conditions on some of the variables, such as the grid temperature, and grid velocity (in the case of symmetry BCs).

3. `scheduleExMomInterpolated` This task actually exists in one of the contact models which can be found in the `Contact` directory. Each of those models has two main tasks. This is the the first of those. It is responsible for modifying the grid velocity computed by interpolateParticlesToGrid according to the rules for the particular contact model chosen in the input file. These models are briefly described in Section 7.5.

4. `scheduleComputeInternalForce` This task computes the volume integral of the divergence of stress. Specifically, it carries out the operation given in Equation 7.3. It also computes some diagnostic data, if requested in the input file, such as the reaction forces (tractions) on the boundaries of the computational domain.

5. `scheduleComputeAndIntegrateAcceleration` As described previously, this task carries out the operations described in Equations 7.4 and 7.5.

6. `scheduleExMomIntegrated` This is the second of the contact tasks (see above). It is responsible for modifiying the time advanced grid velocity computed in `computeAndIntegrateAcceleration.`

7. `scheduleSetGridBoundaryConditions` This task sets boundary conditions on the time advanced grid velocity. It also sets an acceleration boundary condition as well. However, rather than just setting the acceleration to a given value, it is computed by solving Equation 7.5 for acceleration, and then recomputing the acceleration (on all nodes) as:

$$\mathbf{a}_i = \frac{\mathbf{v}_i^L - \mathbf{v}_i}{\Delta t} \tag{7.19}$$

Doing this operation on all nodes has several advantages. For most interior nodes, the value for acceleration will be unchanged, but for nodes on the where the velocity has been altered by enforcing boundary conditions, and for nodes at which the contact models have altered the velocity, the acceleration will be modified to reflect that alteration.

8. `scheduleComputeStressTensor` The task, `computeStressTensor,` exists in each of the models in the `ConstitutiveModel` directory. Each model is responsible for carrying out the operations given in Equation 7.8, and of course, as the name implies, it also computes the material stress. This task has one additional important function, and that is computing the timestep size for the subsequent step. The CFL condition dictates that the timestep size be limited according to:

$$\Delta t < \frac{\Delta x}{c + |u|} \tag{7.20}$$

where Δx is the cell spacing, c is the wavespeed in the material, and $|u|$ is the magnitude of the local velocity. Because the wavespeed may depend on the state of stress that a material is in, this task provides a convenient time at which to make this calculation. A timestep size is computed for all particles, and the minimum for the particle set on a given patch is put into a "reduction variable". The Uintah infrastructure then does a global reduction to select the smallest timestep from across the domain.

9. `scheduleInterpolateToParticlesAndUpdate` This task carries out the operations in Equations 7.9 and 7.10, namely updating the particle state based on the grid solution.

10. `scheduleParticleRelocation` This task is not actually located in the MPM code, but in the Uintah infrastructure. The idea is that as particles move, some will cross patch boundaries, and their data will need to be sent to other processors. This task is responsible for identifying particles that have left the patch that they were on, finding where they went, and sending their data to the correct processor.

7.5 Uintah Specification

Uintah input files are constructed in XML format. Each begins with:

```
<?xml version='1.0' encoding='ISO-8859-1' ?>
```

while the remainder of the file is enclosed within the following tags:

```
<Uintah_specification>
</Uintah_specification>
```

The following subsections describe the remaining inputs needed to construct an input file for an MPM simulation. The order of the various sections of the input file is not important. **The MPM, ICE and MPMICE components are dimensionless calculations. It is the responsibility of the analyst to provide the following inputs using a consistent set of units.**

Common Inputs

Each Uintah component is invoked using a single executable called *sus* , which chooses the type of simulation to execute based on the *SimulationComponent* tag in the input file. For the case of MPM simulations, this looks like:

```
<SimulationComponent type="mpm" />
```

There are a number of fields that are required for any component. The first is that describing the timestepping parameters, these are largely common to all components, and are described in Section 2.5. The only one that bears commenting on at this point is:

```
<timestep_multiplier>    0.5     </timestep_multiplier>
```

This is effectively the CFL number for MPM simulations, that is the number multiplied by the timestep size that is automatically calculated by the MPM code. Experience indicates that one should generally keep this value below 0.5, and should expect to use smaller values for high-rate, large-deformation simulations.

The next field common to the input files for all components is:

```
<DataArchiver>
</DataArchiver>
```

This is described in Section 2.6. To see a list of variables available for saving in MPM simulations, execute the following command from the `StandAlone` directory:

```
inputs/labelNames mpm
```

Note that for visualizing particle data, one must save `p.x,` and at least one other variable by which to color the particles.

The other principle common field is that which describes the computational grid. For MPM, this is typically broken up into two parts, the `<Level>` section specifies the physical extents and spatial resolution of the grid. For more information, consult Section 2.10. The other part specifies kinematic boundary conditions on the grid boundaries. These are discussed below in Section 7.5.

Physical Constants

The only physical constant required (or optional for that matter) for MPM simulations is gravity, this is specified as:

```
<PhysicalConstants>
   <gravity>            [0,0,0]   </gravity>
</PhysicalConstants>
```

MPM Flags

There are many options available when running MPM simulations. These are generally specified in the `<MPM>` section of the input file. Below is a list of these options taken from `inputs/UPS_SPEC/mpm_spec.xml` This file also gives possible values, or at least expected datatype, for these flags. A description of their functionality is forthcoming, in the meantime, consult the code and input files. A default value is set for many, see `MPM/MPMFlags.cc` for more.

```
<MPM>
 <!-- These are commonly used options -->
  <artificial_damping_coeff           spec="OPTIONAL DOUBLE 'positive'"/>
  <artificial_viscosity               spec="OPTIONAL BOOLEAN" />
  <artificial_viscosity_coeff1        spec="OPTIONAL DOUBLE" />
  <artificial_viscosity_coeff2        spec="OPTIONAL DOUBLE" />
  <axisymmetric                       spec="OPTIONAL BOOLEAN" />
  <boundary_traction_faces            spec="OPTIONAL STRING" />
  <DoExplicitHeatConduction           spec="OPTIONAL BOOLEAN" />
  <DoPressureStabilization            spec="OPTIONAL BOOLEAN" />
  <erosion                            spec="OPTIONAL NO_DATA"
        attribute1="algorithm REQUIRED STRING 'none, KeepStress, ZeroStress, RemoveMass'" />
  <interpolator                       spec="OPTIONAL STRING 'linear, gimp, 3rdorderBS, 4thor
  <minimum_particle_mass              spec="OPTIONAL DOUBLE 'positive'"/>
  <minimum_mass_for_acc               spec="OPTIONAL DOUBLE 'positive'"/>
  <maximum_particle_velocity          spec="OPTIONAL DOUBLE 'positive'"/>
  <testForNegTemps_mpm                spec="OPTIONAL BOOLEAN" />
  <time_integrator                    spec="OPTIONAL STRING 'explicit, fracture, implicit'"
  <use_load_curves                    spec="OPTIONAL BOOLEAN" />
  <UsePrescribedDeformation           spec="OPTIONAL BOOLEAN" />
  <withColor                          spec="OPTIONAL BOOLEAN" />

 <!-- These are not commonly used options -->
  <accumulate_strain_energy           spec="OPTIONAL BOOLEAN" />
  <CanAddMPMMaterial                  spec="OPTIONAL BOOLEAN" />
  <create_new_particles               spec="OPTIONAL BOOLEAN" />
  <do_contact_friction_heating        spec="OPTIONAL BOOLEAN" />
  <do_grid_reset                      spec="OPTIONAL BOOLEAN" />
  <DoThermalExpansion                 spec="OPTIONAL BOOLEAN" />
  <ForceBC_force_increment_factor     spec="OPTIONAL DOUBLE" />
  <manual_new_material                spec="OPTIONAL BOOLEAN" />
```

```
  <interpolateParticleTempToGridEveryStep spec="OPTIONAL BOOLEAN" />
  <temperature_solve                  spec="OPTIONAL BOOLEAN" />

 <!-- THE FOLLOWING APPLY ONLY TO THE IMPLICIT MPM CODE -->
  <dynamic                            spec="OPTIONAL BOOLEAN" />
  <solver                             spec="OPTIONAL STRING 'petsc, simple'" />
  <convergence_criteria_disp          spec="OPTIONAL DOUBLE 'positive'"/>
  <convergence_criteria_energy        spec="OPTIONAL DOUBLE 'positive'"/>
  <num_iters_to_decrease_delT         spec="OPTIONAL INTEGER" />
  <num_iters_to_increase_delT         spec="OPTIONAL INTEGER" />
  <iters_before_timestep_restart      spec="OPTIONAL INTEGER" />
  <DoTransientImplicitHeatConduction  spec="OPTIONAL BOOLEAN" />
  <delT_decrease_factor               spec="OPTIONAL DOUBLE" />
  <delT_increase_factor               spec="OPTIONAL DOUBLE" />
  <DoImplicitHeatConduction           spec="OPTIONAL BOOLEAN" />
  <DoMechanics                        spec="OPTIONAL BOOLEAN" />

  <!-- THE FOLLOWING APPLY ONLY TO THE FRACTURE MPM CODE -->
  <dadx                               spec="OPTIONAL DOUBLE" />
  <smooth_crack_front                 spec="OPTIONAL BOOLEAN" />
  <calculate_fracture_parameters      spec="OPTIONAL BOOLEAN" />
  <do_crack_propagation               spec="OPTIONAL BOOLEAN" />
  <use_volume_integral                spec="OPTIONAL BOOLEAN" />
</MPM>
```

Material Properties

The `Material Properties` section of the input file actually contains not only those, but also the geometry and initial condition data as well. Below is a simple example, copied from `inputs/MPM/disks.ups`. The `name` field is optional. The first field is the material `<density>`. The `<constitutive_model>` field refers to the model used to generate a stress tensor on each material point. The use of these models is described in detail in Section 7.5. Next are the thermal transport properties, `<thermal_conductivity>` and `<specific_heat>`. Note that these are required even if heat conduction is not being computed. These are the required material properties. There are additional optional parameters that are used in other auxiliary calculations, for a list of these see the `inputs/UPS_SPEC/mpm_spec.xml` .

Next is the specification of the geometry, and, along with it, the initial state of the material contained in that geometry. For more information on how initial geometry can be specified, see Section 2.8. Within the `<geom_object>` is the `<res>` field. This indicates how many particles per cell are to be used in each of the coordinate directions. Following that are initial values for velocity and temperature. Finally, the `<color>` designation has a number of uses, for example when one wishes to identify initially distinct regions of the same material. In Section 7.5 is a description of how this field is used to identify particles for on the fly data extraction.

An arbitray number of `<material>` fields can be specified. As the calculation

proceeds, each of these materials has their own field variables, and, as such, each material behaves independently of the others. Interactions between materials occur as a result of "contact" models. Their use is described in detail in Section 7.5.

```
<MaterialProperties>
   <MPM>
       <material name="disks">
          <density>1000.0</density>
          <constitutive_model type="comp_mooney_rivlin">
             <he_constant_1>100000.0</he_constant_1>
             <he_constant_2>20000.0</he_constant_2>
             <he_PR>.49</he_PR>
          </constitutive_model>
          <thermal_conductivity>1.0</thermal_conductivity>
          <specific_heat>5</specific_heat>
          <geom_object>
              <cylinder label = "gp1">
                 <bottom>[.25,.25,.05]</bottom>
                 <top>[.25,.25,.1]</top>
                 <radius> .2 </radius>
              </cylinder>
              <res>[2,2,2]</res>
              <velocity>[2.0,2.0,0]</velocity>
              <temperature>300</temperature>
              <color>             0               </color>
           </geom_object>
       </material>

       <contact>
         <type>null</type>
         <materials>[0]</materials>
       </contact>
   </MPM>
</MaterialProperties>
```

Constitutive Models

The MPM code contains a large number of constitutive models that provide a Cauchy stress on each particle based on the velocity gradient computed at that particle. The following is a list and very brief description of the most commonly used models. The reader may wish to consult the `inputs/MPM` and `inputs/MPMICE` directories to find explicit examples of the use of these models, and others not described below.

1. **Compressible Neo-Hookean Models** There are a number of implementations based on a hyperelastic-plastic model described by Simo and Hughes[47] (pp. 307 – 321). Several of these models should be combined, but for now, they are separate. Below the usage for each is given. These models are very robust, and hyperelastic models don't require rotation back and forth between laboratory and material frames of reference.

<comp_neo_hook> is a basic elastic model.

```
<constitutive_model type="comp_neo_hook">
    <bulk_modulus>2000.0</bulk_modulus>
    <shear_modulus>1500.0</shear_modulus>
</constitutive_model>
```

<comp_neo_hook_plastic> is the basic elastic model extended to include plasticity with isotropic linear hardening.

```
<constitutive_model type="comp_neo_hook_plastic">
  <bulk_modulus>2000.0</bulk_modulus>
  <shear_modulus>1500.0</shear_modulus>
  <yield_stress>100.0</yield_stress>
  <hardening_modulus>500.0</hardening_modulus>
  <alpha> 0.0 </alpha>  <!-- optional defaults to 0.0 -->
</constitutive_model>
```

<cnh_damage> is a basic elastic model, with an extension to failure based on a stress or strain as given below, thus yielding an elastic-brittle failure model. This model also allows a distribution of failure strain (or stress) based on normal or Weibull distributions. Note that the post-failure behaviour of simulations is not always robust.

When either this or the subsequent model is chosen, one must also specify the following MPMFlag

```
<!-- choices are: "AllowNoTension", "ZeroStress" -->
<erosion algorithm="ZeroStress"/>
```

in the <MPM> section of the input file.

```
<constitutive_model type="cnh_damage">
     <bulk_modulus> 8.9e9  </bulk_modulus>
     <shear_modulus>3.52e9  </shear_modulus>

      <!-- choices are true or false (default) -->
      <failure_by_stress>true </failure_by_stress>

     <!-- when failure_by_stress is true, values are stress not strain -->
     <failure_strain_mean> 900 </failure_strain_mean>
     <failure_strain_std> 0.1 </failure_strain_std>

     <!-- choices are "constant", "gauss" or "weibull" -->
     <failure_strain_distrib> "constant" </failure_strain_distrib>
</constitutive_model>
```

<cnhp_damage> is the elastic plastic model above, with an extension to failure based on a stress or strain as given below, thus yielding an elastic-plastic model

with failure. Note that the post-failure behaviour of simulations is not always robust.

```
<constitutive_model type="cnhp_damage">
   <bulk_modulus> 8.9e9  </bulk_modulus>
   <shear_modulus>3.52e9  </shear_modulus>
   <yield_stress>100.0</yield_stress>
   <hardening_modulus>500.0</hardening_modulus>

   <!-- choices are true or false (default) -->
   <failure_by_stress>true </failure_by_stress>

   <!-- when failure_by_stress is true, values are stress not strain -->
   <failure_strain_mean> 900 </failure_strain_mean>
   <failure_strain_std> 0.1 </failure_strain_std>

   <!-- choices are "constant", "gauss" or "weibull" -->
   <failure_strain_distrib> "constant" </failure_strain_distrib>
</constitutive_model>
```

2. **Compressible Mooney-Rivlin Model** This model is generally parameterized for rubber type materials. Usage is as follows:

```
<constitutive_model type="comp_mooney_rivlin">
   <he_constant_1>100000.0</he_constant_1>
   <he_constant_2>20000.0</he_constant_2>
   <he_PR>.49</he_PR>
 </constitutive_model>
```

   where `<he_constant_(1,2)>` are usually referred to as $C1$ and $C2$ in the literature.

3. **Kayenta** This is the model formerly known as the Sandia Geomodel. Use is limited to licensees, see Rebecca Brannon for details. It also requires an obscene number of input parameters which are best covered in the users guide for this model. For a simple list, see the source code in `Kayenta.cc`.

4. **Water** This is a model for water, reported in [17]. The P-V relationship is given by:

$$p = \kappa \left[\left(\frac{\rho}{\rho_0} \right)^{\gamma} - 1 \right] \tag{7.21}$$

   Shear stress is simple Newtonian behavior. It has not been validated, but gives qualitatively reasonable behavior. Usage is given by:

```
<constitutive_model type="water">
   <bulk_modulus>15000.0</bulk_modulus>
   <viscosity>.5</viscosity>
   <gamma>7.0</gamma>
 </constitutive_model>
```

5. **Ideal Gas** This is simply an equation of state, with no shear stress. Usage is given by:

```
<constitutive_model type="ideal_gas">
    <specific_heat>  717.5        </specific_heat>
    <gamma>  1.4        </gamma>
</constitutive_model>
```

6. **Rigid Material** This model was designed for use with the `specified` contact model described in Section 7.5. It is designed to compute zero stress and deformation of the material, and is basically a fast place holder for materials that won't be developing a stress anyway.

7. **ElasticPlastic** The `<elastic_plastic>` model is a general purpose model that was primarily implemented for the purpose of modeling high strain rate metal plasticity. Dr. Biswajit Banerjee has written an extensive description of the theory, implementation and use of this model. Because of the amount of detail involved, and because these subtopics are interwoven, this model is given its own section below.

There is a large number remaining models but these are not frequently utilized. This includes models for viscoelasticity, soil models, and transverse isotropic materials (i.e., fiber reinforced composites). Examples of their use can be found in the `inputs` directory. Input files can also be constructed by checking the source code to see what parameters are required.

There are a few models whose use is explicitly not recommended. In particular, `HypoElasticPlastic, Membrane and SmallStrainPlastic.` Input files calling for the first of these should be switched to the `ElasticPlastic` model instead.

Hypo-Elastic Plasticity in Uintah

The hypoelastic-plastic stress update is based on an additive decomposition of the rate of deformation tensor into elastic and plastic parts. Incompressibility is assumed for plastic deformations. The volumetric response is therefore determined either by a bulk modulus and the trace of the rate of deformation tensor or using an equation of state. The deviatoric response is determined either by an elastic constitutive equation or using a plastic flow rule in combination with a yield condition.

The material models that can be varied in these stress update approaches are (this list is not exhaustive):

1. The elasticity model, for example,

    - Isotropic linear elastic model.
    - Anisotropic linear elastic models.

- Isotropic nonlinear elastic models.
- Anisotropic nonlinear elastic models.

2. Isotropic hardening or Kinematic hardening using a back stress evolution rule, for example,
   - Ziegler evolution rule .
3. The flow rule and hardening/softening law, for example,
   - Perfect plasticity/power law hardening plasticity.
   - Johnson-Cook plasticity .
   - Mechanical Threshold Stress (MTS) plasticity .
   - Anand plasticity .
4. The yield condition, for example,
   - von Mises yield condition.
   - Drucker-Prager yield condition.
   - Mohr-Coulomb yield condition.
5. A continuum or nonlocal damage model with damage evolution given by, for example,
   - Johnson-Cook damage model.
   - Gurson-Needleman-Tvergaard model.
   - Sandia damage model.
6. An equation of state to determine the pressure (or volumetric response), for example,
   - Mie-Gruneisen equation of state.

The currently implemented stress update algorithms in Uintah do not allow for arbitrary elasticity models, kinematic hardening, arbitrary yield conditions and continuum or nonlocal damage (however a damage parameter is updated and used in the erosion algorithm). The models that can be varied are the flow rule models, damage variable evolution models and the equation of state models. Note that there are no checks to prevent users from mixing and matching inappropriate models.

This section describes the current implementation of the hypoelastic- plastic model. The stress update algorithm is a slightly modified version of the approach taken by Nemat-Nasser et al. (1991,1992) [38, 39], Wang (1994) [57], Maudlin (1996) [36], and Zocher et al. (2000) [62].

Simplified theory for hypoelastic-plasticity A simplified version of the theory behind the stress update algorithm (in the contex of von Mises plasticity) is given below.

Following [36], the rotated spatial rate of deformation tensor ($\boldsymbol{d}$) is decomposed into an elastic part ($\boldsymbol{d}^e$) and a plastic part ($\boldsymbol{d}^p$)

$$\boldsymbol{d} = \boldsymbol{d}^e + \boldsymbol{d}^p \tag{7.22}$$

If we assume plastic incompressibility ($\mathrm{tr}(\boldsymbol{d}^p) = 0$), we get

$$\boldsymbol{\eta} = \boldsymbol{\eta}^e + \boldsymbol{\eta}^p \tag{7.23}$$

where $\boldsymbol{\eta}$, $\boldsymbol{\eta}^e$, and $\boldsymbol{\eta}^p$ are the deviatoric parts of $\boldsymbol{d}$, $\boldsymbol{d}^e$, and $\boldsymbol{d}^p$, respectively. For isotropic materials, the hypoelastic constitutive equation for deviatoric stress is

$$\dot{\boldsymbol{s}} = 2\mu(\boldsymbol{\eta} - \boldsymbol{\eta}^p) \tag{7.24}$$

where $\boldsymbol{s}$ is the deviatoric part of the stress tensor and μ is the shear modulus. We assume that the flow stress obeys the Huber-von Mises yield condition

$$f := \sqrt{\frac{3}{2}}\,\|\boldsymbol{s}\| - \sigma_y \leq 0 \quad \text{or,} \quad F := \frac{3}{2}\boldsymbol{s} : \boldsymbol{s} - \sigma_y^2 \leq 0 \tag{7.25}$$

where σ_y is the flow stress. Assuming an associated flow rule, and noting that $\boldsymbol{d}^p = \boldsymbol{\eta}^p$, we have

$$\boldsymbol{\eta}^p = \boldsymbol{d}^p = \lambda\frac{\partial f}{\partial \boldsymbol{\sigma}} = \Lambda\frac{\partial F}{\partial \boldsymbol{\sigma}} = 3\Lambda\boldsymbol{s} \tag{7.26}$$

where $\boldsymbol{\sigma}$ is the stress. Let $\mathbf{u}$ be a tensor proportional to the plastic straining direction, and define γ as

$$\mathbf{u} = \sqrt{3}\frac{\boldsymbol{s}}{\|\boldsymbol{s}\|}; \quad \gamma := \sqrt{3}\Lambda\,\|\boldsymbol{s}\| \quad \Longrightarrow \gamma\mathbf{u} = 3\Lambda\boldsymbol{s} \tag{7.27}$$

Therefore, we have

$$\boldsymbol{\eta}^p = \gamma\mathbf{u}; \quad \dot{\boldsymbol{s}} = 2\mu(\boldsymbol{\eta} - \gamma\mathbf{u}) \tag{7.28}$$

From the consistency condition, if we assume that the deviatoric stress remains constant over a timestep, we get

$$\gamma = \frac{\boldsymbol{s} : \boldsymbol{\eta}}{\boldsymbol{s} : \mathbf{u}} \tag{7.29}$$

which provides an initial estimate of the plastic strain-rate. To obtain a semi-implicit update of the stress using equation (7.28), we define

$$\tau^2 := \frac{3}{2}\boldsymbol{s} : \boldsymbol{s} = \sigma_y^2 \tag{7.30}$$

Taking a time derivative of equation (7.30) gives us

$$\sqrt{2}\dot{\tau} = \sqrt{3}\frac{\boldsymbol{s} : \dot{\boldsymbol{s}}}{\|\boldsymbol{s}\|} \tag{7.31}$$

Plugging equation (7.31) into equation $(7.28)_2$ we get

$$\dot{\tau} = \sqrt{2}\mu(\mathbf{u} : \boldsymbol{\eta} - \gamma \mathbf{u} : \mathbf{u}) = \sqrt{2}\mu(d - 3\gamma) \tag{7.32}$$

where $d = \mathbf{u} : \boldsymbol{\eta}$. If the initial estimate of the plastic strain-rate is that all of the deviatoric strain-rate is plastic, then we get an approximation to γ, and the corresponding error (γ_{er}) given by

$$\gamma_{\text{approx}} = \frac{d}{3}; \quad \gamma_{\text{er}} = \gamma_{\text{approx}} - \gamma = \frac{d}{3} - \gamma \tag{7.33}$$

The incremental form of the above equation is

$$\Delta\gamma = \frac{d^* \Delta t}{3} - \Delta\gamma_{\text{er}} \tag{7.34}$$

Integrating equation (7.32) from time t_n to time $t_{n+1} = t_n + \Delta t$, and using equation (7.34) we get

$$\tau_{n+1} = \tau_n + \sqrt{2}\mu(d^* \Delta t - 3\Delta\gamma) = \tau_n + 3\sqrt{2}\mu\Delta\gamma_{\text{er}} \tag{7.35}$$

where d^* is the average value of d over the timestep. Solving for $\Delta\gamma_{\text{er}}$ gives

$$\Delta\gamma_{\text{er}} = \frac{\tau_{n+1} - \tau_n}{3\sqrt{2}\mu} = \frac{\sqrt{2}\sigma_y - \sqrt{3}\,\|\boldsymbol{s}_n\|}{6\mu} \tag{7.36}$$

The direction of the total strain-rate ($\mathbf{u}^\eta$) and the direction of the plastic strain-rate ($\mathbf{u}^s$) are given by

$$\mathbf{u}^\eta = \frac{\boldsymbol{\eta}}{\|\boldsymbol{\eta}\|}; \quad \mathbf{u}^s = \frac{\boldsymbol{s}}{\|\boldsymbol{s}\|} \tag{7.37}$$

Let θ be the fraction of the time increment that sees elastic straining. Then

$$\theta = \frac{d^* - 3\gamma_n}{d^*} \tag{7.38}$$

where $\gamma_n = d_n/3$ is the value of γ at the beginning of the timestep. We also assume that

$$d^* = \sqrt{3}\boldsymbol{\eta} : [(1 - \theta)\mathbf{u}^\eta + \frac{\theta}{2}(\mathbf{u}^\eta + \mathbf{u}^s)] \tag{7.39}$$

Plugging equation (7.38) into equation (7.39) we get a quadratic equation that can be solved for d^* as follows

$$\frac{2}{\sqrt{3}}(d^*)^2 - (\boldsymbol{\eta} : \mathbf{u}^s + \|\boldsymbol{\eta}\|)d^* + 3\gamma_n(\boldsymbol{\eta} : \mathbf{u}^s - \|\boldsymbol{\eta}\|) = 0 \tag{7.40}$$

The real positive root of the above quadratic equation is taken as the estimate for d. The value of $\Delta\gamma$ can now be calculated using equations (7.34) and (7.36). A semi-implicit estimate of the deviatoric stress can be obtained at this stage by integrating

equation $(7.28)_2$

$$\tilde{\boldsymbol{s}}_{n+1} = \boldsymbol{s}_n + 2\mu\left(\eta\Delta t - \sqrt{3}\Delta\gamma\frac{\tilde{\boldsymbol{s}}_{n+1}}{\|\boldsymbol{s}_{n+1}\|}\right) \tag{7.41}$$

$$= \boldsymbol{s}_n + 2\mu\left(\eta\Delta t - \frac{3}{\sqrt{2}}\Delta\gamma\frac{\tilde{\boldsymbol{s}}_{n+1}}{\sigma_y}\right) \tag{7.42}$$

Solving for $\tilde{\boldsymbol{s}}_{n+1}$, we get

$$\tilde{\boldsymbol{s}}_{n+1} = \frac{\boldsymbol{s}^{\text{trial}}_{n+1}}{1 + 3\sqrt{2}\mu\dfrac{\Delta\gamma}{\sigma_y}} \tag{7.43}$$

where $\boldsymbol{s}^{\text{trial}}_{n+1} = \boldsymbol{s}_n + 2\mu\Delta t\boldsymbol{\eta}$. A final radial return adjustment is used to move the stress to the yield surface

$$\boldsymbol{s}_{n+1} = \sqrt{\frac{2}{3}}\sigma_y\frac{\tilde{\boldsymbol{s}}_{n+1}}{\|\tilde{\boldsymbol{s}}_{n+1}\|} \tag{7.44}$$

A pathological situation arises if $\gamma_n = \mathbf{u}_n : \boldsymbol{\eta}_n$ is less than or equal to zero or $\Delta\gamma_{\text{er}} \geq \frac{d^*}{3}\Delta t$. This can occur is the rate of plastic deformation is small compared to the rate of elastic deformation or if the timestep size is too small (see [39]). In such situations, we use a locally implicit stress update that uses Newton iterations (as discussed in [46], page 124) to compute $\tilde{\boldsymbol{s}}$.

Equation of State Models The elastic-plastic stress update assumes that the volumetric part of the Cauchy stress can be calculated using an equation of state. There are three equations of state that are implemented in Uintah. These are

1. A default hypoelastic equation of state.
2. A neo-Hookean equation of state.
3. A Mie-Gruneisen type equation of state.

Default hypoelastic equation of state In this case we assume that the stress rate is given by

$$\dot{\boldsymbol{\sigma}} = \lambda\ \text{tr}(\boldsymbol{d}^e)\ \boldsymbol{1} + 2\ \mu\ \boldsymbol{d}^e \tag{7.45}$$

where $\boldsymbol{\sigma}$ is the Cauchy stress, $\boldsymbol{d}^e$ is the elastic part of the rate of deformation, and λ, μ are constants.

If $\boldsymbol{\eta}^e$ is the deviatoric part of $\boldsymbol{d}^e$ then we can write

$$\dot{\boldsymbol{\sigma}} = \left(\lambda + \frac{2}{3}\ \mu\right)\ \text{tr}(\boldsymbol{d}^e)\ \boldsymbol{1} + 2\ \mu\ \boldsymbol{\eta}^e = \kappa\ \text{tr}(\boldsymbol{d}^e)\ \boldsymbol{1} + 2\ \mu\ \boldsymbol{\eta}^e\ . \tag{7.46}$$

If we split $\boldsymbol{\sigma}$ into a volumetric and a deviatoric part, i.e., $\boldsymbol{\sigma} = p\ \mathbf{1} + \boldsymbol{s}$ and take the time derivative to get $\dot{\boldsymbol{\sigma}} = \dot{p}\ \mathbf{1} + \dot{\boldsymbol{s}}$ then

$$\dot{p} = \kappa\ \mathrm{tr}(\boldsymbol{d}^e)\ . \tag{7.47}$$

In addition we assume that $\boldsymbol{d} = \boldsymbol{d}^e + \boldsymbol{d}^p$. If we also assume that the plastic volume change is negligible, we can then write that

$$\dot{p} = \kappa\ \mathrm{tr}(\boldsymbol{d})\ . \tag{7.48}$$

This is the equation that is used to calculate the pressure p in the default hypoelastic equation of state, i.e.,

$$\boxed{p_{n+1} = p_n + \kappa\ \mathrm{tr}(\boldsymbol{d}_{n+1})\ \Delta t\ .} \tag{7.49}$$

To get the derivative of p with respect to J, where $J = \det(\boldsymbol{F})$, we note that

$$\dot{p} = \frac{\partial p}{\partial J}\ \dot{J} = \frac{\partial p}{\partial J}\ J\ \mathrm{tr}(\boldsymbol{d})\ . \tag{7.50}$$

Therefore,

$$\boxed{\frac{\partial p}{\partial J} = \frac{\kappa}{J}\ .} \tag{7.51}$$

This model is invoked in Uintah using

```
<equation_of_state type="default_hypo">
</equation_of_state>
```

The code is in `.../MPM/ConstitutiveModel/PlasticityModels/DefaultHypoElasticEOS.cc`
If an EOS is not specified then this model is the **default**.

Default hyperelastic equation of state In this model the pressure is computed using the relation

$$p = \frac{1}{2}\ \kappa\ \left(J^e - \frac{1}{J^e}\right) \tag{7.52}$$

where κ is the bulk modulus and J^e is determinant of the elastic part of the deformation gradient.

We can also compute

$$\frac{dp}{dJ} = \frac{1}{2}\ \kappa\ \left(1 + \frac{1}{(J^e)^2}\right)\ . \tag{7.53}$$

This model is invoked in Uintah using

```
<equation_of_state type="default_hyper">
</equation_of_state>
```

The code is in `.../MPM/ConstitutiveModel/PlasticityModels/HyperElasticEOS.cc`.

Mie-Gruneisen equation of state The pressure (p) is calculated using a Mie-Grüneisen equation of state of the form ([58, 62])

$$\boxed{p_{n+1} = -\frac{\rho_0\ C_0^2\ (1 - J^e_{n+1})[1 - \Gamma_0(1 - J^e_{n+1})/2]}{[1 - S_\alpha(1 - J^e_{n+1})]^2} - \Gamma_0\ e_{n+1}\ ; \quad J^e := \det \boldsymbol{F}^e} \tag{7.54}$$

where C_0 is the bulk speed of sound, ρ_0 is the initial mass density, Γ_0 is the Grüneisen's gamma at the reference state, $S_\alpha = dU_s/dU_p$ is a linear Hugoniot slope coefficient, U_s is the shock wave velocity, U_p is the particle velocity, and e is the internal energy density (per unit reference volume), $\boldsymbol{F}^e$ is the elastic part of the deformation gradient. For isochoric plasticity,

$$J^e = J = \det(\boldsymbol{F}) = \frac{\rho_0}{\rho}\ .$$

The internal energy is computed using

$$E = \frac{1}{V_0}\int C_v dT \approx \frac{C_v(T - T_0)}{V_0} \tag{7.55}$$

where $V_0 = 1/\rho_0$ is the reference specific volume at temperature $T = T_0$, and C_v is the specific heat at constant volume. Also,

$$\boxed{\frac{\partial p}{\partial J^e} = \frac{\rho_0\ C_0^2\ [1 + (S_\alpha - \Gamma_0)\ (1 - J^e)]}{[1 - S_\alpha\ (1 - J^e)]^3} - \Gamma_0\ \frac{\partial e}{\partial J^e}.} \tag{7.56}$$

We neglect the $\frac{\partial e}{\partial J^e}$ term in our calculations.

This model is invoked in Uintah using

```
<equation_of_state type="mie_gruneisen">
  <C_0>5386</C_0>
  <Gamma_0>1.99</Gamma_0>
  <S_alpha>1.339</S_alpha>
</equation_of_state>
```

The code is in `.../MPM/ConstitutiveModel/PlasticityModels/MieGruneisenEOS.cc`.

Melting Temperature

Default model The default model is to use a constant melting temperature. This model is invoked using

```
<melting_temp_model type="constant_Tm">
</melting_temp_model>
```

SCG melt model We use a pressure dependent relation to determine the melting temperature (T_m). The Steinberg-Cochran-Guinan (SCG) melt model ([48]) has been used for our simulations of copper. This model is based on a modified Lindemann law and has the form

$$T_m(\rho) = T_{m0} \exp\left[2a\left(1 - \frac{1}{\eta}\right)\right] \eta^{2(\Gamma_0 - a - 1/3)}; \quad \eta = \frac{\rho}{\rho_0} \tag{7.57}$$

where T_{m0} is the melt temperature at $\eta = 1$, a is the coefficient of the first order volume correction to Grüneisen's gamma (Γ_0).

This model is invoked with

```
<melting_temp_model type="scg_Tm">
  <T_m0> 2310.0 </T_m0>
  <Gamma_0> 3.0 </Gamma_0>
  <a> 1.67 </a>
</melting_temp_model>
```

BPS melt model An alternative melting relation that is based on dislocation-mediated phase transitions - the Burakovsky-Preston-Silbar (BPS) model ([13]) can also be used. This model has been used to determine the melt temperature for 4340 steel. The BPS model has the form

$$T_m(p) = T_m(0)\left[\frac{1}{\eta} + \frac{1}{\eta^{4/3}}\frac{\mu_0^{'}}{\mu_0}\, p\right] \;; \quad \eta = \left(1 + \frac{K_0^{'}}{K_0}\, p\right)^{1/K_0^{'}} \tag{7.58}$$

$$T_m(0) = \frac{\kappa\lambda\mu_0\ v_{WS}}{8\pi \ln(z-1)\ k_b} \ln\left(\frac{\alpha^2}{4\ b^2\rho_c(T_m)}\right) \tag{7.59}$$

where p is the pressure, $\eta = \rho/\rho_0$ is the compression, μ_0 is the shear modulus at room temperature and zero pressure, $\mu_0^{'} = \partial\mu/\partial p$ is the derivative of the shear modulus at zero pressure, K_0 is the bulk modulus at room temperature and zero pressure, $K_0^{'} = \partial K/\partial p$ is the derivative of the bulk modulus at zero pressure, κ is a constant, $\lambda = b^3/v_{WS}$ where b is the magnitude of the Burgers' vector, v_{WS} is the Wigner-Seitz volume, z is the coordination number, α is a constant, $\rho_c(T_m)$ is the critical density of dislocations, and k_b is the Boltzmann constant.

This model is invoked with

```
<melting_temp_model type="bps_Tm">
  <B0> 137e9 </B0>
  <dB_dp0> 5.48 <dB_dp0>
  <G0> 47.7e9 <G0>
  <dG_dp0> 1.4 <dG_dp0>
  <kappa> 1.25 <kappa>
  <z> 12 <z>
  <b2rhoTm> 0.64 <b2rhoTm>
```

```
    <alpha> 2.9 <alpha>
    <lambda> 1.41 <lambda>
    <a> 3.6147e-9<a>
    <v_ws_a3_factor> 1/4 <v_ws_a3_factor>
    <Boltzmann_Constant> <Boltzmann_Constant>
  </melting_temp_model>
```

Shear Modulus Three models for the shear modulus (μ) have been tested in our simulations. The first has been associated with the Mechanical Threshold Stress (MTS) model and we call it the MTS shear model. The second is the model used by Steinberg-Cochran-Guinan and we call it the SCG shear model while the third is a model developed by Nadal and Le Poac that we call the NP shear model.

Default model The default model gives a constant shear modulus. The model is invoked using

```
<shear_modulus_model type="constant_shear">
</shear_modulus_model>
```

MTS Shear Modulus Model The simplest model is of the form suggested by [55] ([14])

$$\mu(T) = \mu_0 - \frac{D}{exp(T_0/T) - 1} \tag{7.60}$$

where μ_0 is the shear modulus at 0K, and D, T_0 are material constants.

The model is invoked using

```
<shear_modulus_model type="mts_shear">
  <mu_0>28.0e9</mu_0>
  <D>4.50e9</D>
  <T_0>294</T_0>
</shear_modulus_model>
```

SCG Shear Modulus Model The Steinberg-Cochran-Guinan (SCG) shear modulus model ([48, 62]) is pressure dependent and has the form

$$\mu(p, T) = \mu_0 + \frac{\partial \mu}{\partial p}\frac{p}{\eta^{1/3}} + \frac{\partial \mu}{\partial T}(T - 300); \quad \eta = \rho/\rho_0 \tag{7.61}$$

where, μ_0 is the shear modulus at the reference state($T = 300$ K, $p = 0$, $\eta = 1$), p is the pressure, and T is the temperature. When the temperature is above T_m, the shear modulus is instantaneously set to zero in this model.

The model is invoked using

```
<shear_modulus_model type="scg_shear">
  <mu_0> 81.8e9 </mu_0>
  <A> 20.6e-12 </A>
  <B> 0.16e-3 </B>
</shear_modulus_model>
```

NP Shear Modulus Model A modified version of the SCG model has been developed by [37] that attempts to capture the sudden drop in the shear modulus close to the melting temperature in a smooth manner. The Nadal-LePoac (NP) shear modulus model has the form

$$\mu(p,T) = \frac{1}{\mathcal{J}(\widehat{T})}\left[\left(\mu_0 + \frac{\partial\mu}{\partial p}\frac{p}{\eta^{1/3}}\right)(1-\widehat{T}) + \frac{\rho}{Cm}\,k_b\,T\right]; \quad C := \frac{(6\pi^2)^{2/3}}{3}f^2 \tag{7.62}$$

where

$$\mathcal{J}(\widehat{T}) := 1 + \exp\left[-\frac{1+1/\zeta}{1+\zeta/(1-\widehat{T})}\right] \quad \text{for} \quad \widehat{T} := \frac{T}{T_m} \in [0, 1+\zeta], \tag{7.63}$$

μ_0 is the shear modulus at 0 K and ambient pressure, ζ is a material parameter, k_b is the Boltzmann constant, m is the atomic mass, and f is the Lindemann constant.

The model is invoked using

```
<shear_modulus_model type="np_shear">
  <mu_0>26.5e9</mu_0>
  <zeta>0.04</zeta>
  <slope_mu_p_over_mu0>65.0e-12</slope_mu_p_over_mu0>
  <C> 0.047 </C>
  <m> 26.98 </m>
</shear_modulus_model>
```

PTW Shear model The PTW shear model is a simplified version of the SCG shear model. The inputs can be found in `.../MPM/ConstitutiveModel/PlasticityModel/PTWShea`

Flow Stress We have explored five temperature and strain rate dependent models that can be used to compute the flow stress:

1. the Johnson-Cook (JC) model
2. the Steinberg-Cochran-Guinan-Lund (SCG) model.
3. the Zerilli-Armstrong (ZA) model.
4. the Mechanical Threshold Stress (MTS) model.
5. the Preston-Tonks-Wallace (PTW) model.

JC Flow Stress Model The Johnson-Cook (JC) model ([29]) is purely empirical and gives the following relation for the flow stress (σ_y)

$$\sigma_y(\epsilon_p, \dot{\epsilon}_p, T) = [A + B(\epsilon_p)^n]\left[1 + C\ln(\dot{\epsilon}_p^*)\right][1 - (T^*)^m] \tag{7.64}$$

where ϵ_p is the equivalent plastic strain, $\dot{\epsilon}_p$ is the plastic strain rate, A, B, C, n, m are material constants,

$$\dot{\epsilon}_p^* = \frac{\dot{\epsilon}_p}{\dot{\epsilon}_{p0}}; \quad T^* = \frac{(T - T_0)}{(T_m - T_0)}\,, \tag{7.65}$$

$\dot{\epsilon}_{p0}$ is a user defined plastic strain rate, T_0 is a reference temperature, and T_m is the melt temperature. For conditions where $T^* < 0$, we assume that $m = 1$.

The inputs for this model are

```
<plasticity_model type="johnson_cook">
  <A>792.0e6</A>
  <B>510.0e6</B>
  <C>0.014</C>
  <n>0.26</n>
  <m>1.03</m>
  <T_r>298.0</T_r>
  <T_m>1793.0</T_m>
  <epdot_0>1.0</epdot_0>
</plasticity_model>
```

SCG Flow Stress Model The Steinberg-Cochran-Guinan-Lund (SCG) model is a semi-empirical model that was developed by [48] for high strain rate situations and extended to low strain rates and bcc materials by [49]. The flow stress in this model is given by

$$\sigma_y(\epsilon_p, \dot{\epsilon}_p, T) = [\sigma_a f(\epsilon_p) + \sigma_t(\dot{\epsilon}_p, T)]\,\frac{\mu(p,T)}{\mu_0} \tag{7.66}$$

where σ_a is the athermal component of the flow stress, $f(\epsilon_p)$ is a function that represents strain hardening, σ_t is the thermally activated component of the flow stress, $\mu(p,T)$ is the shear modulus, and μ_0 is the shear modulus at standard temperature and pressure. The strain hardening function has the form

$$f(\epsilon_p) = [1 + \beta(\epsilon_p + \varepsilon_{pi})]^n; \quad \sigma_a f(\epsilon_p) \le \sigma_{\max} \tag{7.67}$$

where β, n are work hardening parameters, and ε_{pi} is the initial equivalent plastic strain. The thermal component σ_t is computed using a bisection algorithm from the following equation (based on the work of [28])

$$\dot{\epsilon}_p = \left[\frac{1}{C_1}\exp\left[\frac{2U_k}{k_b\,T}\left(1 - \frac{\sigma_t}{\sigma_p}\right)^2\right] + \frac{C_2}{\sigma_t}\right]^{-1}; \quad \sigma_t \le \sigma_p \tag{7.68}$$

where $2U_k$ is the energy to form a kink-pair in a dislocation segment of length L_d, k_b is the Boltzmann constant, σ_p is the Peierls stress. The constants C_1, C_2 are given by the relations

$$C_1 := \frac{\rho_d L_d a b^2 \nu}{2w^2}; \quad C_2 := \frac{D}{\rho_d b^2} \tag{7.69}$$

where ρ_d is the dislocation density, L_d is the length of a dislocation segment, a is the distance between Peierls valleys, b is the magnitude of the Burgers' vector, ν is the Debye frequency, w is the width of a kink loop, and D is the drag coefficient.

The inputs for this model are of the form

```
<plasticity_model type="steinberg_cochran_guinan">
  <mu_0> 81.8e9 </mu_0>
  <sigma_0> 1.15e9 </sigma_0>
  <Y_max> 0.25e9 </Y_max>
  <beta> 2.0 </beta>
  <n> 0.50 </n>
  <A> 20.6e-12 </A>
  <B> 0.16e-3 </B>
  <T_m0> 2310.0 </T_m0>
  <Gamma_0> 3.0 </Gamma_0>
  <a> 1.67 </a>
  <epsilon_p0> 0.0 </epsilon_p0>
</plasticity_model>
```

ZA Flow Stress Model The Zerilli-Armstrong (ZA) model ([60, 61, 59]) is based on simplified dislocation mechanics. The general form of the equation for the flow stress is

$$\sigma_y(\epsilon_p, \dot{\epsilon}_p, T) = \sigma_a + B\exp(-\beta(\dot{\epsilon}_p)T) + B_0\sqrt{\epsilon_p}\exp(-\alpha(\dot{\epsilon}_p)T) \tag{7.70}$$

where σ_a is the athermal component of the flow stress given by

$$\sigma_a := \sigma_g + \frac{k_h}{\sqrt{l}} + K\epsilon_p^n, \tag{7.71}$$

σ_g is the contribution due to solutes and initial dislocation density, k_h is the microstructural stress intensity, l is the average grain diameter, K is zero for fcc materials, B, B_0 are material constants. The functional forms of the exponents α and β are

$$\alpha = \alpha_0 - \alpha_1\ln(\dot{\epsilon}_p); \quad \beta = \beta_0 - \beta_1\ln(\dot{\epsilon}_p); \tag{7.72}$$

where $\alpha_0, \alpha_1, \beta_0, \beta_1$ are material parameters that depend on the type of material (fcc, bcc, hcp, alloys). The Zerilli-Armstrong model has been modified by [1] for better performance at high temperatures. However, we have not used the modified equations in our computations.

The inputs for this model are of the form

```
<bcc_or_fcc> fcc </bcc_or_fcc>
<c2> </c2>
<c3> </c3>
<c4> </c4>
<n> </n>
```

MTS Flow Stress Model The Mechanical Threshold Stress (MTS) model ([19, 20, 33]) gives the following form for the flow stress

$$\sigma_y(\epsilon_p, \dot{\epsilon}_p, T) = \sigma_a + (S_i\sigma_i + S_e\sigma_e)\frac{\mu(p,T)}{\mu_0} \tag{7.73}$$

where σ_a is the athermal component of mechanical threshold stress, μ_0 is the shear modulus at 0 K and ambient pressure, σ_i is the component of the flow stress due to intrinsic barriers to thermally activated dislocation motion and dislocation-dislocation interactions, σ_e is the component of the flow stress due to microstructural evolution with increasing deformation (strain hardening), (S_i, S_e) are temperature and strain rate dependent scaling factors. The scaling factors take the Arrhenius form

$$S_i = \left[1 - \left(\frac{k_b\ T}{g_{0i}b^3\mu(p,T)}\ln\frac{\dot{\epsilon}_{p0i}}{\dot{\epsilon}_p}\right)^{1/q_i}\right]^{1/p_i} \tag{7.74}$$

$$S_e = \left[1 - \left(\frac{k_b\ T}{g_{0e}b^3\mu(p,T)}\ln\frac{\dot{\epsilon}_{p0e}}{\dot{\epsilon}_p}\right)^{1/q_e}\right]^{1/p_e} \tag{7.75}$$

where k_b is the Boltzmann constant, b is the magnitude of the Burgers' vector, (g_{0i}, g_{0e}) are normalized activation energies, $(\dot{\epsilon}_{p0i}, \dot{\epsilon}_{p0e})$ are constant reference strain rates, and (q_i, p_i, q_e, p_e) are constants. The strain hardening component of the mechanical threshold stress (σ_e) is given by a modified Voce law

$$\frac{d\sigma_e}{d\epsilon_p} = \theta(\sigma_e) \tag{7.76}$$

where

$$\theta(\sigma_e) = \theta_0[1 - F(\sigma_e)] + \theta_{IV}F(\sigma_e) \tag{7.77}$$

$$\theta_0 = a_0 + a_1\ln\dot{\epsilon}_p + a_2\sqrt{\dot{\epsilon}_p} - a_3T \tag{7.78}$$

$$F(\sigma_e) = \frac{\tanh\left(\alpha\dfrac{\sigma_e}{\sigma_{es}}\right)}{\tanh(\alpha)} \tag{7.79}$$

$$\ln(\frac{\sigma_{es}}{\sigma_{0es}}) = \left(\frac{kT}{g_{0es}b^3\mu(p,T)}\right)\ln\left(\frac{\dot{\epsilon}_p}{\dot{\epsilon}_{p0es}}\right) \tag{7.80}$$

and θ_0 is the hardening due to dislocation accumulation, θ_{IV} is the contribution due to stage-IV hardening, $(a_0, a_1, a_2, a_3, \alpha)$ are constants, σ_{es} is the stress at zero strain hardening rate, σ_{0es} is the saturation threshold stress for deformation at 0 K, g_{0es} is a constant, and $\dot{\epsilon}_{p0es}$ is the maximum strain rate. Note that the maximum strain rate is usually limited to about 10^7/s.

The inputs for this model are of the form

```
<plasticity_model type="mts_model">
  <sigma_a>363.7e6</sigma_a>
  <mu_0>28.0e9</mu_0>
  <D>4.50e9</D>
  <T_0>294</T_0>
  <koverbcubed>0.823e6</koverbcubed>
  <g_0i>0.0</g_0i>
  <g_0e>0.71</g_0e>
  <edot_0i>0.0</edot_0i>
  <edot_0e>2.79e9</edot_0e>
  <p_i>0.0</p_i>
  <q_i>0.0</q_i>
  <p_e>1.0</p_e>
  <q_e>2.0</q_e>
  <sigma_i>0.0</sigma_i>
  <a_0>211.8e6</a_0>
  <a_1>0.0</a_1>
  <a_2>0.0</a_2>
  <a_3>0.0</a_3>
  <theta_IV>0.0</theta_IV>
  <alpha>2</alpha>
  <edot_es0>3.42e8</edot_es0>
  <g_0es>0.15</g_0es>
  <sigma_es0>1679.3e6</sigma_es0>
</plasticity_model>
```

PTW Flow Stress Model The Preston-Tonks-Wallace (PTW) model ([41]) attempts to provide a model for the flow stress for extreme strain rates (up to 10^{11}/s) and temperatures up to melt. The flow stress is given by

$$\sigma_y(\epsilon_p, \dot{\epsilon}_p, T) = \begin{cases} 2\left[\tau_s + \alpha \ln\left[1 - \varphi \exp\left(-\beta - \dfrac{\theta \epsilon_p}{\alpha \varphi}\right)\right]\right] \mu(p,T) & \text{thermal regime} \\ 2\tau_s \mu(p,T) & \text{shock regime} \end{cases} \tag{7.81}$$

with

$$\alpha := \frac{s_0 - \tau_y}{d}; \quad \beta := \frac{\tau_s - \tau_y}{\alpha}; \quad \varphi := \exp(\beta) - 1 \tag{7.82}$$

where τ_s is a normalized work-hardening saturation stress, s_0 is the value of τ_s at 0K, τ_y is a normalized yield stress, θ is the hardening constant in the Voce hardening law, and d is a dimensionless material parameter that modifies the Voce hardening law. The saturation stress and the yield stress are given by

$$\tau_s = \max\left\{ s_0 - (s_0 - s_\infty)\text{erf}\left[\kappa \widehat{T} \ln\left(\frac{\gamma \dot{\xi}}{\dot{\epsilon}_p}\right)\right], s_0 \left(\frac{\dot{\epsilon}_p}{\gamma \dot{\xi}}\right)^{s_1} \right\} \tag{7.83}$$

$$\tau_y = \max\left\{ y_0 - (y_0 - y_\infty)\text{erf}\left[\kappa \widehat{T} \ln\left(\frac{\gamma \dot{\xi}}{\dot{\epsilon}_p}\right)\right], \min\left\{ y_1 \left(\frac{\dot{\epsilon}_p}{\gamma \dot{\xi}}\right)^{y_2}, s_0 \left(\frac{\dot{\epsilon}_p}{\gamma \dot{\xi}}\right)^{s_1} \right\} \right\} \tag{7.84}$$

where s_∞ is the value of τ_s close to the melt temperature, (y_0, y_∞) are the values of τ_y at 0K and close to melt, respectively, (κ, γ) are material constants, $\widehat{T} = T/T_m$, (s_1, y_1, y_2) are material parameters for the high strain rate regime, and

$$\dot{\xi} = \frac{1}{2}\left(\frac{4\pi\rho}{3M}\right)^{1/3}\left(\frac{\mu(p,T)}{\rho}\right)^{1/2} \tag{7.85}$$

where ρ is the density, and M is the atomic mass.

The inputs for this model are of the form

```
<plasticity_model type="preston_tonks_wallace">
  <theta> 0.025 </theta>
  <p> 2.0 </p>
  <s0> 0.0085 </s0>
  <sinf> 0.00055 </sinf>
  <kappa> 0.11 </kappa>
  <gamma> 0.00001 </gamma>
  <y0> 0.0001 </y0>
  <yinf> 0.0001 </yinf>
  <y1> 0.094 </y1>
  <y2> 0.575 </y2>
  <beta> 0.25 </beta>
  <M> 63.54 </M>
  <G0> 518e8 </G0>
  <alpha> 0.20 </alpha>
  <alphap> 0.20 </alphap>
</plasticity_model>
```

Adiabatic Heating and Specific Heat A part of the plastic work done is converted into heat and used to update the temperature of a particle. The increase in temperature (ΔT) due to an increment in plastic strain $(\Delta\epsilon_p)$ is given by the equation

$$\Delta T = \frac{\chi\sigma_y}{\rho C_p}\Delta\epsilon_p \tag{7.86}$$

where χ is the Taylor-Quinney coefficient, and C_p is the specific heat. The value of the Taylor-Quinney coefficient is taken to be 0.9 in all our simulations (see [44] for more details on the variation of χ with strain and strain rate).

The Taylor-Quinney coefficient is taken as input in the ElasticPlastic model using the tags

```
<taylor_quinney_coeff> 0.9 </taylor_quinney_coeff>
```

Default specific heat model The default model returns a constant specific heat and is invoked using

```
<specific_heat_model type="constant_Cp">
</specific_heat_model>
```

Specific heat model for copper The specific heat model for copper is of the form

$$Cp = \begin{cases} A_0\ T^3 - B_0\ T^2 + C_0\ T - D_0 & \text{if } T < T_0 \\ A_1\ T + B_1 & \text{if } T \geq T_0\ . \end{cases} \tag{7.87}$$

The model is invoked using

```
<specific_heat_model type = "copper_Cp"> </specific_heat_model>
```

Specific heat model for steel A relation for the dependence of C_p upon temperature is used for the steel ([34]).

$$C_p = \begin{cases} A_1 + B_1\ t + C_1\ |t|^{-\alpha} & \text{if } T < T_c \\ A_2 + B_2\ t + C_2\ t^{-\alpha^{'}} & \text{if } T > T_c \end{cases} \tag{7.88}$$

$$t = \frac{T}{T_c} - 1 \tag{7.89}$$

where T_c is the critical temperature at which the phase transformation from the α to the γ phase takes place, and $A_1, A_2, B_1, B_2, \alpha, \alpha^{'}$ are constants.

The model is invoked using

```
<specific_heat_model type = "steel_Cp"> </specific_heat_model>
```

The heat generated at a material point is conducted away at the end of a time step using the transient heat equation. The effect of conduction on material point temperature is negligible (but non-zero) for the high strain-rate problems simulated using Uintah.

Adding new models In the parallel implementation of the stress update algorithm, sockets have been added to allow for the incorporation of a variety of plasticity, damage, yield, and bifurcation models without requiring any change in the stress update code. The algorithm is shown in Algorithm 7.1. The equation of state, plasticity model, yield condition, damage model, and the stability criterion are all polymorphic objects created using a factory idiom in C++ ([16]).

Addition of a new model requires the following steps (the example below is only for the flow stress model but the same idea applies to other models) :

1. Creation of a new class that encapsulates the plasticity model. The template for this class can be copied from the existing plasticity models. The data that is unique to the new model are specified in the form of

   - A structure containing the constants for the plasticity model.
   - Particle variables that specify the variables that evolve in the plasticity model.

Table 7.1: Stress Update Algorithm

Persistent:Initial moduli, temperature, porosity,
scalar damage, equation of state, plasticity model,
yield condition, stability criterion, damage model
Temporary:Particle state at time t
Output: Particle state at time $t + \Delta t$

For *all the patches in the domain*
Read the particle data and initialize updated data storage
For *all the particles in the patch*
Compute the velocity gradient and the rate of deformation tensor
Compute the deformation gradient and the rotation tensor
Rotate the Cauchy stress and the rate of deformation tensor
to the material configuration
Compute the current shear modulus and melting temperature
Compute the pressure using the equation of state,
update the hydrostatic stress, and
compute the trial deviatoric stress
Compute the flow stress using the plasticity model
Evaluate the yield function
If *particle is elastic*
Update the elastic deviatoric stress from the trial stress
Rotate the stress back to laboratory coordinates
Update the particle state
Else
Compute the elastic-plastic deviatoric stress
Compute updated porosity, scalar damage, and
temperature increase due to plastic work
Compute elastic-plastic tangent modulus and evaluate stability condition
Rotate the stress back to laboratory coordinates
Update the particle state
End If
If *Temperature* > *Melt Temperature* or *Porosity* > *Critical Porosity* or *Unstable*
Tag particle as failed
End If
Convert failed particles into a material with a different velocity field
End For
End For

2. The implementation of the plasticity model involves the following steps.

   - Reading the input file for the model constants in the constructor.
   - Adding the variables that evolve in the plasticity model appropriately to the task graph.
   - Adding the appropriate flow stress calculation method.

3. The `PlasticityModelFactory` is then modified so that it recognizes the added plasticity model.

Damage Models and Failure Only the Johnson-Cook damage evolution rule has been added to the DamageModelFactory so far. The damage model framework is designed to be similar to the plasticity model framework. New models can be added using the approach described in the previous section.

A particle is tagged as "failed" when its temperature is greater than the melting point of the material at the applied pressure. An additional condition for failure is when the porosity of a particle increases beyond a critical limit and the strain exceeds the fracture strain of the material. Another condition for failure is when a material bifurcation condition such as the Drucker stability postulate is satisfied. Upon failure, a particle is either removed from the computation by setting the stress to zero or is converted into a material with a different velocity field which interacts with the remaining particles via contact. Either approach leads to the simulation of a newly created surface. More details of the approach can be found in [2, 3, 4].

Yield conditions When failure is to be simulated we can use the Gurson-Tvergaard-Needleman yield condition instead of the von Mises condition.

The von Mises yield condition The von Mises yield condition is the default and is invoked using the tags

```
<yield_condition type="vonMises">
</yield_condition>
```

The Gurson-Tvergaard-Needleman (GTN) yield condition The Gurson-Tvergaard-Needleman (GTN) yield condition [23, 53] depends on porosity. An associated flow rule is used to determine the plastic rate parameter in either case. The GTN yield condition can be written as

$$\Phi = \left(\frac{\sigma_{eq}}{\sigma_f}\right)^2 + 2q_1 f_* \cosh\left(q_2 \frac{Tr(\sigma)}{2\sigma_f}\right) - (1 + q_3 f_*^2) = 0 \tag{7.90}$$

where q_1, q_2, q_3 are material constants and f_* is the porosity (damage) function given by

$$f* = \begin{cases} f & \text{for } f \leq f_c, \\ f_c + k(f - f_c) & \text{for } f > f_c \end{cases} \tag{7.91}$$

where k is a constant and f is the porosity (void volume fraction). The flow stress in the matrix material is computed using either of the two plasticity models discussed earlier. Note that the flow stress in the matrix material also remains on the undamaged matrix yield surface and uses an associated flow rule.

This yield condition is invoked using

```
<yield_condition type="gurson">
  <q1> 1.5 </q1>
  <q2> 1.0 </q2>
  <q3> 2.25 </q3>
  <k> 4.0 </k>
  <f_c> 0.05 </f_c>
</yield_condition>
```

Porosity model The evolution of porosity is calculated as the sum of the rate of growth and the rate of nucleation [43]. The rate of growth of porosity and the void nucleation rate are given by the following equations [15]

$$\dot{f} = \dot{f}_{\text{nucl}} + \dot{f}_{\text{grow}} \tag{7.92}$$

$$\dot{f}_{\text{grow}} = (1 - f)\text{Tr}(\boldsymbol{D}_p) \tag{7.93}$$

$$\dot{f}_{\text{nucl}} = \frac{f_n}{(s_n\sqrt{2\pi})} \exp\left[-\frac{1}{2}\frac{(\epsilon_p - \epsilon_n)^2}{s_n^2}\right] \dot{\epsilon}_p \tag{7.94}$$

where $\boldsymbol{D}_p$ is the rate of plastic deformation tensor, f_n is the volume fraction of void nucleating particles , ϵ_n is the mean of the distribution of nucleation strains, and s_n is the standard deviation of the distribution.

The inputs tags for porosity are of the form

```
<evolve_porosity> true </evolve_porosity>
<initial_mean_porosity>         0.005 </initial_mean_porosity>
<initial_std_porosity>          0.001 </initial_std_porosity>
<critical_porosity>             0.3   </critical_porosity>
<frac_nucleation>               0.1   </frac_nucleation>
<meanstrain_nucleation>         0.3   </meanstrain_nucleation>
<stddevstrain_nucleation>       0.1   </stddevstrain_nucleation>
<initial_porosity_distrib>      gauss </initial_porosity_distrib>
```

Damage model After the stress state has been determined on the basis of the yield condition and the associated flow rule, a scalar damage state in each material point

can be calculated using the Johnson-Cook model [30]. The Johnson-Cook model has an explicit dependence on temperature, plastic strain, ans strain rate.

The damage evolution rule for the Johnson-Cook damage model can be written as

$$\dot{D} = \frac{\dot{\epsilon_p}}{\epsilon_p^f} \; ; \quad \epsilon_p^f = \left[D_1 + D_2 \exp\left(\frac{D_3}{3}\sigma^* \right) \right] \left[1 + D_4 \ln(\dot{\epsilon_p}^*) \right] \left[1 + D_5 T^* \right] \; ; \quad \sigma^* = \frac{\mathrm{Tr}(\boldsymbol{\sigma})}{\sigma_{eq}} \; ; \tag{7.95}$$

where D is the damage variable which has a value of 0 for virgin material and a value of 1 at fracture, ϵ_p^f is the fracture strain, D_1, D_2, D_3, D_4, D_5 are constants, $\boldsymbol{\sigma}$ is the Cauchy stress, and T^* is the scaled temperature as in the Johnson-Cook plasticity model.

The input tags for the damage model are :

```
<damage_model type="johnson_cook">
  <D1>0.05</D1>
  <D2>3.44</D2>
  <D3>-2.12</D3>
  <D4>0.002</D4>
  <D5>0.61</D5>
</damage_model>
```

An initial damage distribution can be created using the following tags

```
<evolve_damage>                 true  </evolve_damage>
<initial_mean_scalar_damage>    0.005  </initial_mean_scalar_damage>
<initial_std_scalar_damage>     0.001 </initial_std_scalar_damage>
<critical_scalar_damage>        1.0   </critical_scalar_damage>
<initial_scalar_damage_distrib> gauss </initial_scalar_damage_distrib>
```

Erosion algorithm Under normal conditions, the heat generated at a material point is conducted away at the end of a time step using the heat equation. If special adiabatic conditions apply (such as in impact problems), the heat is accumulated at a material point and is not conducted to the surrounding particles. This localized heating can be used to determine whether a material point has melted.

The determination of whether a particle has failed can be made on the basis of either or all of the following conditions:

- The particle temperature exceeds the melting temperature.
- The TEPLA-F fracture condition [31] is satisfied. This condition can be written as

  $$(f/f_c)^2 + (\epsilon_p/\epsilon_p^f)^2 = 1 \tag{7.96}$$

  where f is the current porosity, f_c is the maximum allowable porosity, ϵ_p is the current plastic strain, and ϵ_p^f is the plastic strain at fracture.
- An alternative to ad-hoc damage criteria is to use the concept of bifurcation to determine whether a particle has failed or not. Two stability criteria have

been explored in this paper - the Drucker stability postulate [18] and the loss of hyperbolicity criterion (using the determinant of the acoustic tensor) [45, 40].

The simplest criterion that can be used is the Drucker stability postulate [18] which states that time rate of change of the rate of work done by a material cannot be negative. Therefore, the material is assumed to become unstable (and a particle fails) when

$$\dot{\boldsymbol{\sigma}} : \boldsymbol{D}^p \leq 0 \tag{7.97}$$

Another stability criterion that is less restrictive is the acoustic tensor criterion which states that the material loses stability if the determinant of the acoustic tensor changes sign [45, 40]. Determination of the acoustic tensor requires a search for a normal vector around the material point and is therefore computationally expensive. A simplification of this criterion is a check which assumes that the direction of instability lies in the plane of the maximum and minimum principal stress [10]. In this approach, we assume that the strain is localized in a band with normal $\boldsymbol{n}$, and the magnitude of the velocity difference across the band is $\boldsymbol{g}$. Then the bifurcation condition leads to the relation

$$R_{ij}g_j = 0 \ ; \quad R_{ij} = M_{ikjl}n_k n_l + M_{ilkj}n_k n_l - \sigma_{ik}n_j n_k \tag{7.98}$$

where M_{ijkl} are the components of the co-rotational tangent modulus tensor and σ_{ij} are the components of the co-rotational stress tensor. If $\det(R_{ij}) \leq 0$, then g_j can be arbitrary and there is a possibility of strain localization. If this condition for loss of hyperbolicity is met, then a particle deforms in an unstable manner and failure can be assumed to have occurred at that particle. We use a combination of these criteria to simulate failure.

Since the material in the container may unload locally after fracture, the hypoelastic-plastic stress update may not work accurately under certain circumstances. An improvement would be to use a hyperelastic-plastic stress update algorithm. Also, the plasticity models are temperature dependent. Hence there is the issue of severe mesh dependence due to change of the governing equations from hyperbolic to elliptic in the softening regime [27, 9, 54]. Viscoplastic stress update models or nonlocal/gradient plasticity models [42, 25] can be used to eliminate some of these effects and are currently under investigation.

The tags used to control the erosion algorithm are in two places. In the `<MPM> </MPM>` section the following flags can be set

```
<erosion algorithm = "ZeroStress"/>
<create_new_particles>          false      </create_new_particles>
<manual_new_material>           false      </manual_new_material>
```

If the erosion algorithm is `"none"` then no particle failure is done.

In the `<constitutive_model type="elastic_plastic">` section, the following flags can be set

```
<evolve_porosity>                true  </evolve_porosity>
<evolve_damage>                  true  </evolve_damage>
<do_melting>                     true  </do_melting>
<useModifiedEOS>                 true  </useModifiedEOS>
<check_TEPLA_failure_criterion> true  </check_TEPLA_failure_criterion>
<check_max_stress_failure>       false </check_max_stress_failure>
<critical_stress>               12.0e9 </critical_stress>
```

Implementation The elastic response is assumed to be isotropic. The material constants that are taken as input for the elastic response are the bulk and shear modulus. The flow rule is determined from the input and the appropriate plasticity model is created using the `PlasticityModelFactory` class. The damage evolution rule is determined from the input and a damage model is created using the `DamageModelFactory` class. The equation of state that is used to determine the pressure is also determined from the input. The equation of state model is created using the `MPMEquationOfStateFactory` class.

In addition, a damage evolution variable (D) is stored at each time step (this need not be the case and will be transfered to the damage models in the future). The left stretch and rotation are updated incrementally at each time step (instead of performing a polar decomposition) and the rotation tensor is used to rotate the Cauchy stress and rate of deformation to the material coordinates at each time step (instead of using a objective stress rate formulation).

Any evolution variables for the plasticity model, damage model or the equation of state are specified in the class that encapsulates the particular model.

The flow stress is calculated from the plasticity model using a function call of the form

```
double flowStress = d_plasticity->computeFlowStress(tensorEta, tensorS,
                                                    pTemperature[idx],
                                                    delT, d_tol, matl, idx);
```

A number of plasticity models can be evaluated using the inputs in the `computeFlowStress` call. The variable `d_plasticity` is polymorphic and can represent any of the plasticity models that can be created by the plasticity model factory. The plastic evolution variables are updated using a polymorphic function along the lines of `computeFlowStress`.

The equation of state is used to calculate the hydrostatic stress using a function call of the form

```
Matrix3 tensorHy = d_eos->computePressure(matl, bulk, shear,
                                          tensorF_new, tensorD,
                                          tensorP, pTemperature[idx],
                                          rho_cur, delT);
```

Similarly, the damage model is called using a function of the type

```
double damage = d_damage->computeScalarDamage(tensorEta, tensorS,
                                              pTemperature[idx],
```

```
                                                    delT, matl, d_tol,
                                                    pDamage[idx]);
```

Therefore, the plasticity, damage and equation of state models are easily be inserted into any other type of stress update algorithm without any change being needed in them as can be seen in the hyperelastic-plastic stress update algorithm discussed below.

Example input file for the elastic-plastic model An example of the portion of an input file that specifies a copper body with a hypoelastic stress update, Johnson-Cook plasticity model, Johnson-Cook Damage Model and Mie-Gruneisen Equation of State is shown below.

```
<material>

  <include href="inputs/MPM/MaterialData/MaterialConstAnnCopper.xml"/>
  <constitutive_model type="elastic_plastic">
    <tolerance>5.0e-10</tolerance>
    <include href="inputs/MPM/MaterialData/IsotropicElasticAnnCopper.xml"/>
    <include href="inputs/MPM/MaterialData/JohnsonCookPlasticAnnCopper.xml"/>
    <include href="inputs/MPM/MaterialData/JohnsonCookDamageAnnCopper.xml"/>
    <include href="inputs/MPM/MaterialData/MieGruneisenEOSAnnCopper.xml"/>
  </constitutive_model>

  <geom_object>
    <cylinder label = "Cylinder">
      <bottom>[0.0,0.0,0.0]</bottom>
      <top>[0.0,2.54e-2,0.0]</top>
      <radius>0.762e-2</radius>
    </cylinder>
    <res>[3,3,3]</res>
    <velocity>[0.0,-208.0,0.0]</velocity>
    <temperature>294</temperature>
  </geom_object>

</material>
```

The general material constants for copper are in the file `MaterialConstAnnCopper.xml`. The contents are shown below

```
<?xml version='1.0' encoding='ISO-8859-1' ?>
<Uintah_Include>
  <density>8930.0</density>
  <toughness>10.e6</toughness>
  <thermal_conductivity>1.0</thermal_conductivity>
  <specific_heat>383</specific_heat>
  <room_temp>294.0</room_temp>
  <melt_temp>1356.0</melt_temp>
</Uintah_Include>
```

The elastic properties are in the file `IsotropicElasticAnnCopper.xml`. The contents of this file are shown below.

```
<?xml version='1.0' encoding='ISO-8859-1' ?>
<Uintah_Include>
  <shear_modulus>45.45e9</shear_modulus>
  <bulk_modulus>136.35e9</bulk_modulus>
</Uintah_Include>
```

The constants for the Johnson-Cook plasticity model are in the file `JohnsonCookPlasticAnnCopp` The contents of this file are shown below.

```
<?xml version='1.0' encoding='ISO-8859-1' ?>
<Uintah_Include>
  <plasticity_model type="johnson_cook">
    <A>89.6e6</A>
    <B>292.0e6</B>
    <C>0.025</C>
    <n>0.31</n>
    <m>1.09</m>
  </plasticity_model>
</Uintah_Include>
```

The constants for the Johnson-Cook damage model are in the file `JohnsonCookDamageAnnCopper` The contents of this file are shown below.

```
<?xml version='1.0' encoding='ISO-8859-1' ?>
<Uintah_Include>
  <damage_model type="johnson_cook">
    <D1>0.54</D1>
    <D2>4.89</D2>
    <D3>-3.03</D3>
    <D4>0.014</D4>
    <D5>1.12</D5>
  </damage_model>
</Uintah_Include>
```

The constants for the Mie-Gruneisen model (as implemented in the Uintah Computational Framework) are in the file `MieGruneisenEOSAnnCopper.xml`. The contents of this file are shown below.

```
<?xml version='1.0' encoding='ISO-8859-1' ?>
<Uintah_Include>
  <equation_of_state type="mie_gruneisen">
    <C_0>3940</C_0>
    <Gamma_0>2.02</Gamma_0>
    <S_alpha>1.489</S_alpha>
  </equation_of_state>
</Uintah_Include>
```

As can be seen from the input file, any other plasticity model, damage model and equation of state can be used to replace the Johnson-Cook and Mie-Gruneisen models without any extra effort (provided the models have been implemented and the data exist).

The material data can easily be taken from a material database or specified for a new material in an input file kept at a centralized location. At this stage material data for a range of materials is kept in the directory `.../Uintah/StandAlone/inputs/MPM/MaterialData`.

Contact

When multiple materials are specified in the input file, each material interacts with its own field variables. In other words, each material has its own mass, velocity, acceleration, etc. Without any mechanism for their interaction, each material would behave as if it were the only one in the domain. Contact models provide the mechanism by which to specify rules for inter material interactions. There are a number of contact models from which to choose, the use of each is described next. See the input file segment in Section 7.5 for an example of their proper placement in the input file, namely, after all of the MPM materials have been described.

The simplest contact model is the `null` model, which indicates that no inter material interactions are to take place. This is typically only used in single material simulations. Its usage looks like:

```
<contact>
  <type>null</type>
</contact>
```

The next simplest model is the `single_velocity` model. The basic MPM formulation provides "free" no-slip, no-interpenetration contact, assuming that all particle data communicates with a single field on the grid. For a single material simulation with multiple objects, that is the case. If one wishes to achieve that behavior in Uintah-MPM when multiple materials are present, the `single_velocity` contact model should be used. It is specified as:

```
<contact>
  <type>single_velocity</type>
  <materials>[0,1]</materials>
</contact>
```

Note that for this, and all of the contact models, the `<materials>` tag is optional. If it is omitted, the assumption is that all materials will interact via the same contact model. (This will be further discussed below.)

The ultimate in contact models is the `friction` contact model. For a full description, the reader is directed to the paper by Bardenhagen et al.[7]. Briefly, the model both overcomes some deficiences in the single velocity field contact (either the "free" contact or the model described above, which behave identically), and it enables some additional features. With single velocity field contact, initially adjacent objects are treated as if they are effectively stuck together. The friction contact model overcomes this by detecting if materials are approaching or departing at a given node. If they are

approaching, contact is "enforced" and if they are departing, another check is made to determine if the objects are in compression or tension. If they are in compression, then they are still rebounding from each other, and so contact is enforced. If tension is detected, they are allowed to move apart independently. Frictional sliding is allowed, based on the value specified for `<mu>` and the normal force between the objects. An example of the use of this model is given here:

```
<contact>
   <type>friction</type>
   <materials>[0,1,2]</materials>
   <mu> 0.5 </mu>
</contact>
```

A slightly simplified version of the friction model is the `<approach>` model. It is the same as the frictional model above, except that it doesn't make the additional check on the traction between two bodies at each node. At times, it is necessary to neglect this, but some loss of energy will result. Specification is of the model is also nearly identical:

```
<contact>
   <type>approach</type>
   <materials>[0,1,2]</materials>
   <mu> 0.5 </mu>
</contact>
```

Note, at this time, neither of these models works properly with the axisymmetric formulation, due to the necessary gradient calculations. This will be fixed in subseqent releases of Uintah.

Finally, the contact infrastructure is also used to provide a moving displacement boundary condition. Imagine a billet being smashed by a rigid platen, for example. Usage of this model, known as `<specified>` contact, looks like:

```
<contact>
  <type>specified</type>
  <filename>TXC.txt</filename>
  <materials>[0,1,2]</materials>
  <master_material>[0]</master_material>
  <direction>[1,1,1]</direction>
  <stop_time>1.0 </stop_time>
  <velocity_after_stop>[0, 0, 0]</velocity_after_stop>
</contact>
```

For reasons of backwards compatibility, the `<type>specified</type>` is interchangable with `<type>rigid</type>`. By default, when either model is chosen, material 0 is the "rigid" material, although this can be over ridden by the use of the `<master_material>` field. If no `<filename>` field is specified, then the particles of the rigid material proceed

with the velocity that they were given as their initial condition, either until the reach a computational boundary, or until the simulation time has reached `<stop_time>,` after which, their velocity becomes that given in the `<velocity_after_stop>` field. The `<direction>` field indicates in which cartesian directions contact should be specified. Values of 1 indicate that contact should be specified, 0 indicates that the subject materials should be allowed to slide in that direction. If a `<filename>` field *is* specified, then the user can create a text file which contains four entries per line. These are:

```
time1 velocity_x1 velocity_y1 velocity_z1
time2 velocity_x2 velocity_y2 velocity_z2
     .
     .
     .
```

The velocity of the rigid material particles will be set to these values, based on linear interpolation between times, until `<stop_time>` is reached.

Finally, it is possible to specify more than one contact model. Suppose one has a simulation with three materials, one rigid, and the other two deformable. The user may want to have the rigid material interact in a rigid manner with the other two materials, while the two deformable materials interact with each other in a single velocity field manner. Specification for this, assuming the rigid material is 0 would look like:

```
<contact>
    <type>single_velocity</type>
    <materials>[1,2]</materials>
</contact>

<contact>
    <type>specified</type>
    <filename>prof.txt</filename>
    <stop_time>1.0</stop_time>
    <direction>[0, 0, 1]</direction>
</contact>
```

An example of this usage can be found in `inputs/MPM/twoblock-single-rigid.ups.`

BoundaryConditions

Boundary conditions must be specified on each face of the computational domain $(x^-, x^+, y^-, y^+, z^-, z^+)$ for each material. An example of their specification is as follows, where the entire `<Grid>` field is included for context:

```
<Grid>
   <BoundaryConditions>
     <Face side = "x-">
         <BCType id = "all" var = "Dirichlet" label = "Velocity">
               <value> [0.0,0.0,0.0] </value>
         </BCType>
```

```
    </Face>
    <Face side = "x+">
       <BCType id = "all" var = "Neumann" label = "Velocity">
            <value> [0.0,0.0,0.0] </value>
       </BCType>
    </Face>
    <Face side = "y-">
      <BCType id = "all" var = "Dirichlet" label = "Velocity">
             <value> [0.0,0.0,0.0] </value>
      </BCType>
    </Face>
    <Face side = "y+">
      <BCType id = "all" var = "Neumann" label = "Velocity">
             <value> [0.0,0.0,0.0] </value>
      </BCType>
    </Face>
    <Face side = "z-">
      <BCType id = "all" var = "symmetry" label = "Symmetric"> </BCType>
    </Face>
    <Face side = "z+">
      <BCType id = "all" var = "symmetry" label = "Symmetric"> </BCType>
    </Face>
  </BoundaryConditions>
  <Level>
```

... See Section 2.10 ...

```
  </Level>
</Grid>
```

The three main types of numerical boundary conditions (BCs) that can be applied are "Neumann", "Dirichlet", and "Symmetric", and the use of each is illustrated above. In the case of MPM simulations, Neumann BCs are used when one wishes to allow particles to advect freely out of the computational domain. Dirichlet BCs are used to specify a velocity, zero or otherwise (indicated by the `<value>` tag), on one of the computational boundaries. Symmetric BCs are used to indicate a plane of symmetry. This has a variety of uses. The most obvious is simply when a simulation of interest has symmetry that one can take advantage of to reduce the cost of a calculation. Similarly, since Uintah is a three-dimensional code, if one wishes to achieve plane-strain conditions, this can be done by carrying out a simulation that is one cell thick with Symmetric BCs applied to each face of the plane, as in the example above. Finally, Symmetric BCs also provide a free slip boundary.

There is also the field `id = "all"` . In principal, one could set different boundary condition types for different materials. In practice, this is rarely used, so the usage illustrated here should be used.

Physical Boundary Conditions

It is often more convenient to apply a specified load at the MPM particles. The load may be a function of time. Such a load versus time curve is called a **load curve**. In Uintah, the load curve infrastructure is available for general use (and not only for particles). However, it has been implemented only for a special case of pressure loading. Namely, a surface is specified through the use of the `<geom_object>` description, and a pressure vs. time curve is described by specifying their values at discrete points in time, between which linear interpolation is used to find values at any time. At $t = 0$, those particles in the vicinity of the the surface are tagged with a load curve ID, and those particles are assigned external forces such that the desired pressure is achieved.

We invoke the load curve in the `<MPM>` section (See Section 7.5)of the input file using `<use_load_curves> true </use_load_curves>`. The default value is `<use_load_curves> false`

In Uintah, a load curve infrastructure is implemented in the file `.../MPM/PhysicalBC/LoadCurve.h`. This file is essentially a templated structure that has the following private data

```
// Load curve information
std::vector<double> d_time;
std::vector<T> d_load;
int d_id;
```

The variable `d_id` is the load curve ID, `d_time` is the time, and `d_load` is the load. Note that the load can have any form - scalar, vector, matrix, etc.

In our current implementation, the actual specification of the load curve information is in the `<PhysicalBC>` section of the input file. The implementation is limited in that it applies only to pressure boundary conditions for some special geometries (the implementation is in `.../MPM/PhysicalBC/PressureBC.cc`). However, the load curve template can be used in other, more general, contexts.

A sample input file specification of a pressure load curve is shown below. In this case, a pressure is applied to the inside and outside of a cylinder. The pressure is ramped up from 0 to 1 GPa on the inside and from 0 to 0.1 MPa on the outside over a time of 10 microsecs.

```
<PhysicalBC>
  <MPM>
    <pressure>
      <geom_object>
        <cylinder label = "inner cylinder">
          <bottom>           [0.0,0.0,0.0]   </bottom>
          <top>              [0.0,0.0,.02]   </top>
          <radius>           0.5             </radius>
        </cylinder>
      </geom_object>
      <load_curve>
        <id>1</id>
        <time_point>
```

```
          <time> 0 </time>
          <load> 0 </load>
        </time_point>
        <time_point>
          <time> 1.0e-5 </time>
          <load> 1.0e9 </load>
        </time_point>
      </load_curve>
    </pressure>
    <pressure>
      <geom_object>
        <cylinder label = "outer cylinder">
          <bottom>           [0.0,0.0,0.0]   </bottom>
          <top>              [0.0,0.0,.02]   </top>
          <radius>           1.0             </radius>
        </cylinder>
      </geom_object>
      <load_curve>
        <id>2</id>
        <time_point>
          <time> 0 </time>
          <load> 0 </load>
        </time_point>
        <time_point>
          <time> 1.0e-5 </time>
          <load> 101325.0 </load>
        </time_point>
      </load_curve>
    </pressure>
  </MPM>
</PhysicalBC>
```

The complete input file can be found in `inputs/MPM/thickCylinderMPM.ups`. An additional example which is used to achieve triaxial loading can be found at `inputs/MPM/TXC.ups`. There, the material geometry is a block, and so the regions described are flat surfaces upon which the pressure is applied.

On the Fly DataAnalysis

In the event that one wishes to monitor the data for a small region of a simulation at a rate that is more frequent than the what the DataArchiver can reasonably provide (for reasons of data storage and effect on run time), Uintah provides a `<DataAnalysis>` feature. As it applies to MPM, it allows one to specify a group of particles, by assigning those particles a particular value of the `<color>` parameter. In addition, a list of variables and a frequency of output is provided. Then, at run time, a subdirectory (`particleExtract/L-0`) is created inside the uda which contains a series of files, named according to their particle IDs, one for each tagged particle. Each of these files contains the time and position for that particle, along with whatever other

data is specified. **To use this feature, one must include the** `<withColor> true </withColor>` **tag in the** `<MPM>` **section of the input file.** (See Section 7.5.)

The following input file snippet is taken from `inputs/MPM/disks.ups`

```
<DataAnalysis>
   <Module name="particleExtract">

    <material>disks</material>
    <samplingFrequency> 1e10 </samplingFrequency>
    <timeStart>          0   </timeStart>
    <timeStop>          100  </timeStop>
    <colorThreshold>
      0
    </colorThreshold>

    <Variables>
      <analyze label="p.velocity"/>
      <analyze label="p.stress"/>
    </Variables>

  </Module>
</DataAnalysis>
```

For all particles that are assigned a color greater than the `<colorThreshold>`, the variables `p.velocity` and `p.stress` are saved every every 1/`<samplingFrequency>` time units, starting at `<timeStart>` until `<timeStop>`.

It is also possible to save grid based data with this module, see Section 6 for more information.

Prescribed Motion

The prescribed motion capability in Uintah allows the user to prescribe arbitrary material deformations and superimposed rotations. This capability is particularly useful in verifying that the constitutive model is behaving as expected and is frame indifferent. To prescribe material motion the following tag must be included in the `<MPM>` section of the input file:

```
<MPM>
    <UsePrescribedDeformation>true</UsePrescribedDeformation>
</MPM>
```

The desired motion must then be specified in a file named `time_defgrad_rotation`. The format of this file is as follows:

```
t0 F11 F12 F13 F21 F22 F23 F31 F32 F33 theta0 a0 a1 a2
t1 F11 F12 F13 F21 F22 F23 F31 F32 F33 theta1 a0 a1 a2
. . .
```

```
tn F11 F12 F13 F21 F22 F23 F31 F32 F33 thetan a0 a1 a2
```

where the first column is time, columns two through ten are the nine components of the prescribed deformation gradient, the eleventh column is the desired rotation angle, and the remaining three columns are the three components of the axis of prescribed rotation. The components of the deformation gradient are linearly interpolated for times between those specified in the table. The axis of rotation may be changed for each specified time. As a result, the angle of rotation about the specified axis linearly increases from zero to the specified value at the end of the specified interval. For example, the following table:

```
0 1 0 0 0 1 0 0 0 1 0 0 0 0
1 1 0 0 0 1 0 0 0 1 90 0 0 1
2 1 0 0 0 1 0 0 0 1 91 0 0 1
```

specifies a pure rotation (no stretch) about the 3-axis. At time=0 the material will have rotated 90 degrees about the 3-axis. At time=2 the material will have rotated an additional 91 degrees about the 3-axis for a total of 181 degrees of rotation. As a warning to the user, it is possible to specify the deformation gradient such that interpolating between to entries in the table results in a singular deformation gradient. For example:

```
0 1 0 0 0 1 0 0 0 1 0 0 0 0
1 1 0 0 0 1 0 0 0 1 0 0 0 1
2 -1 0 0 0 -1 0 0 0 1 0 0 0 1
```

would result in the simulation failing due to a negative jacobian error between time=1 and time=2 since the 11 and 22 components are linearly varying from 1 to -1 during that time, which will attempt to invert the computational cell. The deformation gradient at time=2 corresponds to a 180 degree rotation about the 3-axis, and can be accomplished using the rotation feature described above.

As a final example the table:

```
0 1 0 0 0 1 0 0 0 1 0 0 0 0
1 0.5 0 0 0 0.5 0 0 0 0.5 45 0 1 0
2 0.5 0 0 0.5 0.5 0 0 0 0.5 90 0 0 1
```

would result in 50% hydrostatic compression at time=1 with a 45 degree superimposed rotation about the 2-axis, followed by simple shear and a 90 degree rotation about the 3-axis between time=1 and time=2.

7.6 Examples

The following examples are meant to be illustrative of a variety of capabilities of Uintah-MPM, but are by no means exhaustive. Input files for the examples given here can be found in:

`inputs/UintahRelease/MPM`

Additional (mostly undocumented) input files that exercise a greater range of code capabilities can be found in:

`inputs/MPM`

Colliding Disks

Problem Description

This is an implementation of an example calculation from [50] in which two elastic disks collide and rebound. See Section 7.3 of that manuscript for a description of the problem.

Simulation Specifics

Component used: MPM

Input file name: disks_sulsky.ups

Command used to run input file: sus disks_sulsky.ups

Simulation Domain: 1.0 x 1.0 x 0.05 m

Cell Spacing:
.05 x .05 x .05 m (Level 0)

Example Runtimes:
4 seconds (1 processor, 3.16 GHz Xeon)

Physical time simulated: 3.0 seconds

Associate VisIt session: disks.session

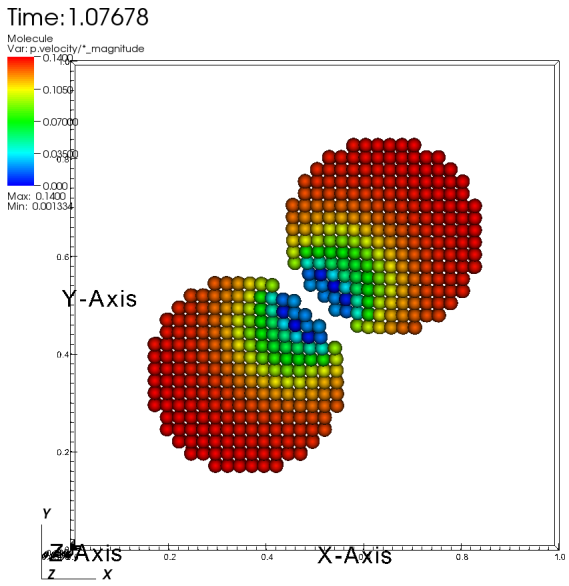

Figure 7.5: Colliding elastic disks. Particles colored according to velocity magnitude.

Results

Figure 7.5 shows a snapshot of the simulation, as the disks are beginning to collide.

Additional data is available within the uda in the form of "dat" files. In this case, both the kinetic and strain energies are avaiable and can be plotted to create a graph similar to that in Fig. 5a of [50]. e.g. using gnuplot:

```
cd disks.uda.000
gnuplot
gnuplot> plot "StrainEnergy.dat", "KineticEnergy.dat"
gnuplot> quit
```

Taylor Impact Test

Problem Description

This is a simulation of an Taylor impact experiment calculation from [24] in a copper cylinder at 718 K that is fired at a rigid anvil at 188 m/s. The copper cylinder has a length of 30 mm and a diameter of 6 mm. The cylinder rebounds from the anvil after 100 μs.

Simulation Specifics

Component used: MPM

Input file name: taylorImpact.ups

Command used to run input file: sus taylorImpact.ups

Simulation Domain: 8 mm x 33 mm x 8 mm

Cell Spacing:
1/3 mm x 1/3 mm x 1/3 mm (Level 0)

Example Runtimes:
1 hour (1 processor, Xeon 3.16 GHz)

Physical time simulated: 100 μseconds

Associate VisIt session: taylorImpact.session

Results

Figure 7.6 shows a snapshot from the end of the simulation. There, the cylinder is allowed to slide laterally across the plate due to the following optional specification in the `<contact>` section:

```
<direction>[1,1,1]</direction>
```

Figure 7.7 shows a snapshot from the end of a similar simulation. In this case, the cylinder is restricted from sliding laterally across the plate by altering the `<contact>` section as follows:

```
<direction>[0,1,0]</direction>
```

Sphere Rolling Down an Inclined Plane

Problem Description

Here, a sphere of soft plastic, initially at rest, rolls under the influence of gravity down a plane of a harder plastic. Gravity is oriented such that the plane is effectively angled at 45 degrees to the horizontal. This simulation demonstrates the effectiveness of the contact algorithm, described in [5]. Frictional contact, using a friction coefficient of $\mu = 0.495$ causes the ball to start rolling as it impacts the plane, after being dropped from barely above it. The same simulation is also run using a friction coefficient of $\mu = 0.0$. The difference in the results is shown below.

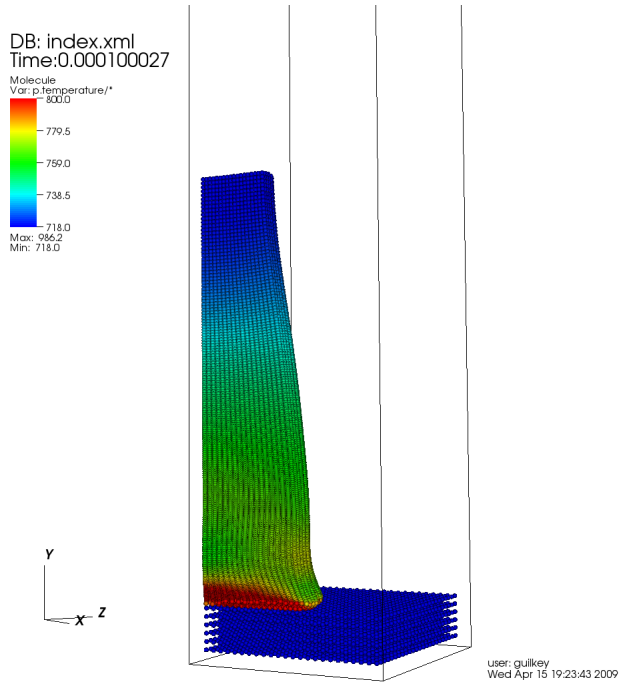

Figure 7.6: Taylor impact simulation with sliding between cylinder and target. Particles colored according to temperature.

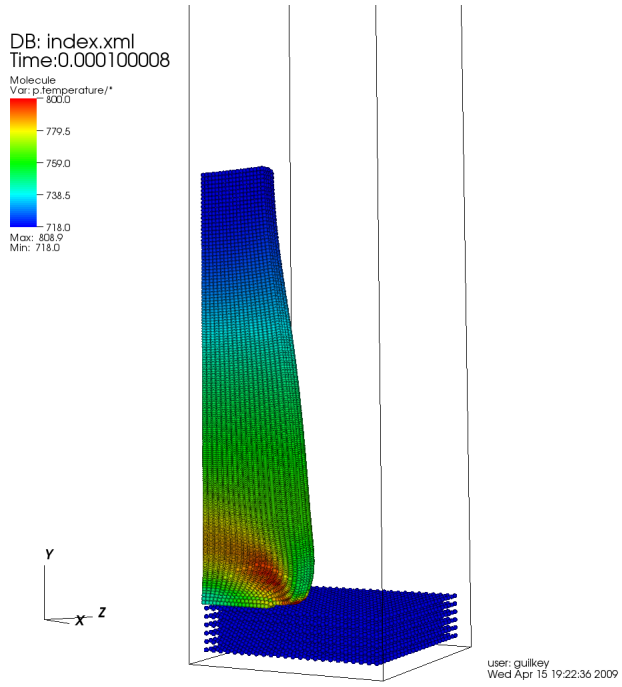

Figure 7.7: Taylor impact simulation with sliding prohibited between cylinder and target. Particles colored according to temperature.

Simulation Specifics

Component used: MPM

Input file name: inclinedPlaneSphere.ups

Command used to run input file: sus inclinedPlaneSphere.ups

Simulation Domain: 12.0 x 2.0 x 4.8 m

Cell Spacing:
.2 x .2 x .2 m (Level 0)

Example Runtimes:
2.7 hours (1 core, 3.16 GHz Xeon)

Physical time simulated: 2.2 seconds

Associate VisIt session: incplane.session

Results

Figure 7.8 and Figure 7.9 show snapshots of the simulation, as the sphere is about halfway down the plane.

Crushing a Foam Microstructure

Problem Description

This calculation demonstrates two important strength of MPM. The first is the ability to quickly generate a computational representation of complex geometries. The second is the ability of the method to handle large deformations, including self contact.

In particular, in this calculation a small sample of foam, the geometry for which was collected using microCT, is represented via material points. The sample is crushed to 87.5% compaction through the use of a rigid plate, which acts as a constant velocity boundary condition on the top of the sample. This calculation is a small example of those described in [12]. The geometry of the foam is created by image procesing the CT data, and based on the intensity of each voxel in the image data, the space represented by that voxel either recieves a particle with the material properties of the foam's constituent material, or is left as void space. This particle representation avoids the time consuming steps required to build a suitable unstructured mesh for this very complicated geometry.

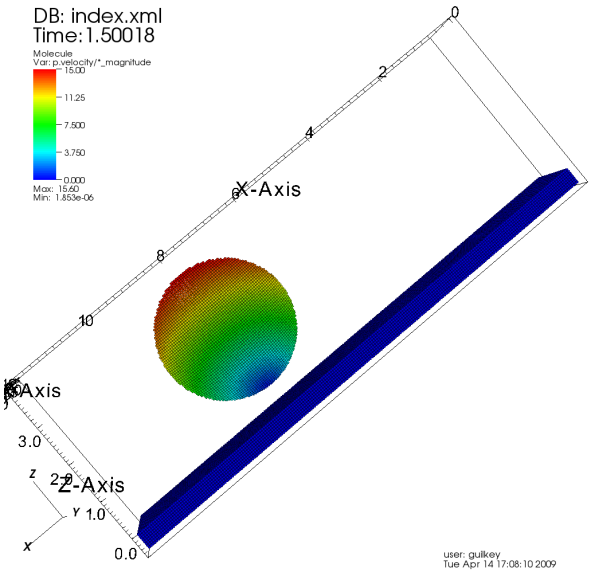

Figure 7.8: Sphere rolling down an "inclined" plane. The gravity vector is oriented at a 45 degree angle relative to the plane. Particles are colored by velocity magnitude. A friction coefficient of $\mu = 0.495$ is used. Particles are colored according to velocity magnitude, note that the particles at the top of the sphere are moving most rapidly, and those near the surface of the plane are basically stationary, as expected.

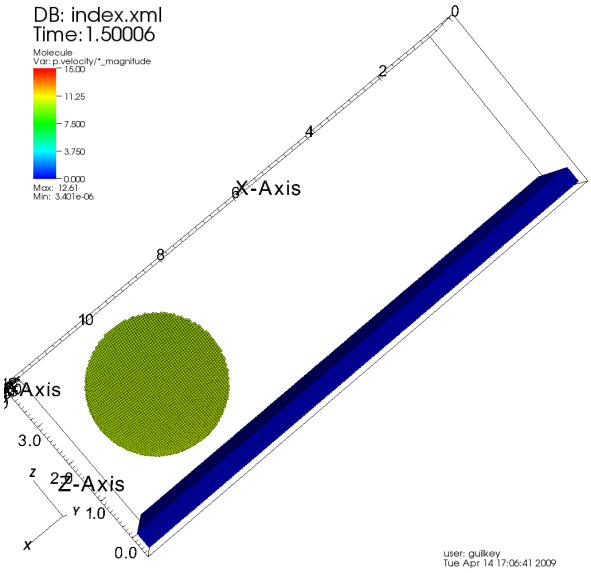

Figure 7.9: Sphere rolling down an "inclined" plane. The gravity vector is oriented at a 45 degree angle relative to the plane. Particles are colored by velocity magnitude. A friction coefficient of $\mu = 0.0$ is used. Particles are colored according to velocity magnitude. In this case, the particles throughout the sphere are moving at roughly the same velocity, because the sphere is sliding as it moves down the plane, as opposed to sticking and rolling.

Simulation Specifics

Component used: MPM

Input file name: foam.ups

Instruction to run input file: First, copy foam.ups and foam.pts.gz to the same directory as sus. Adjust the number of patches in the ups file based on the number of processors available to you for this run. First, uncompress the pts file:

```
gunzip foam.pts.gz
```

Then the command:

```
tools/pfs/pfs foam.ups
```

will divide the foam.pts file, which contains the geometric description of the foam, into number of patches smaller files, named foam.pts.0, foam.pts.1, etc. This is done so that for large simulations, each processor is only reading that data which it needs, and prevents the thrashing of the file system that would occur if each processor needed to read the entire pts file. This command only needs to be done once, or anytime the patch distibution is changed. Note that this step must be done even if only one processor is available.

To run this simulation:

```
mpirun -np NP sus foam.ups
```

where NP is the number of processors being used.

Simulation Domain: 0.2 X 0.2 X 0.2125 mm

Number of Computational Cells:
102 X 102 X 85 (Level 0)

Example Runtimes:
2.4 hours (4 cores, 3.16 GHz Xeon)

Physical time simulated: 3.75 seconds

Associated VisIt session 1: foam.iso.session

Associated VisIt session 2: foam.part.session

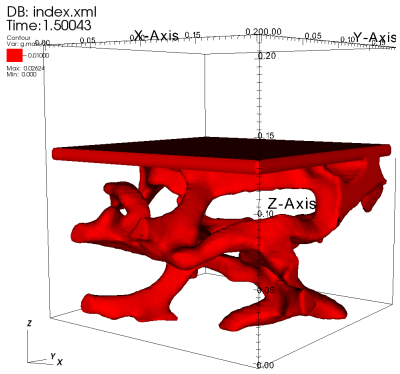

Figure 7.10: Compaction of a foam microstructure shown via isosurfacing.

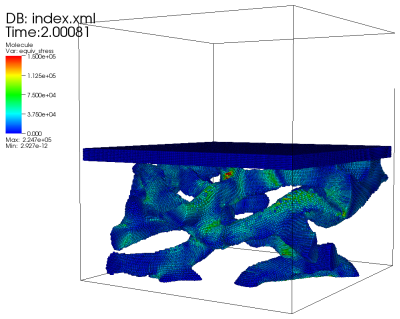

Figure 7.11: Compaction of a foam microstructure rendered as particles colored by equivalent stress.

Results

Figure 7.10 shows a snapshot of the simulation via isosurfacing, as the foam is at about 50% compaction.

Figure 7.11 shows a snapshot of the simulation via particles colored by equivalent stress as the foam is at about 60% compaction.

In this simulation, the reaction forces at 5 of the 6 computational boundaries are also recorded and can be viewed using a simple plotting package such as gnuplot. At each timestep, the internal force at each of the boundaries is accumulated and stored in "dat" files within the uda, e.g. BndyForce_zminus.dat. Because the reaction force is a vector, it is enclosed in square brackets which may be removed by use of a script in the inputs directory:

```
cd foam.uda.000
../inputs/ICE/Scripts/removeBraces BndyForce\_zminus.dat
gnuplot
gnuplot> plot "BndyForce\_zminus.dat" using 1:4
gnuplot> quit
```

These reaction forces are similar to what would be measured on a mechanical testing device, and help to understand the material behavior.

Hole in an Elastic Plate

Problem Description

A flat plate with a hole in the center is loaded in tension. To achieve a quasi-static solution, the load is applied slowly and a viscous damping force is used to reduce transients in the solution. As such, this simulation demonstrates those two capabilities. Specifically, take note of:

```
<use_load_curves> true </use_load_curves>
<artificial_damping_coeff>1.0</artificial_damping_coeff>
```

in the `<MPM>` section of the input file, and:

```
<PhysicalBC>
  <MPM>
    <pressure>
     .
     .
     .
```

section below that.

Simulation Specifics

Component used: MPM

Input file name: holePlate.ups

Command used to run input file: sus holePlate.ups

Simulation Domain: 5.0 m x 5.0 m x 0.1 m

Cell Spacing:
0.1 m x 0.1 m x 0.1 m (Level 0)

Example Runtimes:
2 minutes (1 processor, Xeon 3.16 GHz)

Physical time simulated: 10 seconds

Associate VisIt session: holeInPlate.session

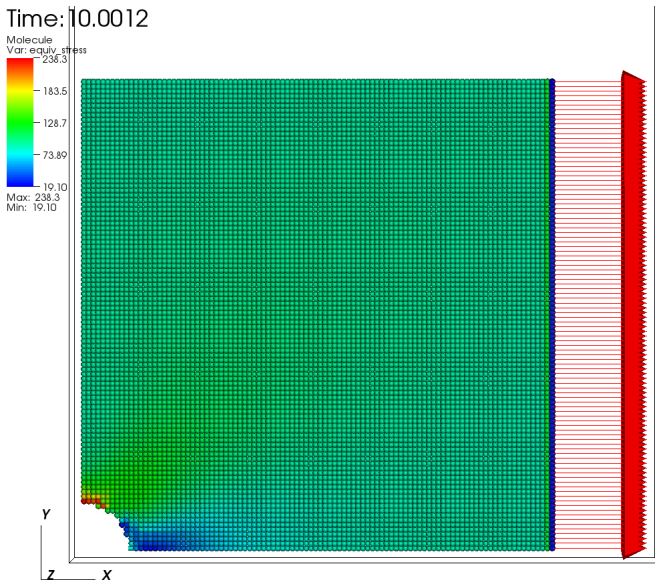

Figure 7.12: Elastic plate with a hole loaded in tension. Particles are colored by equivalent stress, vectors indicate applied load.

Results

Figure 7.12 shows a snapshot of the equivalent stress throughout the plate, as well as the load applied to the vectors near the edge of the plate. Expected maximum stress is $300Pa$. The $238Pa$ maximum observed here is significantly lower, but upon doubling the resolution in the x and y directions, the maximum stress is $308Pa$.

Tungsten Sphere Impacting a Steel Target

Problem Description

A $1mm$ tungsten sphere with an initial velocity of $5000m/s$ impacts a steel target. Axisymmetric conditions are used in this case, conversion of the input file to the full 3D simulation is straightforward. The user may wish to do both simulations of both to gain confidence in the applicability of axisymmetry.

This simulation exercises the `elastic_plastic` constitutive model for the steel material. This includes sub-models for equations of state, variable shear modulus, melting, plasticity, etc. The tungsten is modeled using the `comp_neo_hook_plastic,` which is simple vonMises plasticity with linear hardening. One difficulty with using the more sophisticated models is that parameters can be difficult to find for many materials.

Simulation Specifics

Component used: MPM

Input file name: WSphereIntoSteel.axi.ups

Command used to run input file: sus WSphereIntoSteel.axi.ups

Simulation Domain: 1.0 cm x 1.5 cm x axisymmetric

Cell Spacing:
0.333 mm x 0.333 mm x axisymmetry (Level 0)

Example Runtimes:
15 seconds (1 processor, Xeon 3.16 GHz)

Physical time simulated: 4 μseconds

Associate VisIt session: WSphereSteel.session

Results

Figure 7.13 shows the initial configuration for this simulation, with particles colored by the magnitude of their velocity. Figure 7.14 shows the state of the simulation after 4μseconds this simulation, with particles still colored by velocity magnitude.

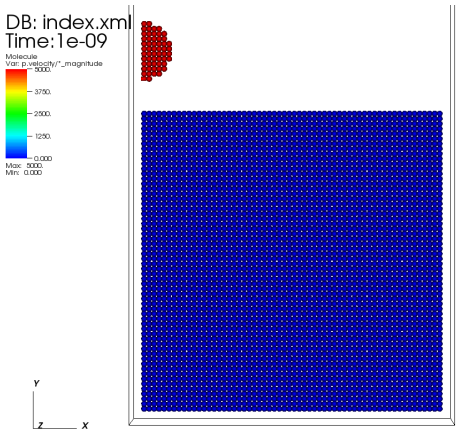

Figure 7.13: Initial configuration of hypervelocity impact of tungsten sphere into a steel target. Particles are colored by velocity magnitude.

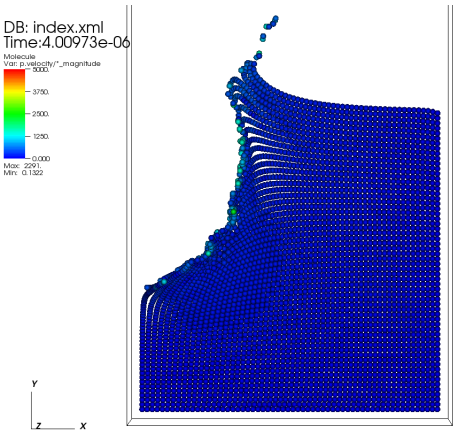

Figure 7.14: State of the tunsgsten and steel after 4μseconds. Particles are colored by velocity magnitude.

Bibliography

[1] F. H. Abed and G. Z. Voyiadjis. A consistent modified Zerilli-Armstrong flow stress model for bcc and fcc metals for elevated temperatures. *Acta Mechanica*, 175:1–18, 2005.

[2] B. Banerjee. Material point method simulations of fragmenting cylinders. In *Proc. 17th ASCE Engineering Mechanics Conference (EM2004)*, Newark, Delaware, 2004.

[3] B. Banerjee. MPM validation: Sphere-cylinder impact: Low resolution simulations. Technical Report C-SAFE-CD-IR-04-002, Center for the Simulation of Accidental Fires and Explosions, University of Utah, USA, 2004.

[4] B. Banerjee. Simulation of impact and fragmentation with the material point method. In *Proc. 11th International Conference on Fracture*, Turin, Italy, 2005.

[5] S. G. Bardenhagen, J. E. Guilkey, K. M Roessig, J. U. BrackBill, W. M. Witzel, and J. C. Foster. An improved contact algorithm for the material point method and application to stress propagation in granular material. *Computer Methods in the Engineering Sciences*, 2(4):509–522, 2001.

[6] S.G. Bardenhagen, J.U. Brackbill, and D. Sulsky. The material-point method for granular materials. *Comput. Methods Appl. Mech. Engrg.*, 187:529–541, 2000.

[7] S.G. Bardenhagen, J.E. Guilkey, K.M. Roessig, J.U. Brackbill, W.M. Witzel, and J.C. Foster. An improved contact algorithm for the material point method and application to stress propagation in granular material. *Computer Modeling in Engineering and Sciences*, 2:509–522, 2001.

[8] S.G. Bardenhagen and E.M. Kober. The generalized interpolation material point method. *Computer Modeling in Engineering and Sciences*, 5:477–495, 2004.

[9] Z. P. Bazant and T. Belytschko. Wave propagation in a strain-softening bar: Exact solution. *ASCE J. Engg. Mech*, 111(3):381–389, 1985.

[10] R. Becker. Ring fragmentation predictions using the gurson model with material stability conditions as failure criteria. *Int. J. Solids Struct.*, 39:3555–3580, 2002.

[11] J.U. Brackbill and H.M. Ruppel. Flip: A low-dissipation, particle-in-cell method for fluid flows in two dimensions. *J. Comp. Phys.*, 65:314–343, 1986.

[12] A.D. Brydon, S.G. Bardenhagen, E.A. Miller, and G.T. Seidler. Simulation of the densification of real open-celled foam microstructures. *Journal of the Mechanics and Physics of Solids*, 53:2638–2660, 2005.

[13] L. Burakovsky, D. L. Preston, and R. R. Silbar. Analysis of dislocation mechanism for melting of elements: pressure dependence. *J. Appl. Phys.*, 88(11):6294–6301, 2000.

[14] S. R. Chen and G. T. Gray. Constitutive behavior of tantalum and tantalum-tungsten alloys. *Metall. Mater. Trans. A*, 27A:2994–3006, 1996.

[15] C. C. Chu and A. Needleman. Void nucleation effects in biaxially stretched sheets. *ASME J. Engg. Mater. Tech.*, 102:249–256, 1980.

[16] J. O. Coplien. *Advanced C++ Programming Styles and Idioms*. Addison-Wesley, Reading, MA, 1992.

[17] L. Cueto-Felgueroso, G. Mosqueira, F. Navarrina, and M. Casteleiro. On the galerkin formulation of the smoothed particle hydrodynamics method. *Int. J. Numer. Meth. Engng*, 60:1475–1512, 2004.

[18] D. C. Drucker. A definition of stable inelastic material. *J. Appl. Mech.*, 26:101–106, 1959.

[19] P. S. Follansbee and U. F. Kocks. A constitutive description of the deformation of copper based on the use of the mechanical threshold stress as an internal state variable. *Acta Metall.*, 36:82–93, 1988.

[20] D. M. Goto, J. F. Bingert, W. R. Reed, and R. K. Garrett. Anisotropy-corrected MTS constitutive strength modeling in HY-100 steel. *Scripta Mater.*, 42:1125–1131, 2000.

[21] J. E. Guilkey and J. A. Weiss. Implicit time integration for the material point method: Quantitative and algorithmic comparisons with the finite element method. *Int. J. Numer. Meth. Engng.*, 57(9):1323–1338, 2003.

[22] Y Guo and JA Nairn. Three-dimensional dynamic fracture analysis using the material point method. *Computer Modeling in Engineering and Sciences*, 6:295–308, 2004.

[23] A. L. Gurson. Continuum theory of ductile rupture by void nucleation and growth: Part 1. Yield criteria and flow rules for porous ductile media. *ASME J. Engg. Mater. Tech.*, 99:2–15, 1977.

[24] W. H. Gust. High impact deformation of metal cylinders at elevated temperatures. *J. Appl. Phys.*, 53(5):3566–3575, 1982.

[25] S. Hao, W. K. Liu, and D. Qian. Localization-induced band and cohesive model. *J. Appl. Mech.*, 67:803–812, 2000.

[26] F.H. Harlow. The particle-in-cell computing method for fluid dynamics. *Methods Comput. Phys.*, 3:319–343, 1963.

[27] R. Hill and J. W. Hutchinson. Bifurcation phenomena in the plane tension test. *J. Mech. Phys. Solids*, 23:239–264, 1975.

[28] K. G. Hoge and A. K. Mukherjee. The temperature and strain rate dependence of the flow stress of tantalum. *J. Mater. Sci.*, 12:1666–1672, 1977.

[29] G. R. Johnson and W. H. Cook. A constitutive model and data for metals subjected to large strains, high strain rates and high temperatures. In *Proc. 7th International Symposium on Ballistics*, pages 541–547, 1983.

[30] G. R. Johnson and W. H. Cook. Fracture characteristics of three metals subjected to various strains, strain rates, temperatures and pressures. *Int. J. Eng. Fract. Mech.*, 21:31–48, 1985.

[31] J. N. Johnson and F. L. Addessio. Tensile plasticity and ductile fracture. *J. Appl. Phys.*, 64(12):6699–6712, 1988.

[32] B.A. Kashiwa. A multifield model and method for fluid-structure interaction dynamics. Technical Report LA-UR-01-1136, Los Alamos National Laboratory, Los Alamos, 2001.

[33] U. F. Kocks. Realistic constitutive relations for metal plasticity. *Materials Science and Engrg.*, A317:181–187, 2001.

[34] F. L. Lederman, M. B. Salamon, and L. W. Shacklette. Experimental verification of scaling and test of the universality hypothesis from specific heat data. *Phys. Rev. B*, 9(7):2981–2988, 1974.

[35] J. Ma, H. Lu, and R. Komanduri. Structured mesh refinement in generalized interpolation material point method (gimp) for simulation of dynamic problems. *Computer Modeling in Engineering and Sciences*, 12:213–227, 2006.

[36] P. J. Maudlin and S. K. Schiferl. Computational anisotropic plasticity for high-rate forming applications. *Comput. Methods Appl. Mech. Engrg.*, 131:1–30, 1996.

[37] M.-H. Nadal and P. Le Poac. Continuous model for the shear modulus as a function of pressure and temperature up to the melting point: analysis and ultrasonic validation. *J. Appl. Phys.*, 93(5):2472–2480, 2003.

[38] S. Nemat-Nasser. Rate-independent finite-deformation elastoplasticity: a new explicit constitutive algorithm. *Mech. Mater.*, 11:235–249, 1991.

[39] S. Nemat-Nasser and D. T. Chung. An explicit constitutive algorithm for large-strain, large-strain-rate elastic-viscoplasticity. *Comput. Meth. Appl. Mech. Engrg*, 95(2):205–219, 1992.

[40] P. Perzyna. Constitutive modelling of dissipative solids for localization and fracture. In Perzyna P., editor, *Localization and Fracture Phenomena in Inelastic Solids: CISM Courses and Lectures No. 386*, pages 99–241. SpringerWien, New York, 1998.

[41] D. L. Preston, D. L. Tonks, and D. C. Wallace. Model of plastic deformation for extreme loading conditions. *J. Appl. Phys.*, 93(1):211–220, 2003.

[42] S. Ramaswamy and N. Aravas. Finite element implementation of gradient plasticity models Part I: Gradient-dependent yield functions. *Comput. Methods Appl. Mech. Engrg.*, 163:11–32, 1998.

[43] S. Ramaswamy and N. Aravas. Finite element implementation of gradient plasticity models Part II: Gradient-dependent evolution equations. *Comput. Methods Appl. Mech. Engrg.*, 163:33–53, 1998.

[44] G. Ravichandran, A. J. Rosakis, J. Hodowany, and P. Rosakis. On the conversion of plastic work into heat during high-strain-rate deformation. In *Proc. , 12th APS Topical Conference on Shock Compression of Condensed Matter*, pages 557–562. American Physical Society, 2001.

[45] J. W. Rudnicki and J. R. Rice. Conditions for the localization of deformation in pressure-sensitive dilatant materials. *J. Mech. Phys. Solids*, 23:371–394, 1975.

[46] J. C. Simo and T. J. R. Hughes. *Computational Inelasticity*. Springer-Verlag, New York, 1998.

[47] JC Simo and TJR Hughes. *Computational Inelasticity*. Springer-Verlag, New York, 1998.

[48] D. J. Steinberg, S. G. Cochran, and M. W. Guinan. A constitutive model for metals applicable at high-strain rate. *J. Appl. Phys.*, 51(3):1498–1504, 1980.

[49] D. J. Steinberg and C. M. Lund. A constitutive model for strain rates from 10^{-4} to 10^{6} s^{-1}. *J. Appl. Phys.*, 65(4):1528–1533, 1989.

[50] D. Sulsky, Z. Chen, and H.L. Schreyer. A particle method for history dependent materials. *Comput. Methods Appl. Mech. Engrg.*, 118:179–196, 1994.

[51] D. Sulsky and H.L. Schreyer. Axisymmetric form of the material point method with applications to upsetting and taylor impact problems. *Computer Methods in Applied Mechanics and Engineering*, 139:409–429, 1996.

[52] D. Sulsky, S. Zhou, and H.L. Schreyer. Application of a particle-in-cell method to solid mechanics. *Computer Physics Communications*, 87:236–252, 1995.

[53] V. Tvergaard and A. Needleman. Analysis of the cup-cone fracture in a round tensile bar. *Acta Metall.*, 32(1):157–169, 1984.

[54] V. Tvergaard and A. Needleman. Ductile failure modes in dynamically loaded notched bars. In J. W. Ju, D. Krajcinovic, and H. L. Schreyer, editors, *Damage Mechanics in Engineering Materials: AMD 109/MD 24*, pages 117–128. American Society of Mechanical Engineers, New York, NY, 1990.

[55] Y. P. Varshni. Temperature dependence of the elastic constants. *Physical Rev. B*, 2(10):3952–3958, 1970.

[56] P. C. Wallstedt and J. E. Guilkey. An evaluation of explicit time integration schemes for use with the generalized interpolation material point method. *J. Comp. Phys.*, 227:9628–9642, 2008.

[57] L. H. Wang and S. N. Atluri. An analysis of an explicit algorithm and the radial return algorithm, and a proposed modification, in finite elasticity. *Computational Mechanics*, 13:380–389, 1994.

[58] M. L. Wilkins. *Computer Simulation of Dynamic Phenomena*. Springer-Verlag, Berlin, 1999.

[59] F. J. Zerilli. Dislocation mechanics-based constitutive equations. *Metall. Mater. Trans. A*, 35A:2547–2555, 2004.

[60] F. J. Zerilli and R. W. Armstrong. Dislocation-mechanics-based constitutive relations for material dynamics calculations. *J. Appl. Phys.*, 61(5):1816–1825, 1987.

[61] F. J. Zerilli and R. W. Armstrong. Constitutive relations for the plastic deformation of metals. In *High-Pressure Science and Technology - 1993*, pages 989–992, Colorado Springs, Colorado, 1993. American Institute of Physics.

[62] M. A. Zocher, P. J. Maudlin, S. R. Chen, and E. C. Flower-Maudlin. An evaluation of several hardening models using Taylor cylinder impact data. In *Proc. , European Congress on Computational Methods in Applied Sciences and Engineering*, Barcelona, Spain, 2000. ECCOMAS.

Chapter 8

MPMICE

8.1 Introduction

MPMICE is a marriage of the multi-material ICE method, described in Section 6 and MPM, described in Section 7. The equations of motion solved for both fluid and solid are essentially the same, although the physical behavior of these two states of matter differ, largely due to their constitutive relationships. MPM is used to track the evolution of solid materials in a Lagrangian frame of reference, while fluids are evolved in the Eulerian frame.

8.2 Theory - Algorithm Description

At this time, the reader is directed to the manuscript by Guilkey, Harman and Banerjee [2] for the theoretical and algorithmic description of the method.

8.3 HE Combustion Models

Three models exist for reaction of high explosive materials. Each simulation using one of these models utilize MPMICE's material interactions as its foundation. The components work by taking several material specific constants as well as a reactant and product material from the model input section of the .ups file. Following are brief descriptions of each model, as well as their input parameters.

8.3.1 Simple Burn

Simple Burn, as the name implies, is a simple model of combustion of HMX based on the rate equation:

$$\dot{m} = AP^{0.778} \tag{8.1}$$

Where $\dot{m}$ is the mass flux, P is the pressure and n is the pressure dependence coefficient. The pressure coefficient in Equation (8.1) is that of HMX. The models input section for a Simple Burn simulation takes the form:

```
<Models>
  <Model type="Simple_Burn">
    <fromMaterial> reactant      </fromMaterial>
    <toMaterial>   product       </toMaterial>
    <Active>       true          </Active>
    <ThresholdTemp>       450.0  </ThresholdTemp>
    <ThresholdPressure> 50000.0  </ThresholdPressure>
    <Enthalpy>        2000000.0  </Enthalpy>
    <BurnCoeff>            75.3  </BurnCoeff>
    <refPressure>      101325.0  </refPressure>
  </Model>
</Models>
```

The first two tags take names of materials previously defined in the input file, defining both reactant and product used by the model. See Section 6.3.4 and 7.5 for in depth description for defining materials. <Active> is a debugging parameter that takes a boolean value indicating whether the model is on (i.e. the actual computations take place during the timestep). True is the value to set for <Active> in most situations. Each of the other parameters take double values. Threshold temperature and pressure tags define two criteria the cell must have in order to be flagged burning. The reference pressure is used to scale the cell centered pressure as well as make it an unitless value. The burn coefficient corresponds to A in the rate equation. Enthalpy is simply the enthalpy value for conversion of reactant to product.

8.3.2 Steady Burn

Steady Burn is a more accurate model than Simple Burn. It is based on WSB model of combustion developed by Ward, Son and Brewster in [4]. WSB is based on a simplified two-step chemical model with an initial zero-order, thermally activated ($E_c > 0$), mildly exothermic, solid-to-gas reaction, modeled as a thermal decomposition of the solid:

$$A(solid) \rightarrow B(gas) \tag{8.2}$$

Intermediate B, in the presence of any gas phase collision partner M, reacts in a highly exothermic fashion producing a flame. This step is modelled as a second-order, gas phase, free radical chain reaction based on the assumption that $E_g = 0$:

$$B(gas) + M(gas) \rightarrow C(gas) + M(gas) \tag{8.3}$$

As such, this second equation represents the reaction in the gas phase that causes heat convection back to the surface that activate the first reaction. In Steady Burn, a solution is found by iteratively solving two equations: one for mass burning rate $\dot{m}$ and one for surface temperature T_s. Mass flux is initially solved with an assumed value T_s (in the model set to $850.0K$) using WSB:

$$\dot{m}\left(T_s\right) = \sqrt{\frac{\kappa_c \rho_c A_c R T_s^2 \exp\left(\frac{-E_c}{RT_s}\right)}{C_p E_c \left(T_s - T_0 - \frac{Q_c}{2C_p}\right)}} \tag{8.4}$$

The solution to this equation is used to refine the surface temperature and vice-versus until a self-consistent solution for surface temperature and mass flux has been found. The surface temperature equation takes the form:

$$T_s(\dot{m}, P) = T_0 + \frac{Q_c}{C_p} + \frac{Q_g}{Cp\left(1 + \frac{x_g\left(\dot{m}, P\right)}{x_{cd}(\dot{m})}\right)} \tag{8.5}$$

x_g in the third term of Equation (8.5) is the flame standoff distance, computed from:

$$x_g\left(\dot{m}, P\right) = \frac{2x_{cd}\left(\dot{m}\right)}{\sqrt{1 + D_a\left(\dot{m}, P\right)} - 1} \tag{8.6}$$

where x_{cd} and D_a are the convective-diffusive length and Damkohler number, respectively:

$$x_{cd}\left(\dot{m}\right) = \frac{\kappa_g}{\dot{m} C_p} \tag{8.7}$$

$$D_a(\dot{m}, P) = \frac{4B_g M C_p P^2}{R^2 \kappa_g} x_{cd} (\dot{m})^2 \tag{8.8}$$

WSB model is valid as a 1D model, but needs extension to work in a 3D multimaterial CFD environment. As such, Steady Burn is WSB extended with logic for ignition of energetic materials and computation of surface area for burning cells. Ignition of a cell is based on three criteria:

- The cell must contain one particle of energetic solid
- The cell is near a surface of an energetic solid (e.g. ratio of minimum node-centered mass to maximum node-centered mass is less than 0.7)
- One neighboring cell must have at most two particles of energetic material

If a cell is ignited, the model will be applied and mass will be transferred from reactant material to product material. Total mass burned is computed using mass flux $\dot{m}$, Δt of the timestep and the calculated surface area, found using:

$$A = \frac{\delta x \delta y \delta z}{\delta x |g_x| + \delta y |g_y| + \delta z |g_z|} \tag{8.9}$$

where δx, δy, and δz are the dimensions of the cell and components of $\overrightarrow{g}$ are the normalized density gradients of the particle mass in a cell. A more thorough examination of Steady Burn can be read about in [5].

The following table describes the input parameters for Steady Burn. The final column of the table indicates parameters for combustion of HMX.

Steady Burn Input Parameters			
Tag	**Type**	**Description**	**HMX Value**
<fromMaterial>	String	'Name' of reactant material (mass source)	
<toMaterial>	String	'Name' of product material (mass sink)	
<IdealGasConst>	double	Ideal gas constant (R)	$8.314 J/(K \times mol)$
<PreExpCondPh>	double	Condensed phase pre-exponential coefficient (A_c)	$1.637 \times 10^{15} s^{-1}$
<ActEnergyCondPh>	double	Condensed phase activation energy (E_c)	$1.76 \times 10^5 J/mol$
<PreExpGasPh>	double	Gas phase frequency factor (B_g)	$1.6 \times 10^{-3} m^3/(kg \times s \times K)$
<CondPhaseHeat>	double	Condensed phase heat release per unit mass (Q_c)	$4.0 \times 10^5 J/kg$
<GasPhaseHeat>	double	Gas phase heat release per unit mass (Q_g)	$3.018 \times 10^6 J/kg$
<HeatConductGasPh>	double	Thermal conductivity of gas (κ_g)	$0.07 W/(m \times K)$
<HeatConductCondPh>	double	Thermal conductivity of condensed phase (κ_c)	$0.02 W/(m \times K)$
<SpecificHeatBoth>	double	Specific heat at constant pressure (c_p)	$1.4 \times 10^3 J/(kg \times K)$
<MoleWeightGasPh>	double	Molecular weight of gas (W)	$3.42 \times 10^{-2} kg/mol$
<BoundaryParticles>	int	Max # of particles a cell can have and be burning	Resolution dependent
<ThresholdPressure>	double	Threshold pressure cell must have $\geq$ to burn mass	$50000 Pa$
<IgnitionTemp>	double	Temperature cell must have $\geq$ to be burning	$550 K$

8.3.3 Unsteady Burn

Unsteady Burn is a model developed at the University of Utah as an extension of Steady Burn to better represent mass burning rates when pressure at the burning surface fluctuates. A pressure-coupled response is accounted for in the model such that, qualitatively a pressure increase causes gas phase reaction rates to increase as well as move the gas phase reactions closer to the burning surface. Increase of near surface gas phase reactions increases the rate of thermally activated solid state reactions, ultimately causing a higher steady burn rate. Unsteady Burn more accurately models the transition from low pressure to high pressure than Steady Burn by taking into account the initially overshot burn rate at the time when the pressure increases, and the relaxation period to steady burn rate. Similarly, Unsteady Burn models undershot pressures during pressure drops.

The model is an extension of Steady Burn by partial decoupling of the gas phase and solid state Equations (8.4) and (8.5). An expression for the temperature gradient of the solid:

$$\beta = (T_s - T_0)\,\frac{mc_p}{\kappa_c} \tag{8.10}$$

is reaarranged for $(T_s - T_0)$ and substituted in Equation (8.4) leading to the quadradic equation:

$$\dot{m}^2 - \frac{2\beta\kappa_c}{Q_c}\dot{m} + \frac{2A_c R T_s^2 \kappa_c \rho_c}{E_c Q_C} \exp\left(\frac{-E_c}{RT_s}\right) = 0 \tag{8.11}$$

which allows independent tracking of temperature gradient β and surface temperature T_s. The gas phase response is computed using a runnning average of T_s as it approaches the steady burning value. A solid state response is obtained by computing a running average of β as it approaches the steady burning value. A slow relaxation time for β and a fast relaxation time for T_s models the overshoot or undershoot in burn rate. Burning criteria for a cell is the same as Steady Burn. For more information on Unsteady Burn see [5].

The following table describes the input parameters for Unsteady Burn.

Unsteady Burn Input Parameters		
Tag	**Type**	**Description**
<fromMaterial>	String	'Name' of reactant material (mass source)
<toMaterial>	String	'Name' of product material (mass sink)
<IdealGasConst>	double	Ideal gas constant (R)
<PreExpCondPh>	double	Condensed phase pre-exponential coefficient (A_c)
<ActEnergyCondPh>	double	Condensed phase activation energy (E_c)
<PreExpGasPh>	double	Gas phase frequency factor (B_g)
<CondPhaseHeat>	double	Condensed phase heat release per unit mass (Q_c)
<GasPhaseHeat>	double	Gas phase heat release per unit mass (Q_g)
<HeatConductGasPh>	double	Thermal conductivity of gas (κ_g)
<HeatConductCondPh>	double	Thermal conductivity of condensed phase (κ_c)
<SpecificHeatBoth>	double	Specific heat at constant pressure (c_p)
<MoleWeightGasPh>	double	Molecular weight of gas (W)
<BoundaryParticles>	int	Max # of particles a cell can have and be burning
<BurnrateModCoef>	double	if $\neq$1.0, scale unsteady rate with steady rate as $\dot{m}_u = \dot{m}_s \left(\frac{\dot{m}_u}{\dot{m}_s}\right)^{B_m}$
<CondUnsteadyCoef>	double	Coefficient for condensed phase pressure response relaxation
<GasUnsteadyCoef>	double	Coefficient for gas phase pressure response relaxation
<ThresholdPressure>	double	Threshold pressure cell must be $\geq$ to burn mass
<IgnitionTemp>	double	Temperature cell must be at $\geq$ to be burning

8.4 Examples

Mach 2 Wedge

Problem Description

This is a simulation of a symmetric 20^o wedge traveling through initially quiescent air at Mach 2.0. A shock forms at the leading edge of the wedge and an expansion fan over its top. Consultation of oblique shock tables, e.g. [3] (pp.308-309) reveals that the angle of the leading shock compares quite well with the expected value. In addition, this simulation demonstrates a few other useful features of the fluid-structure interaction capability. In this case, the structure is rigid, and as such, essentially provides a boundary condition to the compressible flow calculation. Furthermore, the geometry of the wedge is described via a triangulated surface, rather than the geometric primitives usually used. This allows the user to study flow around arbitrarily complex objects, without the difficulty of generating a body fitted mesh around that object.

Simulation Specifics

Component used: rmpmice (Rigid MPM-ICE)

Input file name: Mach2Wedge.ups

Command used to run input file: sus Mach2Wedge.ups (Note: The files wedge40.pts and wedge40.tri must also be copied to the same directory as sus.)

Simulation Domain: 0.25 x 0.0375 x 0.001 m

Cell Spacing:
.0005 x .0005 x .001 m (Level 0)

Example Runtimes:
20 minutes (1 processor, 3.16 GHz Xeon)

Physical time simulated: 0.3 milliseconds

Associated visit session: M2wedge.session

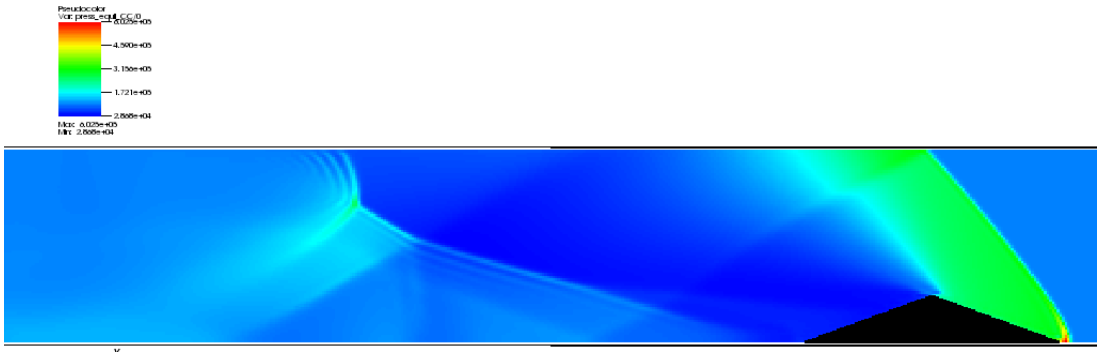

Figure 8.1: 20^o wedge moving at Mach 2.0 through initially stationary air. Contour plot depicts pressure.

Results

Figure 8.1 shows a snapshot of the simulation. Contour plot depicts pressure and reflects the presence of a leading shock and an expansion fan.

Cylinder in a Crossflow

Problem Description

In this example the domain is initially filled with air moving at a uniform velocity of $0.03m/s$ A ridgid cylinder $O.D. = 0.02m$ is placed $0.1m$ from the inlet and a passive scalar is injected into the domain through a $0.002m$ hole on in the inlet boundary of the domain. A velocity perturbation is placed upstream of the cylinder to produce an instablity that will help trigger the onset of the Kármán vortex street.

Simulation Specifics

Component used: rmpmice (Rigid MPM-ICE)

Input file name: `cylinderCrossFlow.ups`

Command used to run input file:

```
mpirun -np 6 sus inputs/UintahRelease/MPMICE/cylinderCrossFlow.ups
```

Simulation Domain: 0.3 x 0.15 x 0.001 m

Cell Spacing:
.00015 x .001 x .001 m (Level 0)

Example Runtimes:
7ish hrs (6 processor, 3.16 GHz Xeon)

Physical time simulated: 60 seconds

Associated visit session: cyl_crossFlow.session

Results

Figure 8.2 shows a snapshot of the simulation at time $t = 60sec$. The contour plot of the passive scalar shows the Kármán vortex street behind the cylinder at $Re = 700$. A movie of the results is located at

```
movies/cyl_crossFlow.mpg
```

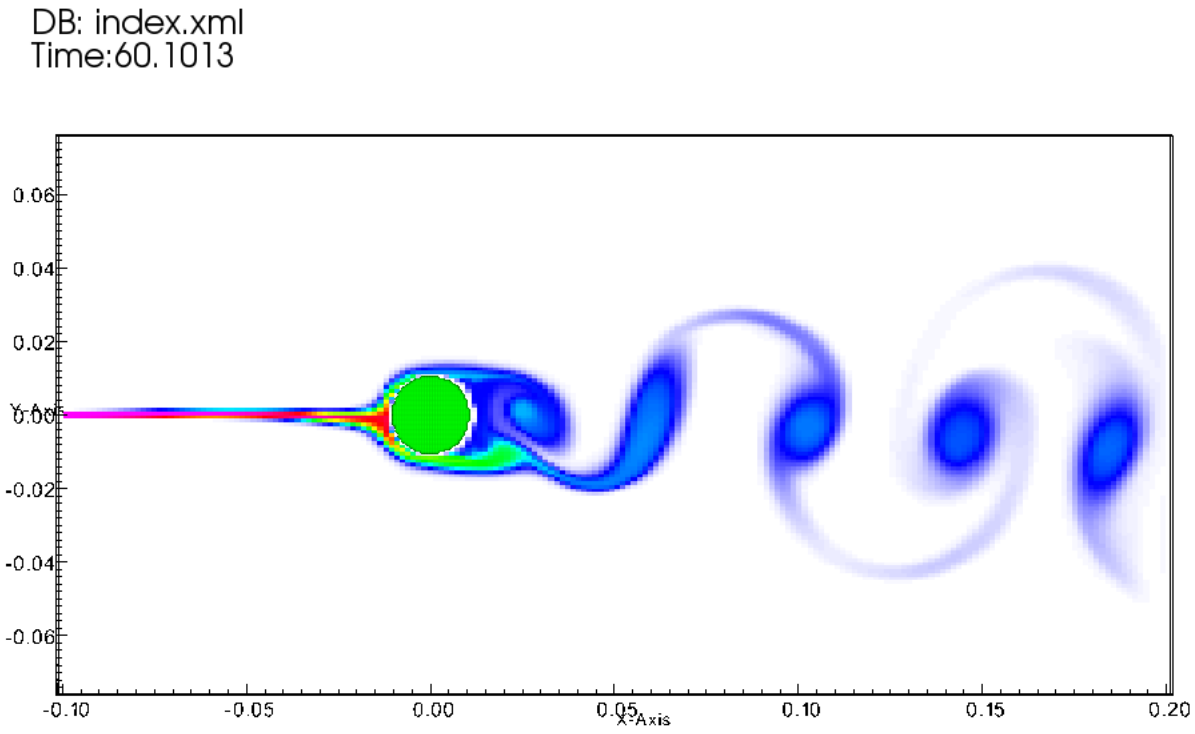

Figure 8.2: Flow over a stationary cylinder, $Re = 700$, a passive scalar is used as a flow marker

Copper Clad Rate Stick (aka "Cylinder Test")

Problem Description

This is a two-dimensional version of the "cylinder test" which is used to characterize equations of state for explosive products. In those tests, a copper tube is filled with a high explosive and a detonation is initiated at one end. Various means are used to measure the velocity of the tube as the high pressure product gases expand inside of it.

Here, a cylinder ($r = 2.54cm$) of QM100 is jacketed with a copper cylinder that has a wall thickness of $0.52cm$. Detonation is initiated by giving a thin layer of the explosive a high initial velocity in the axial direction which generates a pressure that is sufficiently high to reach trigger the detonation model. As the detonation proceeds, the copper is pushed out of the domain by the expanding product gases.

Note that in this example, to make run times brief, the domain is very short in the axial direction, and is probably not sufficient for the detonation to reach steady state. Additionally, the domain has been reduced to two dimensions, as symmetry is assumed in the Z-plane. Finally, the spatial resolution of $1.0mm$ is a bit coarse to achieve convergent results. The full three dimensional result can quickly be obtained by commenting out the symmetry condition on the z+ plane and uncommenting the Neumann conditions, as well as changing the spatial extents and resolution in the Z direction to match those in the Y direction.

Simulation Specifics

Component used: mpmice (MPM-ICE)

Input file name: `QM100CuRS.ups`

Command used to run input file:

```
sus inputs/UintahRelease/MPMICE/QM100CuRS.ups
```

Simulation Domain: 0.055 x 0.032 x 0.0005 m

Cell Spacing:

1.0 mm x 1.0 mm x 1.0 mm (Level 0)

Example Runtimes:

20 minutes (1 processor, 3.16 GHz Xeon)

Physical time simulated: 30 μseconds

Associated visit session: QM100.session

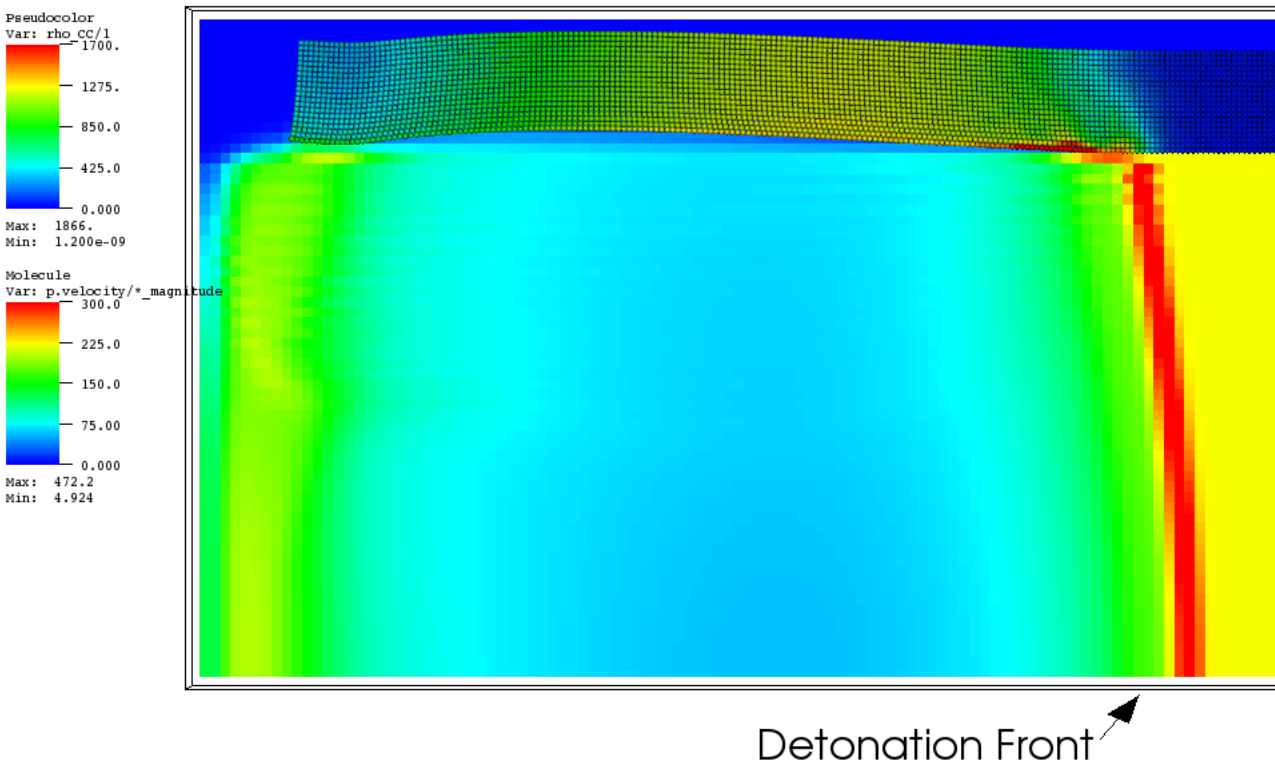

Figure 8.3: Detonation in a copper cylinder (2-D). Particles are colored by velocity magnitude, contours indicate density of unreacted explosive.

Results

Figure 8.3 shows a snapshot of the simulation at time $t = 60sec$. Particles are colored by velocity magnitude, contours reflect the density of explosive, note the highly compressed region near the shock front.

Cylinder Pressurization Using Simple Burn

Problem Description

This example demonstrates use of the Simple Burn algorithm in an explosive scenario. The exact situation consists of a cylinder of PBX encased in steel. For simplicity it is set up as a 2D simulation. It demonstrates Symmetric boundaries as a useful construct for simplifying the computational requirements of a problem. The end result is the pressurization of a quarter of a cylinder by combustion of PBX 9501. Damage and failure models simulate cylinder failure in a detonation scenario. The simulation as it stands falls far short of the required physical time simulated for actual detonation, but demonstrates how Simple Burn can be used to pressurize a cylinder. For description of Simple Burn see 8.3.1.

Simulation Specifics

Component used: mpmice (MPM-ICE)

Input file name: guni2dRT.ups

Preprocessing on input file:

1) Comment out or remove <max_Timesteps> on line 21
2) Comment out <outputTimestepInterval> on line 96
3) add <outputInterval>5e-5<outputInterval> on line 97

Command used to run input file: mpirun -np 4 sus guni2dRT.ups

Simulation Domain: 8.636 x 8.636 x 0.16933 cm

Example Runtimes:

2 minutes (1 processor, 2.8 GHz Xeon)

Physical time simulated: 8 microseconds

Associated visit session: SimpleBurn.session

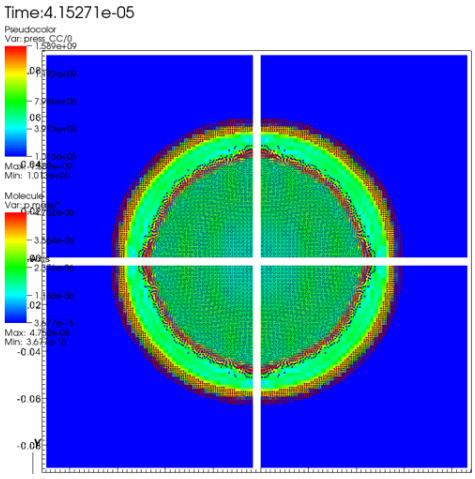

(a) Receding PBX9501 leads to pressure increase in cylindrical steel shell

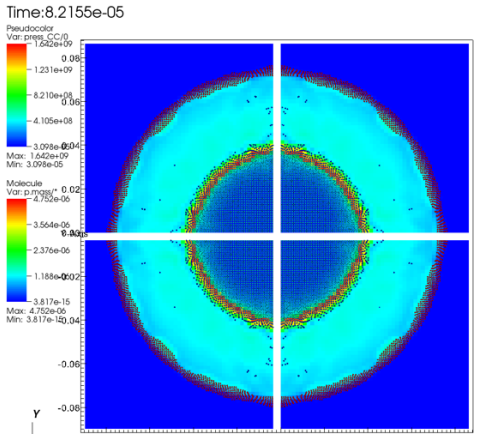

(b) Pressure increase causes cylinder to respond

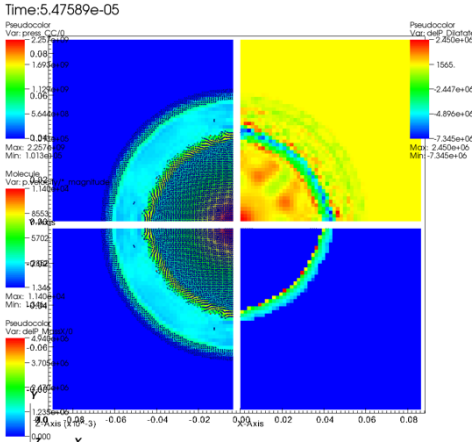

(c) The left half of the image represents particles as spheres colored according to mass and pressure as background color. Top-right shows delP_Dilatate and bottom-right shows delP_MassX

Figure 8.4:

Results

With the recession of mass comes a pressure increase that causes the case to expand outward. A snapshot of pressure after the 0.4 milliseconds can be seen in Figure 8.4a. At this time pressure has increased to three-fold its initial value. A later snapshot Figure 8.4b shows the response of the steel cylinder to increased pressure. Note that mass flux will scale according to 8.1. Another interesting view of the simulation can be seen in Figure 8.4c. On the left is the normal particle and pseudocolor map representing solid mass and pressure respectively. On the top right, change in pressure during the timestep can be seen (delP_Dilatate). The bottom shows change in pressure due to mass exchange (del_MassX). See table 6.3.8 for description of these variables.

Exploding Cylinder Using Steady Burn

Problem Description

This problem consistes of a cylinder initially at 600 K causing burning. Steady Burn acts as the model for burning of HE material. More information on Steady Burn can be found in 8.3.2. The cylinder is build from an outer shell of steel covering a hollow bored cylinder of PBX9501. The simulation demonstrates the violence of explosions when large voids allow rapid expansion of surface area due to collapse of explosive material into the bore. Information on the violence of explosions with solid and hollow cores can be attained in [5].

Simulation Specifics

Component used: mpmice (MPM-ICE)

Input file name: SteadyBurn_2dRT.ups

Preprocessing on input file:

1) Comment out or remove <max_Timesteps>

2) Comment out <outputTimestepInterval> and uncomment <outputInterval> around line 101

Command used to run input file: mpirun -np 4 sus SteadyBurn_2dRT.ups

Simulation Domain: 9 x 9 x 0.1 cm

Example Runtimes:

5 hours (1 processor, 2.8 GHz Xeon)

Physical time simulated: 3 milliseconds

Associated visit session: SteadyBurn.session

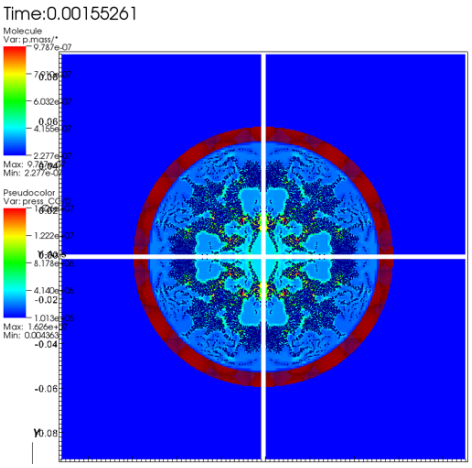

(a) Collapse of PBX into hollow bore of explosive device

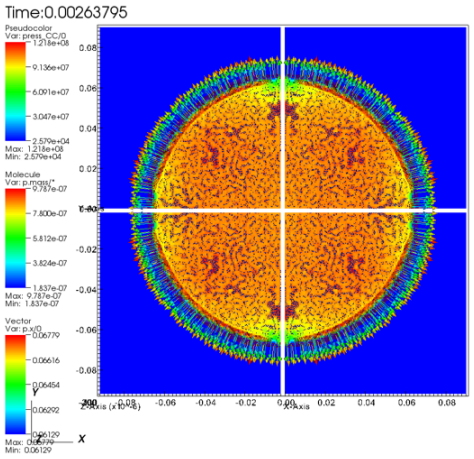

(b) Expansion of steel casing as explosion occurs–response to pressure build-up

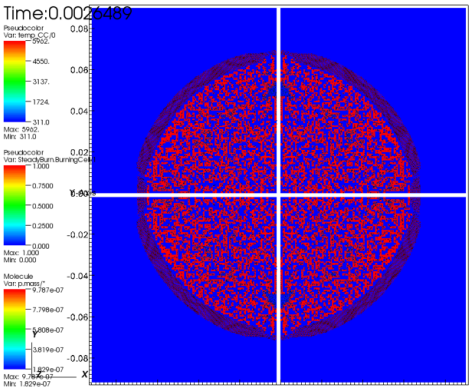

(c) Burning Cells denoted by red squares

Figure 8.5:

Results

Figure 8.5a shows a nice view of the cylinder as the PBX particles within is collapsing into the void, creating more burnable surface area resulting in more violent explosion. Figure 8.5b shows a view of the cylinder as the steel container begins to expand outward. Arrows represent the speed at which the particles in the steel case are expanding outward. Figure 8.5c shows cell flagged as burning by Steady Burn.

T-Burner Example Using Unsteady Burn

Problem Description

The T-Burner problem was inspired by an article by Jerry Finlinson, Richard Stalnaker and Fred Blomshield in which a T-Burner apparatus was pressurized to a given pressure and ignited [1]. The T-Burner composed of a cylinder with HMX on each circular ends, and a pressure inlet halfway between the HMX caps pumps pressure into the vessel parallel to those walls. Finlinson, et. al. measured pressure oscillations in the chamber and this simulation mimics the behavior found of Finlinson's 500 psi experiment. For simplicity and resource minimization, the simulation is set up as a 2D T-Burner. The graphs below shows the pressure oscillations over time compared with that from [1]. This simulation demonstrates the utility of Unsteady Burn in simulations where pressure oscillations occur in small places. For more information on Unsteady Burn see 8.3.3.

Simulation Specifics

Component used: mpmice (MPM-ICE)

Input file name: `TBurner_2dRT.ups`

Command used to run input file: mpirun -np 4 sus TBurner_2dRT.ups

Simulation Domain: 0.822 x 0.138 x 0.003 m

Example Runtimes:
25 minutes (1 processor, 2.8 GHz Xeon)

Physical time simulated: 0.46 milliseconds
0.46 milliseconds of simulation equates flag <max_Timesteps>410< /max_Timesteps>

Notes:
1)Remove line from input file to allow simulation to run full 0.25 seconds
2)Comment out <outputTimestepInterval> and uncomment <outputInterval> to make output Δt constant

Associated visit session: TBurner.session

Results

Figure 8.6a, 8.6b and 8.6c show successive snapshots of the simulation. Contour plot depicts pressure and represents the wave front as it oscillates between two sheets of burning PBX 9501. Figure 8.6d shows velocities of gas cells.

Figure 8.6d shows a snapshot of the simulation at the same instant as the previous figure. The contour plot depicts pressure. The arrows are vectors depicting the importance

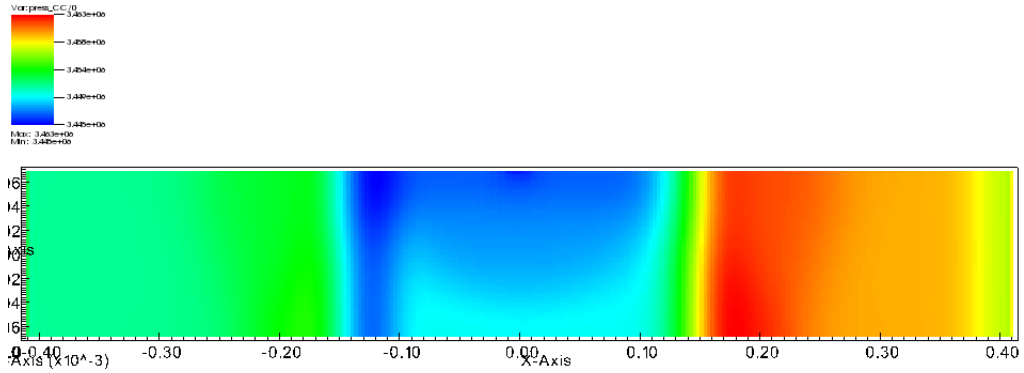

(a) Time 1: Oscillatory behavior in the form of a pressure wave in a T-Burner. Contour plot depicts pressure

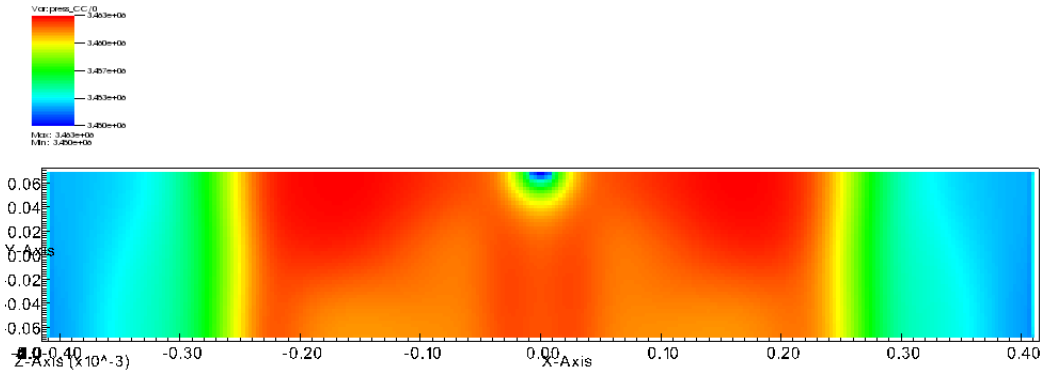

(b) Time 2: Oscillatory behavior in the form of a pressure wave in a T-Burner. Contour plot depicts pressure

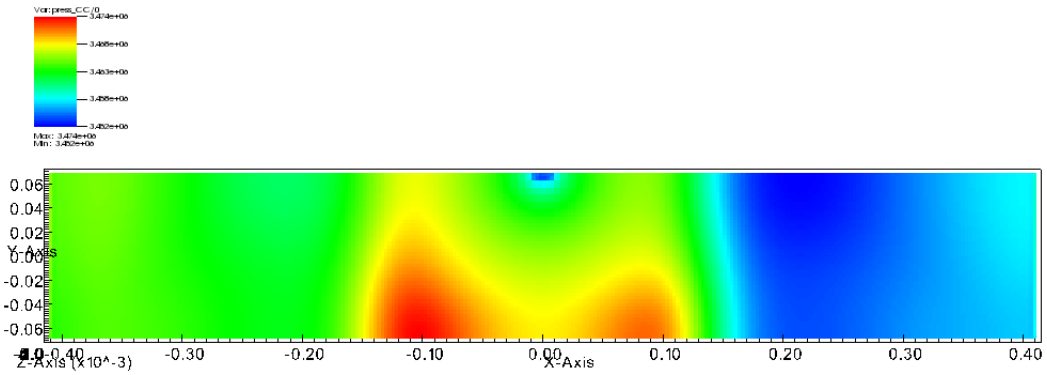

(c) Time 3: Oscillatory behavior in the form of a pressure wave in a T-Burner. Contour plot depicts pressure

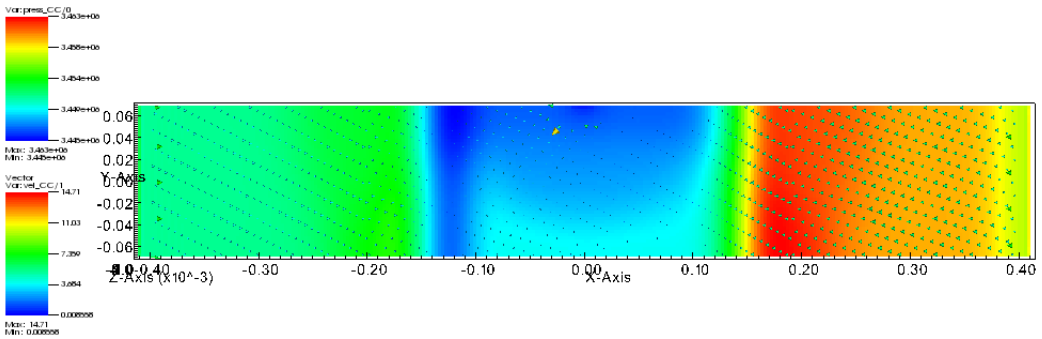

(d) Velocity vectors of cell material. Shows how the pressure causes gas to move

Figure 8.6:

Bibliography

[1] J.C. Finlinson, R. Stalnaker, and Blomshield F.S. Hmx and rdx t-burner pressure coupled response at 200, 500, and 1000 psi. *Proceedings of 36th JANNAF Combustion Meeting*, 1999.

[2] J.E. Guilkey, T.B. Harman, and B. Banerjee. An eulerian-lagrangian approach for simulating explosions of energetic devices. *Computers and Structures*, 85:660–674, 2007.

[3] M. A. Saad. *Compressible Fluid Flow*. Prentice-Hall, New Jersey, 1985.

[4] M.J. Ward, S.F. Son, and M.Q. Brewster. Steady deflagration of hmx with simple kinetics: A gas phase chain reaction model. *Combustion and Flame*, 114:556–568, 1998.

[5] C.A. Wight and E.G. Eddings. Science-based simulation tools for hazard assessment and mitigation. *Advancements in Energetic Materials and Chemical Propulsion*, pages 921–937, 2008.

Chapter 9

Glossary

- Data Warehouse (NewDW, OldDW, DW) - The `Data Warehouse` is an abstraction (and implementation vehicle) used in Uintah to provide data to simulation components (across distributed memory spaces as necessary). OldDW refers to a DW from the previous time step. NewDW refers to the DW for the current time step. In practice, variables are usually pulled from the OldDW, updated, and placed in the NewDW.
- Time step - Uintah is a time dependent code. A time step refers to a unique point in simulation time. The state of the simulation is updated one time step at a time.
- Adaptive Mesh Refinement (AMR) - In brief, AMR allows spending less CPU time on "inactive" (less interesting) areas of the simulation, and spend more time computing where there are many particles reacting. Resolution is low in the center where things are stable, but high at the edges. This feature is in ICE, but not ARCHES.
- CCA - Common Component Architecture.
- CFD - Computational Fluid Dynamics modeling.
- DistCC - Parallel, distributed compiler.
- Doxygen - Doxygen (code documentation) web interface.
- GhostCells (and Extra Cells)
- Grid - The problem's physical domain. The number of cells in the grid determine the resolution of the simulation.
- Handle - Smart pointers. Handles track the number of references to a given object, and when the number reaches zero, de-allocates the memory.

- Level - Not a 'level' in 3d-space, but a level of recursion into an AMR grid. ARCHES doesn't support AMR or nonuniform cells, and therefore doesn't need recursion, so it works on a single level '1'.
- Material Point Method (MPM) - The main component for simulating structures (physcial objects) in the UCF.
- Message Passing Interface (MPI) - Communication library used by many distributed software packages to communicate data between multiple processors. Besides send'ing and recv'ing data, data reduction (UCF Reduction Variables) is supported.
  - OpenMPI
- Patch - A physical region of the grid assigned one to each processor. The processor working on a patch will compute properties for each of the cells contained in the patch. Think of this as a big cube that contains hundreds of little cubes.
- Regression Tester (RT) - Runs nightly accuracy, memory, and completion tests on Uintah simulations.
- SCIRun - A Problem Solving Environment (PSE) originally used to provide core software building blocks for Uintah as well as an extensive visualization package for viewing Uintah data archives.
- SUS - Standalone Uintah Simulator. This is the main executable program in the Uintah project.
- SVN - Subversion code versioning system.
- Uintah - The general name of the C-SAFE simulation code. Sometimes also refered to as the UCF. The name comes from the Uintah mountain range in Utah.
- Uintah Computational Framework (UCF) - The core software infrastructure for Uintah.
  - Variables (CC, NC, FC) - Cell centered, Node centered, and Face centered (respectively) data structures used within the UCF.
- Uintah Data Archive (UDA) - The directory/file/data layout for storing Uintah simulation data.
- Uintah Problem Specification (UPS (Section 2.3)) - An XML based file used to specify Uintah simulation properties.
- Uintah Software Organization

- Visualization
- scinew - a wrapper for the C++ new() function that allows for memory tracking.